Analysis of The Effectiveness of Queue Warning Systems in Freeway Work Zones

by

Han Luo

A thesis submitted to the Graduate Faculty of
Auburn University
in partial fulfillment of the
requirements for the Degree of
Master of Science

Auburn, Alabama
May 6, 2023

Keywords: Freeway, Work Zones, Queue Warning Systems, Crash Modification Factors, Traffic Microsimulation, VISSIM

Approved by

Rod E. Turochy, Chair, James M. Hunnicutt Professor in Traffic Engineering
Huaguo Zhou, Elton Z. and Lois G. Huff Professor of Civil Engineering
Larry Rilett, Director of the Auburn University Transportation Research Institute

ABSTRACT

Work zone safety and mobility have always been a major concern for state DOTs and transportation professionals. While roadway usage has increased substantially in recent years as the U.S. population and number of licensed drivers have grown, the capacity of the highway system has grown very slowly. Increased roadway usage has led to deteriorating quality of road infrastructure, posing a potential risk to the traveling public.

Work zones are necessary components to maintain and improve the quality of the highway infrastructure. However, the presence of work zones disrupts mobility and presents motorists with unforeseen challenges and conditions, increasing the risk of vehicular crashes and traffic delays within and near work zones.

Rear-end crashes were identified as the predominant crash types in freeway work zones. To minimize the impacts of work zones on safety and mobility, Intelligent Transportation Systems (ITS) technologies are being utilized to fill in the gaps of current practices.

Queue Warning Systems (QWS), as an example of ITS technology in work zones, which employs queue detection systems and communication technologies, provide an opportunity to address traffic safety and mobility associated issues in work zones through queue detection and warning systems.

A proper queue warning system is designed to detect traffic conditions in the work zone, such as the presence of queues or accidents, and notify motorists of slow traffic or queues ahead so that they can react in time to the upcoming traffic conditions. Currently, the application of this technology is still in its early stages in Alabama.

The purpose of this study is to analyze the effectiveness of the QWS in a freeway work zone through the evaluation of the impact on traffic safety of QWS and the development of traffic simulation models to estimate the traffic effects of QWS. From the results of the safety performance evaluation, a site-specific crash modification factor specific (CMF) for QWS deployment was developed to be 1.49, and combined with the crash reduction analysis, it was found that specific in this study, the percentage of increased rear-end and sideswipe associated crashes at the control site (without QWS) is lower than that at the treatment site (with QWS). However, these findings were from a very limited study that only included one treatment and one control site making the transferability to other deployments limited until further study with more sites can be performed.

In addition, traffic simulation models were developed and successfully validated to replicate field-observed traffic operations within the work zone area.

The methodology presented in this study for the development of the site-specific crash modification factor related to the QWS deployment in freeway work zones when true control conditions could not be evaluated, and for the VISSIM model development, calibration and validation can be applicable to other state highway agencies and practitioners.

ACKNOWLEDGEMENTS

I would like to express my sincere gratitude to my academic advisors, friends, and family for their support throughout the thesis preparation process.

I am particularly grateful to my advisor, Dr. Rod E. Turochy, for his mentorship and encouragement throughout my graduate studies. Thanks to him for his patience and meticulousness, and the countless hours of meetings that helped me complete this thesis.

Special gratitude to Dr. Turochy and his family for their constant warm gestures and for always making me feel welcome. I am very fortunate to be one of the students working under your guidance. Your gesture of humility, kindness, and wisdom has inspired me a lot, making me become better and better.

I would like to express my sincere appreciation to my committee members, Dr. Huaguo Zhou and Dr. Larry Rilett, for serving on my thesis committee. Thanks for their time and valuable advice.

I would also like to extend my gratitude to the Alabama Department of Transportation for their financial support throughout the research process.

Special gratitude to Dr. Ernest Tufuor for his help and valuable advice during the VISSIM simulation models development.

TABLE OF CONTENTS

LIST OF TABLES

LIST OF FIGURES

LIST OF ABBREVIATIONS

AADT	Annual Average Daily Traffic
ALDOT	Alabama Department of Transportation
ARTBA	American Road & Transportation Builders Association
CARE	Critical Analysis Reporting Environment
CCS	Continuous Count Station
CMF	Crash Modification Factors
DOT	Department of Transportation
EDC-3	Every Day Counts Round 3
EOQ	End-of-Queue
FHWA	Federal Highway Administration
FREVAL-WZ	Freeway Evaluation Tool
GEH	Geoffrey E. Havers
HCM	Highway Capacity Manual
HSM	Highway Safety Manual
ITS	Intelligent Transportation Systems
MUTCD	Manual on Uniform Traffic Control Devices
NB	Northbound
NHS	National Highway System
PCMS	Portable Changeable Message Sign
PDO	Property Damage Only
PRS	Portable Rumble Strips
QUEWZ-98	Queue and User Cost Evaluation of Work Zones
QWS	Queue Warning System
RE	Rear-End
RRMSE	Relative Root Mean Square Error
SB	Southbound
SS	Sideswipe-in-same-direction
SWZ	Smarter Work Zones

TDM	Traffic Data Manager
TTC	Temporary Traffic Control
TTC	Temporary Traffic Control
TxDOT	Texas Department of Transportation
U.S.	United States
VMT	Vehicle Miles Traveled
vphpl	Vehicles Per Hour Per Lane
VSL	Variable Speed Limit

CHAPTER ONE: INTRODUCTION

1.1 BACKGROUND

With the continuous development of the economy, the National Highway System (NHS) has been developed rapidly in the last few decades. As of 2020, although the 220,515 miles on the NHS accounted for only 5.28% of the total mileage, it carried 1.572 trillion vehicle miles traveled (VMT) in 2020, which approximately 54.17% of the total travel (Federal Highway Administration 2020). Among the total VMT, the 48,756 miles of the Interstate System carried 0.727 trillion VMT in 2020 which approximately 25% of the nation's traffic (Federal Highway Administration 2020). Compared to 2004, the share of mileage with good ride quality dropped from 43.1% to 38.4% in 2014, indicating that the situation has worsened on roads with lower traffic volumes (Federal Highway Administration 2020).

With the increase of U.S. population and the number of licensed drivers, the roadway usage has increases substantially, but the capacity of the highway system has grown very slowly in recent year, indicating that demand is growing faster than system capacity. Therefore, the current transportation system needs to be improved to meet these needs (Federal Highway Administration 2020).

In recent years, the U.S. Department of Transportation (DOT) construction focus has shifted from expansion to maintenance and rehabilitation, which has resulted in a significant increase in work area presence nationwide. The presence of work zones disrupts mobility and increases the potential crashes between vehicles. The safe and efficient flow of traffic through work zones is a major concern to transportation professionals (Federal Highway Administration 2022).

In 2019, nearly a quarter of all fatal work zone crashes were identified to be rear-end (RE) crashes, specifically, rear-end crashes increased significantly from 2019 to 2020 as can be seen in Figure 1-1 (Federal Highway Administration 2022).

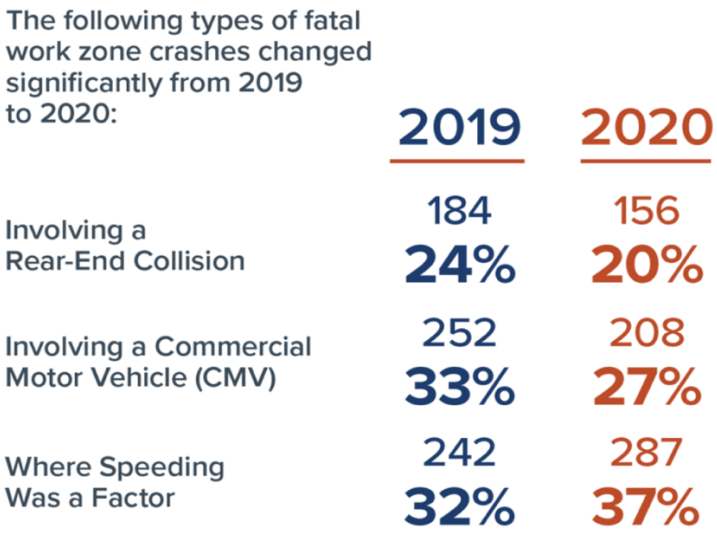

Figure 1-1: Total Work Zone Fatal Traffic Crashes by Type (Federal Highway Administration 2022)

To address the impact of work zone on traffic safety and flow, technological applications to dynamically manage work zone traffic through the deployment of Intelligent Transportation Systems (ITS) such as queue management and speed management has been a focus to minimize the impacts of work zone on safety and mobility according to the FHWA's Every Day Counts Round 3 (EDC-3) Smarter Work Zones program (Federal Highway Administration 2022).

Queue warning system, as an example of smart work zone technology applications, is designed to detect traffic conditions within the work zone such as the presence of queues or incidents and inform motorists about slowed or queued traffic ahead so they can react in a timely manner to the upcoming traffic conditions (ARTBA 2022, Khazraeian et al. 2017).

1.2 PROBLEM STATEMENT

Highway work zones are necessary components of the Alabama Department of Transportation's (ALDOT) effort to maintain and improve the quality of the state's highway infrastructure. However, the presence of work zones can present unforeseen challenges and conditions to motorists, increasing the risk of vehicular crashes and traffic delays within and near work zones. Table 1-1 summarizes the annual average number of total crashes and total fatalities in Alabama work zones, based on the Alabama Traffic Crash Fact Booklet from 2011 to 2019.

Table 1-1: Work Zone Related Crashes and Fatalities
(ALDOT Crash Fact Booklets 2011 – 2019)

Year	Total Crashes	Total Fatalities
2011	3167	21
2012	2232	25
2013	2346	24
2014	2377	23
2015	2435	31
2016	2960	19
2017	3154	31
2018	3806	34
2019	3134	16
Average	**2846**	**25**

It can be seen that the annual average number of work zone related crashes and fatalities over the nine-year period in Alabama were 2846 and 25, respectively. However, the actual number may be higher, as many work zone-related crashes were found to not always be reported as such in crash reports (Prichard 2015).

When work zones exist on high-speed facilities such as freeways, unexpected congestion can cause motorists to misjudge their ability to stop or slow down in a safe and timely manner (Ramirez 2017). In the condition of high-speed driving, improper operation may lead to severe

rear-end crashes. Therefore, the deployment of queue warning systems provides an opportunity to address this issue and improve safety and mobility in freeway work zones.

Past studies focused on the deployment of QWS has shown an estimated reduction in work zone-related crashes of 14% in Illinois and 18% to 45% in Texas. However, current available evaluations related to queuing warning systems are relatively limited. Due to the potential benefits of this technology, FHWA has made the deployment of QWS a priority area for safety improvements, and through grants to support the adoption and implementation of smart work zone technology in states.

In the state of Alabama, ALDOT formed a committee to consider and select potential smart work zone applications statewide for possible deployment. With the suggestion of the committee, this research has been developed for the purpose of evaluating the safety impacts and performance of ALDOT's experience with this QWS deployment and provide guidance on future applications.

1.3 RESEARCH OBJECTIVES

This thesis is intended to support ongoing research related to a project entitled "Analysis of The Safety and Mobility Benefits of Queue Warning Systems in Alabama Work Zones" funded by the Alabama Department of Transportation (ALDOT). As such, the purpose of this study is to analyze the effectiveness of the QWS in a freeway work zone through the evaluation of the impact on traffic safety of QWS and the development of traffic simulation models to estimate the traffic effects of QWS. The objectives of this study are to:

1. Summarize the current state of availability and practice of QWS, as well as the safety and mobility effectiveness of previous deployments.

2. Evaluate the safety performance of QWS deployed in a freeway work zone by developing an approach to estimate expected crashes that would potentially be mitigated by QWS.
3. Develop, calibrate, and validate a series of microsimulation models in VISSIM to replicate field-observed traffic conditions.
4. Develop recommendations for modelers and practitioners, as well as for future research by synthesizing findings from previous tasks.

1.4 ORGANIZATION OF THIS THESIS

This thesis is organized into five chapters and the remainder is as follows: Chapter 2: Literature Review, synthesizes the state-of-the-practice literature focusing on the safety and mobility effects of QWS. Specifically, the literature review addresses the safety analysis focusing on the work zone crash characteristics identification as well as the work zone-related crash modification factor development. The chapter also includes the concept of queue warning system applications, and the most relevant traffic simulation tools available to researchers and practitioners. Chapter 3: Safety Performance Evaluation, describes the mathematical procedures for safety evaluation of QWS. Specifically, a detailed analysis to develop a site-specific crash modification factor (CMF) for freeway work zone QWS deployment is presented. Chapter 4: Traffic Simulation Evaluation, introduces the process of the development, calibration, and validation of the traffic microsimulation models in greater detail. Chapter 5: Conclusion and Recommendations, summarizes the major findings from the safety evaluation and traffic simulation analysis sections and provides recommendations for future research.

CHAPTER TWO: LITERATURE REVIEW

2.1 INTRODUCTION

This chapter synthesizes the state-of-the-practice literature focusing on the safety and mobility effects of QWS. This chapter starts with the relevant freeway work zone safety analysis focusing on the work zone crash characteristics identification as well as the work zone-related crash modification factor development. Then, work zone mobility research focusing on application of Intelligent Transport System (ITS) technology is presented, along with an introduction of queue warning system applications. This chapter also presents the most relevant traffic analysis tools currently available to researchers and practitioners, as well as the application of traffic simulation models specific to this study.

2.2 FREEWAY WORK ZONE SAFETY ANALYSIS

Work zone safety and mobility have always been a priority for both decision makers and practitioners. Previous studies have proven that inefficient operation of traffic within freeway work zones tend to cause an increase not only in travel time delays, queue length, and fuel consumption but also in the number of crashes related to the presence of a work zone (Ishak et al. 2012; Al-Kaisy and Hall 2003).

2.2.1 WORK ZONE CRASH CHARACTERISTICS

Studies on crash analysis specific to upstream of the freeway work zone are limited, especially under queueing condition. However, this section may be of similar hazard as the work zone itself due to the disturbed flow of traffic and potential for queuing.

A study conducted by Venugopal and Tarko examined several potential factors that contribute to crashes within and approach to work zone segment. The authors were able to develop separate regression models to predict the expected crash frequency inside the work zone segment and on approaches to the work zone, since safety effects inside a work zone might not be the same as on approaches to the work zone. The crashes were assigned to the upstream of a work zone if a) the location of a certain crash fell within a queued condition upstream of the work zone and b) the time with respect to the crash coincided with the presence of the work zone; whereas if the location of a certain crash fell between the beginning of an active work zone to the end of the construction zone, and the crash time concurred with the existence of the work zone, then the crashes were assigned to the inside of a work zone. This study indicated that factors including traffic volume, length, and duration of the work zone have significant impacts on the number of crashes upstream of freeway work zones (Venugopal and Tarko 2000).

More specifically, another research study conducted by Garber and Zhao investigated relevant work zone crash characteristics with respect to crash type, crash severity, and crash location in Virginia. The authors were able to evaluate percentage distributions of each crash trait and concluded that the predominant crash type for both advance warning area and transition area was rear-end (RE) crash, specifically, 83% of RE occurred in advance warning area and 54% of RE occurred in transition area. This study was also able to demonstrate a significant increase in sideswipe-in-same-direction (SS) crashes within the transition area when compared to the advance warning area. However, while considered to the crash severity distribution among the upstream of the work zone, the researchers identified a lower fatality rate in the transition area than that in the advance warning area, but the proportion of property damage only (PDO) in the transition area was found almost three times higher than that of the advance warning area (Garber and Zhao 2002).

This finding did not agree with a later research study by Ishak et al. In this study, statistical analysis of crash rates on Louisiana's work zone approaches segment with a conventional lane merge configuration showed that compared to the upstream transition area, the advance warning area experienced higher fatality and PDO crash rates due to merging maneuvers started under high-speed condition (Ishak et al. 2012). Figure 2-1 below describes a generic work zone temporary traffic control (TTC) layout where the four areas were illustrated in detail.

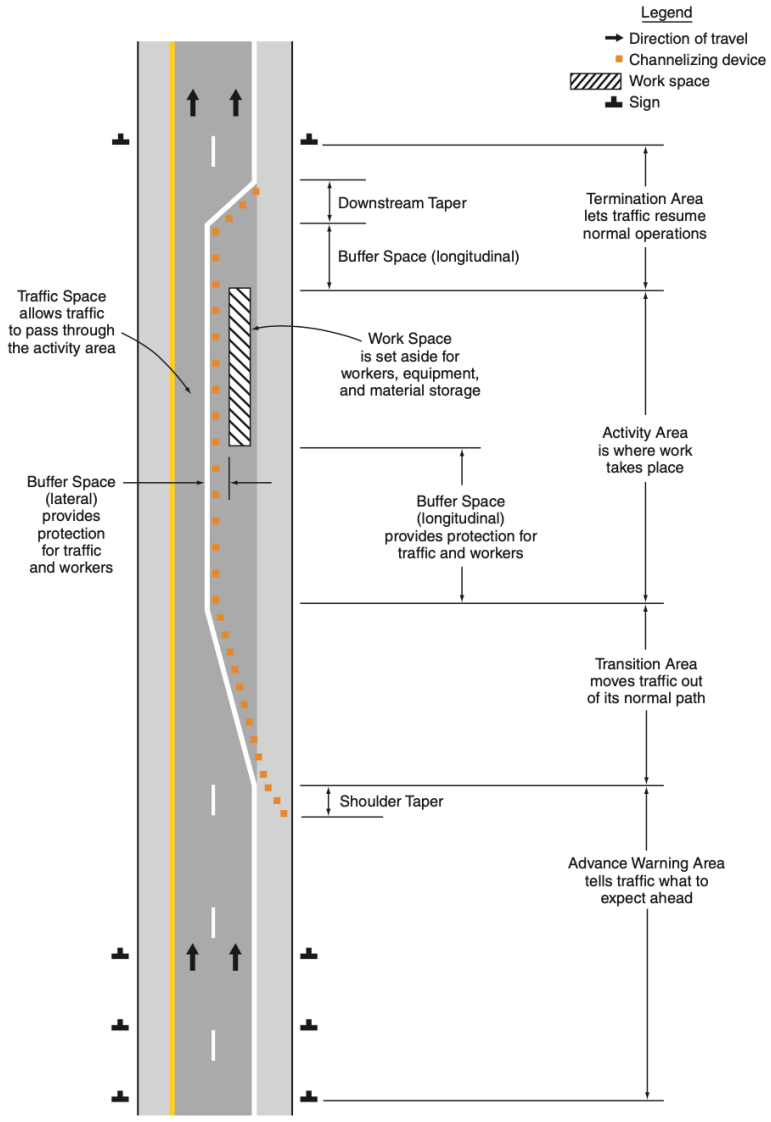

Figure 2-1: Component Parts of a Temporary Traffic Control Zone (Manual on Uniform Traffic Control Devices 2009)

When considering the safety impact of the work zone in urban or rural, Harb et al. developed regression models to evaluate urban and rural freeway work zone crash traits considering interactions and confounding parameters to identify its relationship associated with driver, vehicle, and environmental characteristics. Statistical findings from this study identified that the crash rate in urban freeway work zones was almost twice as high as in rural areas for each of the three evaluation indexes (Harb et al. 2008).

Although numerous studies have attempted to characterize freeway work zone crashes and their causal factors, their results have not been entirely consistent and different research results are possible due to a variety of factors associated with work zone conditions. In a recent study, Yang et al. reviewed and synthesized the state of existing knowledge on work zone safety analysis in the last fifty years, and concluded that rear-end crashes did as the prevalent type of crash involved in freeway work zones. While seeking to find the relationship between work zone-related crashes and other factors such as crash location, crash type, and crash severity, the results from the reviewed studies did not come out with completely consistent (Yang et al. 2015).

2.2.2 WORK ZONE CRASH MODIFICATION FACTORS

A crash modification factor (CMF), a numerical ratio used to provide an estimation of the change in crash frequency that would be expected due to the implementation of a given countermeasure or a specific change in a particular site (Edara et al. 2020; FHWA 2022). A CMF value of less than 1.0 indicates an expected reduction in crashes after the implementation of a safety improvement, while a value of CMF greater than 1.0 indicates an expected increase in crashes if deploy a countermeasure.

A high-quality CMF can be used to quantify the safety benefits of possible work zone improvements and to weigh the safety benefits of implementing work zone countermeasures against various other tradeoffs to assist practitioners in the decision-making process of whether to implement specific work zone countermeasure (Edara et al. 2020).

The currently available CMFs were developed based on extensive research conducted by roadway safety-related professionals that measured the potential of various types of safety improvements in reducing crashes through comparing the number of crashes after deployment of a safety improvement to that before implementation to obtain a measured change in crashes (FHWA 2014).

While there have been developed many studies on the safety evaluation of roadway facilities, only a few of them have focused on CMF development within work zone, and even fewer studies have been done on freeway work zone CMF development. The availability of existing work zone CMFs for researchers and practitioners is very limited. At the time of writing this report, the existing work zone-related CMF values can be found from two sources, the Highway Safety Manual (HSM), and the CMF Clearinghouse, with details included in each source discussed below.

Work Zone CMFs in HSM

The CMFs for specific types of facilities such as work zone length and duration, are provided in Highway Safety Manual (HSM). These work zone-related CMFs were developed with the use of data from 36 high-impact freeway work zones in California. The CMF values for work zone length and duration with representation of all crash severities can be calculated using the following Equation 2-1 and Equation 2-2, respectively (Edara et al. 2020, AASHTO 2014). It can be seen that there is a liner relationship between CMF value and work zone length/duration.

$$CMF_{l,all} = 1.0 + \frac{(\%\ increase\ in\ length \times 0.67)}{100} \quad \text{(Eq. 2-1)}$$

$$CMF_{d,all} = 1.0 + \frac{(\%\ increase\ in\ duration \times 1.11)}{100} \quad \text{(Eq. 2-2)}$$

Work Zone CMFs in CMF Clearinghouse

The CMF Clearinghouse, an online database hosted by FHWA and maintained by the University of North Carolina Highway Safety Research Center, provides all existing CMFs as well as related additional information and resources, based on the synthesis of work zone safety studies. In addition to a single CMF value, the corresponding star quality rating (based on a scale of 1 to 5 with 5 being the best), applicability, research reference and development details are provided as well for reference. An example screenshot from the CMF Clearinghouse regarding a specific CMF for the countermeasure – Active work with no lane closure (compared to no work zone) is provided in Figure 2-2.

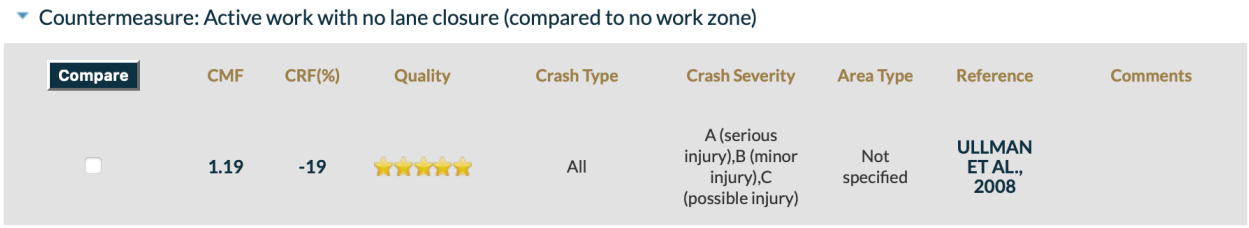

Figure 2-2: Example Screenshot of CMF General Information for Specific Countermeasure (CMF Clearinghouse 2022)

It can be seen from Figure 2-2 that the corresponding CMF for this countermeasure is 1.19 (with a crash reduction factor of -19%) indicating that a 19% increase in crashes should be expected when an active work zone with no lane closure presents. A star rating of 5 identifies the quality of this CMF value is highly reliable. Specifically, detailed applicability information and

relevant additional information are provided in the following Figure 2-3 and Figure 2-4, respectively.

Applicability	
Crash Type:	All
Crash Severity:	A (serious injury),B (minor injury),C (possible injury)
Roadway Types:	Principal Arterial Other Freeways and Expressways

Figure 2-3: Example Screenshot of CMF Applicability
(CMF Clearinghouse 2022)

Development Details	
Date Range of Data Used:	
Municipality:	
State:	
Country:	
Type of Methodology Used:	Before/after using empirical Bayes or full Bayes
Other Details	
Included in Highway Safety Manual?	No
Date Added to Clearinghouse:	Dec-01-2009
Comments:	

Figure 2-4: Example Screenshot of CMF Additional Information
(CMF Clearinghouse 2022)

From Figure 2-3, it can be seen that this CMF value is applicable to all crash type but only specific to serious injury (A), minor injury (B), and possible injury (C). The applicable roadway types include principal arterial, freeways, and expressways. The area type is not specified for this particular CMF. Figure 2-4 provides additional information including development and other details. Specifically, the type of methodology used to develop this CMF value is before/after using Empirical Bayes or Full Bayes. This particular CMF value was added to the CMF Clearinghouse on December 1st, 2009 and not included in HSM.

In general, the available CMFs included in the CMF Clearinghouse for the current work zone-related countermeasures (a total of 9 countermeasures available) are presented in Figure 2-5, which also includes work zone length and duration that already in the HSM.

- Countermeasure: Active work with no lane closure (compared to no work zone)
- Countermeasure: Active work with temporary lane closure (compared to no work zone)
- Countermeasure: Implement left-hand merge and downstream lane shift (Iowa weave)
- Countermeasure: Increase work zone duration
- Countermeasure: Increasing the inside shoulder width inside the work zone by one foot
- Countermeasure: Increasing the outside shoulder width inside the work zone by one foot
- Countermeasure: Modify work zone length
- Countermeasure: No active with no lane closure (compared to no work zone)
- Countermeasure: TLTWO (two way traffic operations - crossover closures) in work zones

Figure 2-5: Available CMFs for Work Zone-Related Countermeasures (CMF Clearinghouse 2022)

In addition to the existing work zone-related CMFs that already included in both HSM and CMF Clearinghouse, some additional work zone CMFs for specific improvements developed by other work zone safety research that are not in the HSM or CMF Clearinghouse are discussed in greater detail elsewhere (Edara et al. 2020). Specifically, since this study focuses on the topic of queue warning system (QWS) deployment within freeway work zones, literature review efforts were conducted mostly on this aspect.

In a study undertaken by Ullman et al., the researchers were able to develop an end-of-queue (EOQ) warning system with a combination of highly-portable transverse rumble strips (PRS) at nighttime temporary work zones along Interstate 35 (I-35) through central Texas. Lane closures were presented at nighttime therefore the EOQ warning system was deployed upstream of lane closures where queuing was expected. The researchers concluded that the system had a positive effect in reducing crashes. Specifically, the combination of EOQ warning system and PRS resulted in a 44% reduction in crashes. In addition, severe crashes and the most common rear-end crashes have also decreased. For this specific work zone safety countermeasure, the researchers computed a CMF value of 0.559, which corresponds to the 44% reduction in crashes, with a p-value of 0.085 indicating that this countermeasure has a statistically positive effect on reducing crashes (Edara et al. 2020; Ullman et al. 2016).

Later on, in a follow up study, a greater detailed analysis on the safety impact of the combination of EOQ warning system and PRS was conducted by Ullman et al. The researchers were able to evaluate individual safety effects between EOQ warning system and PRS in both queuing and non-queuing traffic conditions. Four associated CMFs were developed from this study as presented in Table 2-1. The researchers concluded that the computed CMFs have a range from 0.40 to 0.89 showing that the portable rumble strips (PRS) only or the combination of EOQ

warning system and PRS has safety benefits under both traffic conditions (Edara et al. 2020; Ullman et al. 2018).

Table 2-1: CMFs for Safety Treatment

(Ullman et al. 2018)

Safety Treatment	Traffic Condition	Crash Modification Factor
Only PRS Deployed	Non-queued	0.890
	Queued	0.397
EOQ Warning System & PRS Deployed	Non-queued	0.717
	Queued	0.468

In general, a comprehensive work zone-related literature review effort was performed showing that there are few work zone-related CMFs available to practitioners or researchers. It was also found that in recent work zone safety studies, only a few of them have focused on the development of work zone CMFs. The most recent study conducted by Domenichini et al. generated a series of work zone CMFs for different layout configurations for four and six-lane median divided freeways using data from Italy, making the transferability of the developed CMFs applicable to the United States less feasible. Therefore, additional work zone safety research studies and work zone CMFs are in needed to be developed for the purpose of improving work zone safety (Edara et al. 2020; Domenichini et al. 2017).

For this research, a state-specific freeway work zone crash modification factor for a queue warning system (QWS) deployed in Alabama freeway work zone will be developed and evaluated using the following procedures as presented in Figure 2-6. The processes for the site-specific CMF development are discussed in significant detail in Chapter 3.

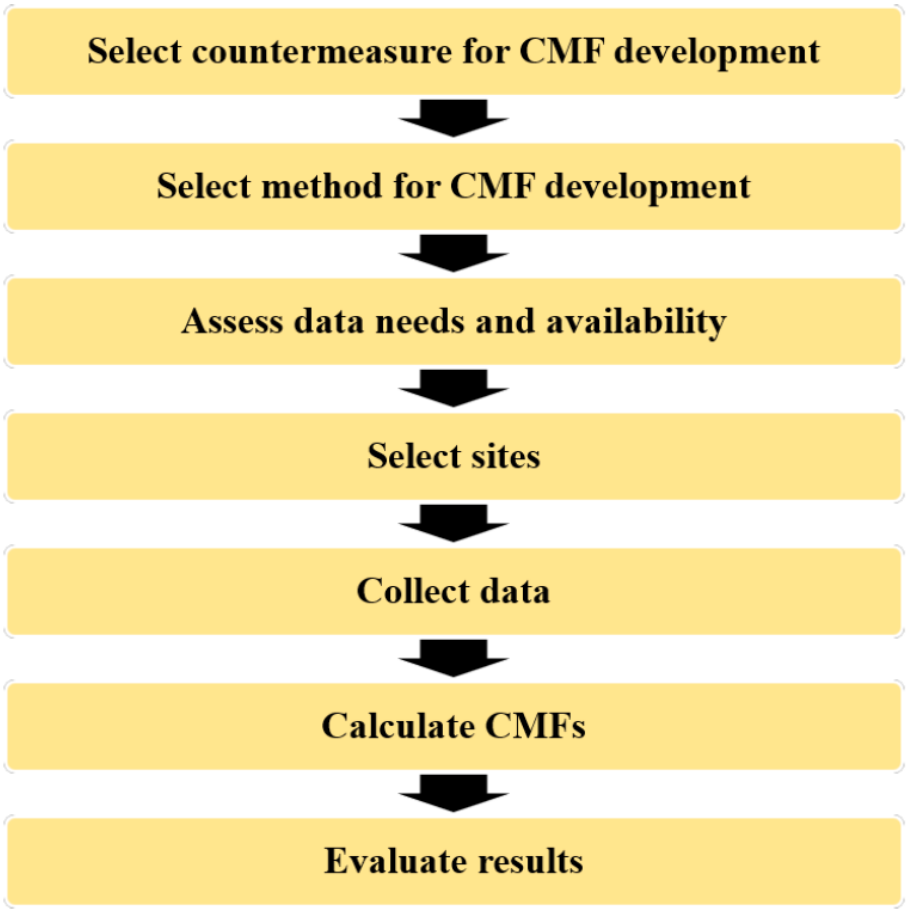

Figure 2-6: Procedure for Development of State-Specific Freeway Work Zone CMF (Edara et al. 2020)

It is worth mentioning in advance that the most important step presented in Figure 2-5 was the selection of an appropriate method for new CMF development, since many factors may affect the determination of the best method for a particular condition, such as data availability for comparison between different time periods, and the availability of control sites specific for QWS analysis (Edara et al. 2020).

In an earlier study on the development of CMFs conducted by Gross et al., 9 study designs for developing CMFs were discussed, which are before-after with comparison group (CG), before-after with empirical bayes (EB), full bayes (FB), cross-sectional, case-control, cohort, meta-

analysis, expert panel, and surrogate measures. The researchers were able to analyze each of the 9 methods with general applicability, strengths, and weaknesses. A detailed flowchart describing the process of selecting an appropriate methodology to develop the desired CMF under specific conditions is provided in Figure 2-7 (Gross et al., 2010). It may be noting that the abbreviations of CG, EB, and FB correspond to Comparison Group, Empirical Bayes, and Full Bayes, respectively.

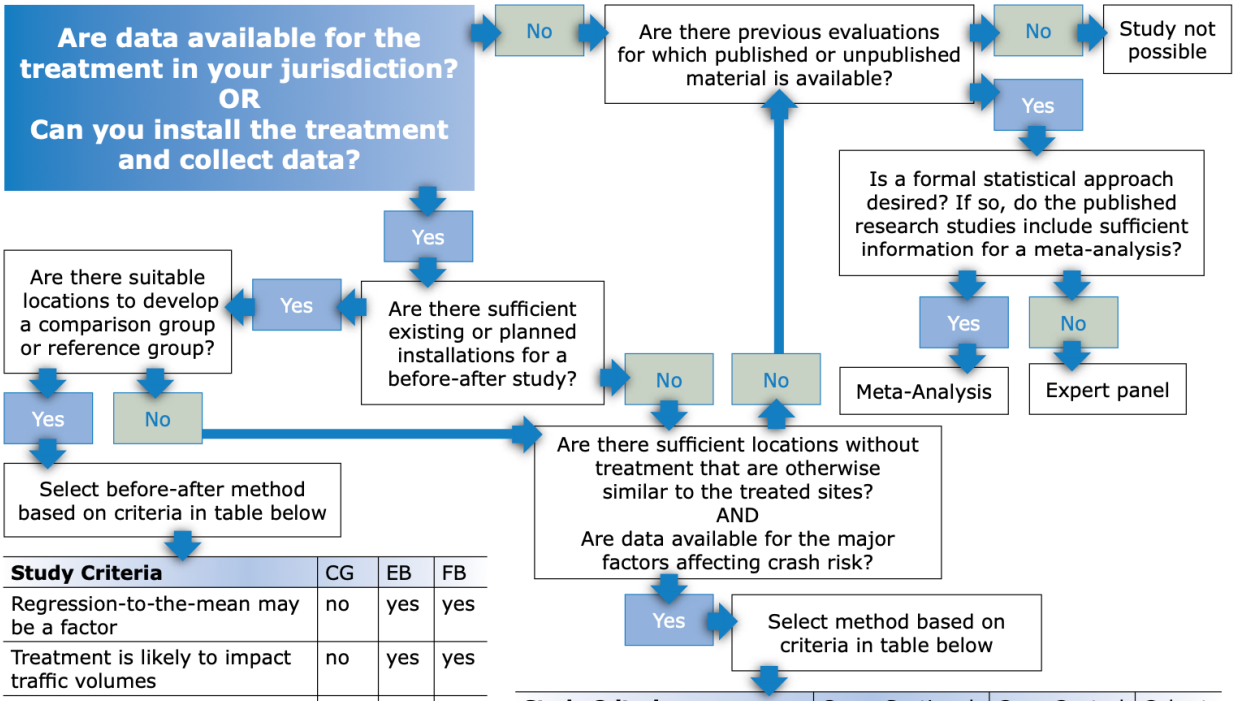

Study Criteria	CG	EB	FB
Regression-to-the-mean may be a factor	no	yes	yes
Treatment is likely to impact traffic volumes	no	yes	yes
Include spatial correlation (either among treated sites or among treated and comparison or reference sites)	no	no	yes
A complex model form is required	no	no	yes
Include prior knowledge of model or CMF estimates in the analysis	no	no	yes

Study Criteria	Cross-Sectional	Case-Control	Cohort
Crash type is rare	no	yes	no
Treatment is rare	no	no	yes
Accounts for locations with multiple crashes (rather than first occurrence)	yes	no	no
CMFunction desired	yes	no	no

Figure 2-7: Flowchart for Study Design Selection
(Gross et al. 2010)

From Figure 2-6, there are only 8 methods included in the study design selection for developing CMFs. However, the box with "Study not possible" in the upper right corner of the

flowchart represents that the surrogate measures (one of the nine methods) need to be explored by analysts for given conditions. The general applicability of this method to generate a CMF is when crash data are unavailable or insufficient such as limited "after" period data or the treatment is rarely implemented. The developed CMF is not based on a crash-based evaluation, therefore, the quality of the generated CMF is questionable.

2.3 FREEWAY WORK ZONE MOBILITY ANALYSIS

With the increasing development of the transportation system, the increasing need for mobility has led to major changes in the transportation infrastructure, and the most important of which are the increase of traffic congestion and the degradation of roadway condition. Therefore, rehabilitation and maintenance of the roadway requires work zones. Inefficient operation within and around work zones not only results in significant time lost, but also reduces the safety of motorists and work zone personnel, increasing exposure to hazard conditions. As such, there is a need to develop more efficient and safer mobility systems applicable for work zone conditions (Dimitrakopoulos and Demestichas 2010; Steger-Vonmetz 2005).

Intelligent Transport System (ITS), which integrate advanced communication, electronic, and computer technologies into transportation infrastructure and vehicles, can mitigate the impact of roadway construction and maintenance on their surroundings. Work zone ITS deployment can improve safety and mobility within and around work zones (Ullman et al. 2014; Luttrell et al. 2008; FHWA 2011; FHWA 2022).

Although ITS technology can be applied in work zones for different intentions, such as traffic monitoring and management, providing traveler information, incident management, enhancing safety of both the road user and worker, increasing capacity, enforcement, tracking and

evaluation of contract incentives/disincentives (performance-based contracting), and work zone planning (FHWA 2022), for the purpose of this study, it was utilized in freeway work zone for traffic monitoring and management, as well as providing real-time information to travelers. The resulting systems by utilizing information from ITS equipment to dynamically manage traffic in and around work zones are often referred to as Smart Work Zones (TxDOT 2018).

2.4 SMART WORK ZONES AND QUEUE WARNING SYSTEMS

During construction, effective traffic management is critical to enhancing the safety of drivers and workers, reducing travel delays, and completing roadwork on time. According to the FHWA's Every Day Counts Round 3 (EDC-3) Smarter Work Zones program, technological applications to dynamically manage work zone traffic through the deployment of Intelligent Transportation Systems (ITS) such as queue management and speed management is a focus for the purpose of minimizing the impacts of work zone on safety and mobility, in which queue management systems incorporate traffic communication technologies to alter drivers in preparing for upcoming traffic conditions, and speed management provides dynamic management of work zone traffic solutions such as variable speed limit (VSL) systems based on real-time conditions such as congestions (FHWA 2022, ARTBA 2022).

In recently, smart work zone (SWZ) systems have been immensely evaluated and applied in field by relevant researchers and practitioners for the purpose of improving public safety and mobility within the construction work area.

A smart work zone system combines computer, communication, and sensor technology and has the characteristics of real-time, reliable, portable and automated. Specifically, the system should have the ability to gather and analyze traffic flow data in real-time within the active work

zone, and automatically generate accurate and reliable information to upstream motorists with upcoming traffic conditions, as well as feature for easy deployment in different locations.

A proper SWZ system would benefit in preparing motorists for upcoming traffic conditions, reducing freeway congestion, and improving safety for motorists and work zone personnel. Specifically, the SWZ system can be utilized in freeway construction work area to provide motorists with accurate and reliable real-time information on the upcoming work zone conditions by predicting travel times, delays, and speeds in a timely manner (FHWA 2017).

One example of smart work zone technology applications is a queue warning system (QWS) designed to detect traffic conditions within the work zone such as the presence of queues or incidents and warn motorists of approaching traffic slow or stop areas (ARTBA 2022). A typical queue warning system consists of a set of speed detectors and portable changeable message signs (PCMS) alongside the roadway with the ability to customize speed threshold for the purpose of detecting queued traffic (Ramirez 2017). A QWS is able to collect real-time traffic data specifically speeds and volumes, analyze the data through an algorithm including a predefined speed threshold (i.e., 35mph) to determine the appropriate warning message, and provide dynamic and actionable guidance through the PCMSs to alert drivers of impending conditions such as "Road Work Ahead", "Stopped/Slowed Traffic XX Mile Ahead", and "Road Work – Expect Delays", etc. QWS deployment in work zones can reduce the severity of crashes and minimize rear-end crashes (FHWA 2022).

As noted earlier, two studies undertaken by Ullman et al. evaluated the safety effects of an end-of-queue (EOQ) warning system combined with portable rumble strips (PRS) in nighttime work zones on Interstate 35 (I-35) in Texas. The findings of these two studies indicated a 44% reduction in crashes as well as a reduction in severe crashes and rear-end crashes due to the

deployment of the combined end-of-queue (EOQ) warning system and PRS. Specifically, in later research, the individual safety impact of the EOQ warning system and PRS in queuing and non-queuing traffic conditions was evaluated. The results indicated a safety benefit of each in reducing crashes (Ullman et al. 2016; Ullman et al. 2018).

With the use of a microscopic traffic simulation model, Pesti et al. were able to evaluate the expected performance and reliability of a queue warning system deployed at a freeway work zone lane closure. The researchers tested various combinations of design parameters such as speed thresholds, data aggregation interval, update interval, and detector spacing, using traffic simulations, and identified the most appropriate setting of these parameters. The study concluded that a queue warning system with a detector spacing of half a mile could detect the end-of-queues more accurately than a system with a one-mile detector spacing. In addition, 35 mph was identified as the queue detection threshold which corresponds a "Stop" traffic condition, and 55 mph as the speed threshold for a "Slow" traffic stream which same as the freeway applications recommendation (Pesti et al. 2013).

2.5 TRAFFIC ANALYSIS TOOLS

Traffic analysis methodologies and tools have evolved significantly over the last few decades. With the increasing maturity of computer technology, computer-based traffic simulation tools have become one of the most useful tools and been widely used to help cope with real-world changing traffic conditions. Based on the FHWA Traffic Analysis Toolbox, in addition to simulation tools, traffic analysis tools can be grouped into several categories. For the purpose of this research and the purpose the tool was designed to fulfill, four categories will be discussed in detail along with the associated advantages and limitations. From most common to most complex, they are sketch-

planning tools, macroscopic simulation models, mesoscopic simulation models, and microscopic simulation models (FHWA Traffic Analysis Toolbox Reports; Jehn 2018; Ramirez 2017).

Sketch-Planning Tools

Sketch-planning tools or analytical/deterministic tools including software such as QUEWZ-98, QuickZone, FREVAL-WZ, are usually specialized models designed for specific tasks or applications (e.g., work zone assessment or ITS analysis) which also include spreadsheet models developed by individuals and state DOTs for specific projects or conditions. These types of tools target a wider range of applications, and most follow the volume-capacity approach contained in the Highway Capacity Manual (HCM).

The strengths of sketch planning tools lie in their relative ease of use and ability to facilitate rapid analysis, as opposed to the limited network complexity and advanced analysis, as well as detailed fidelity (accuracy and level of analysis) information (Hardy and Wunderlich 2008).

Macroscopic Simulation Models

Macroscopic simulation models are described in the FHWA Traffic Analysis Toolbox as deterministic relationships based on flow, speed, and density of traffic streams. The simulation runs in the Macroscopic model are performed section by section, rather than tracking individual vehicles, and cannot simulate the movement of individual vehicles on a network.

Macroscopic models have the ability to cover larger geographic areas, which becomes very useful for a particular condition, for example, when the area affected by a work zone is larger than a corridor or area where geographic features must be considered to better understand the impact.

The main limitation of such models is the simple representation of traffic motion (e.g., no car-following algorithms), which limits the fidelity of the results (Hardy and Wunderlich 2008).

Mesoscopic Simulation Models

Mesoscopic simulation models are thought to be the most recent generation of traffic simulation modeling tools developed in response to the need for intermediate analysis. These models, while providing a higher level of detail than macroscopic models, do not have the same fidelity as microscopic simulation models. Mesoscopic models tend to represent the relative flow of vehicles on network links, but not individual lanes on a link. Advantages of mesoscopic simulation models include the ability to model large geographic areas and corridors when analyzing work zones. Limitations of such models include their limited ability to model detailed operational strategies, as well as the complexity of the overall model and the data requirements needed for accurate results (Hardy and Wunderlich 2008).

Microscopic Simulation Models

Lastly, microscopic simulation models simulate the motion of each vehicle in the network by considering the driver's reaction to the surrounding roadway environment under real-world traffic conditions, based on car-following and lane-changing theories, and other parameters. Unlike deterministic tools discussed above, microsimulation tools are stochastic, meaning that each model run produces a unique result (Jehn 2018).

Microscopic simulation models can effectively evaluate a variety of scenarios, including heavily congested conditions and complex geometric configurations. The main limitation of these

models is that they require substantial amounts of roadway geometry, traffic control, and traffic pattern data.

Commonly available microsimulation tools include CORSIM and VISSIM developed by FHWA and PTV Group, respectively. Three main parameters are used to define the randomness of driving behavior, which are car-following, lane-changing and gap acceptance (Hardy and Wunderlich 2008).

2.6 TRAFFIC SIMULATION MODEL FOR FREEWAY WORK ZONE

As discussed in the previous section, although there are many traffic analysis tools currently available with different focuses for evaluating the safety and mobility impact of roadway construction on traffic, in this study, VISSIM was the chosen microscopic simulation tool due to its customization capabilities and ability to generate detailed output down to the second as well as individual vehicle accuracy (Ramirez 2017).

However, although VISSIM has been widely used by researchers and practitioners with different purpose, the validity of the developed models depends on robust calibration efforts at the later stage for the purpose of obtaining a model with the ability to best replicate the real-world traffic conditions. Recently, several studies have focused on the calibration of VISSIM simulation models by modifying key parameters.

In a recent study undertaken by Jehn and Turochy, the researchers developed and calibrated a rural freeway work zone through the adjustments to the driving behavior and heavy vehicle performance characteristics in VISSIM. Particularly, car-following parameters, such as desired standstill distance (CC0), desired time headway (CC1), and desired safety distance (CC2), were identified as most critical to model development and calibration. The authors also found that the

default key truck characteristics such as power, weight, and acceleration distributions for heavy trucks in VISSIM are not representative of the U.S. truck fleet. This study conducted a set of calibrated parameters which is applicable to this thesis and will be discussed in detail in the mobility analysis in Chapter 4.

2.7 SUMMARY

Freeway work zone often generates potential conflicts between traveling vehicles and work activities. With the application of intelligent transportation system (ITS) technology, freeway work zones safety and mobility can be improved. Queue warning system (QWS), an application of ITS technology, has been widely used in recent years because it can reduce the severity of crashes as well as have the ability to reduce the most common rear-end crashes in work zones, by informing drivers in advance of upcoming traffic conditions (queueing/slowing traffic) so they have enough time to react.

However, due to the complexity of the freeway condition, different work zones have different characteristics such as duration and length, therefore, a site-specific analysis of the safety and mobility impacts of QWS deployment is in need to be developed.

In general, the results of the literature review section indicate that there is a need to develop site-specific freeway work zone crash modification factor for a queue warning system (QWS) deployed in Alabama. To analysis the impact of QWS on traffic flow, based on the findings from literature work, the use of microscopic simulation model was identified since it has the ability to better replicate field conditions.

CHAPTER THREE: SAFETY PERFORMANCE EVALUATION

3.1 INTRODUCTION

This chapter is intended to describe the mathematical procedures of safety evaluation that lead to results, conclusions, and recommendations. One of the major objectives for this safety analysis section was to evaluate the safety performance of QWS deployed in a freeway work zone by developing an approach to estimate expected crashes that would potentially be mitigated by QWS. As such, a site-specific crash modification factor (CMF) for freeway work zone QWS deployment will be developed and discussed in detail in this Chapter.

3.2 OVERVIEW OF STUDY SITE (I-59/I-20)

Deployment of ITS applications in work zones ("smart work zone") is a current focus area of the FHWA's Every Day Counts Round 3 (EDC-3) program which by providing grants to support the adoption and implementation of smart work zone technologies. ALDOT formed a committee to consider and select potential smart work zone applications statewide for possible deployment, and ultimate determined to deploy a QWS on a widening project (level of terrian) on Interstate 59/Interstate 20 just south of Tuscaloosa, Alabama. An aerial map of the study site layout along with the location of sensors and portable changeable message sign (PCMSs) is provided in Figure 3-1. A total of 18 sensors and 4 PCMSs were deployed roadside throughout the project length. It is worth mentioning that a complete project location map from ALDOT construction plans can be found in Appendix A.

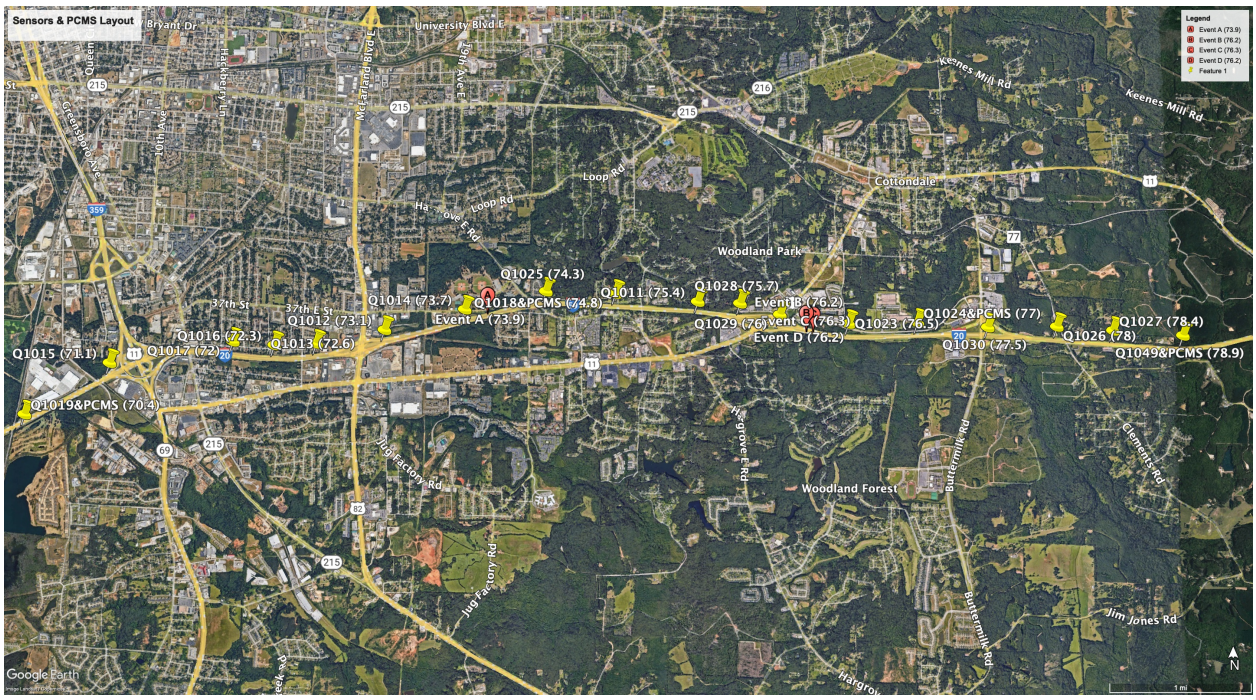

Figure 3-1: Overview of Treatment Site (I-59/I-20)

The I-59 widening project, also referred to the treatment site, with available data from deployed QWS started in March 2018 and ended in December 2019 for a total duration of approximately 22 months, resulting in a 6-lane highway from a 4-lane highway in both directions. To evaluate the safety and mobility impacts of ALDOT's initial deployment of QWS in work zones and provide guidance on future relevant applications, this research has been developed with the analysis addressed in detail in the following Chapters. Specifically, Chapter 3 discusses the procedures utilized to evaluate the safety performance of QWS deployment, and Chapter 4 details in the development of a series of simulation models for the purpose of analyzing the impact of QWS on traffic flow under free-flow conditions and typical crash conditions.

3.3 METHODOLOGY

Due to insufficient study sites available for analysis of both treatment (work zone with QWS) and control (work zone without QWS) conditions, a thorough literature review was conducted on the selection of methodology for developing a specific crash modification factor (CMF) applicable to this situation to evaluate safety performance of QWS deployment. The method eventually determined to generate the CMF was adjusted for an observational before-during study with comparison site (Srinivasan 2011). The comparison site, also referred to the control site and will be used in the following content to avoid confusion, is an untreated (without QWS deployed) active work area and similar to the treatment (with QWS deployed) site used to account for changes in crashes unrelated to the treatment such as time and traffic volume changes.

The identified control site will be used to calculate the comparison ratio (r) of the observed crash frequency in the during-construction period ($N_{obs, C, D}$) to that in the before period ($N_{obs, C, B}$) to illustrate how crash counts are expected to change within the construction zone in the absence of QWS deployed. This comparison ratio (r) is determined by Equation 3-1.

$$r = N_{obs, C, D} / N_{obs, C, B} \quad \text{(Eq. 3-1)}$$

The parameters involved in the following equations are described in detail below:

$N_{exp, T, D}$: the expected crash number for the treatment site with no treatment applied (work zone without QWS) during construction

$N_{obs, T, D}$: the observed crash number for the treatment site (work zone with QWS) during construction

$N_{obs, T, B}$: the observed crash number for the treatment site (work zone with QWS) before construction

$N_{obs,\ C,\ B}$: the observed crash number for the control site (work zone without QWS) before construction

$N_{obs,\ C,\ D}$: the observed crash number for the control site (work zone without QWS) during construction

The comparison ratio is then multiplied by the observed crash frequency before construction ($N_{obs,\ T,\ B}$) at the treatment site to provide an estimate of the expected crashes for the treated site if no QWS was applied. This expected crash number ($N_{exp,\ T,\ D}$) can be obtained using the Equation 3-2, where the expected crashes can be used to compare to the observed crashes during construction at the treatment site to evaluate the safety effect of the treatment (Gross 2010).

$$N_{exp,\ T,\ D} = N_{obs,\ T,\ B} * r \quad \text{(Eq. 3-2)}$$

Equation 3-3 was utilized to estimate variance of the expected crashes for the purpose of improving CMF's accuracy.

$$Var\ (N_{exp,\ T,\ D}) = (N_{exp,\ T,\ D})^2 * (1/N_{obs,\ T,\ B} + 1/N_{obs,\ C,\ B} + 1/N_{obs,\ C,\ D}) \quad \text{(Eq. 3-3)}$$

The CMF then can be calculated as an approximation by dividing the during construction observed crash number for the treatment site ($N_{obs,\ T,\ D}$) and the expected number without treatment ($N_{exp,\ T,\ D}$), with the Equation 3-4 as shown below, to evaluate the safety effect of the treatment.

$$CMF = (N_{obs,\ T,\ D} / N_{exp,\ T,\ D}) / (1 + (Var\ (N_{exp,\ T,\ D}) / N_{exp,\ T,\ D}^{\ 2})) \quad \text{(Eq. 3-4)}$$

3.4 OVERVIEW OF CONTROL SITE (I-65)

As mentioned beforehand, the selection of available control sites was limited across the State. The research team coordinated with the Alabama Department of Transportation (ALDOT) to identify

a potential control site where no QWS was deployed within the work zone as well as a site for which the main features were similar to the treatment site such as work zone length, duration, and temporary traffic control (TTC) deployment, and ultimately selected a similar widening project on Interstate 65 (I-65) from Exit 238 to Exit 242 south of Birmingham, Alabama. A map of the control site is highlighted in Figure 3-2.

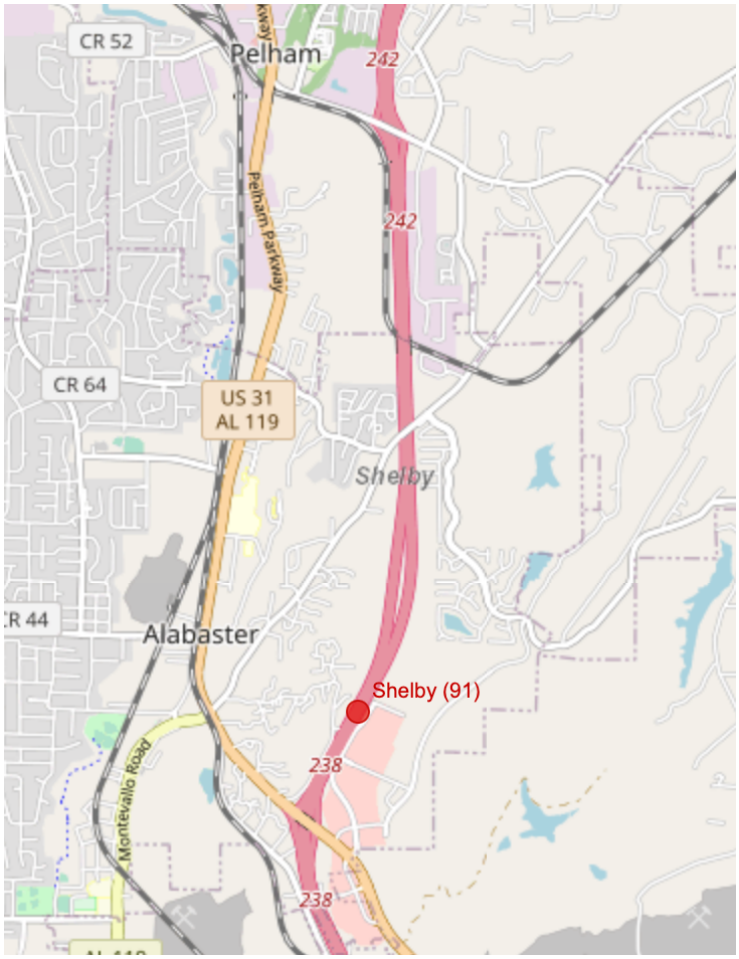

Figure 3-2: Overview of Control Site (I-65)
(Alabama Traffic Data Manager 2020)

The I-65 widening project, also referred to the control site, started in March 2018 and ended in December 2019 for a total duration of approximately 22 months, similar to the treatment site. During the construction period, the temporary concrete barriers were installed throughout the

entire length of the project from milepost 237.56 to milepost 241.80 with various access points for trucks and contractor's equipment to gain access to the work zone. As with the treatment site, lane closures were not permitted at the control site, since the purpose of this widening project was to expand from 4-lane to 8-lane in both directions and the only time that the interstate was permitted to be reduced to one lane in either direction was at night, and only when absolutely necessary. Therefore, generally, two lanes remained open in either direction during construction.

The key features between the selected control site and treatment site are listed as follows:

- Both have a project duration of 22 months;
- Both are widening projects without lane closure from 4-lane to 6-lane (treatment) and 8-lane (control) in both direction;
- Construction area length: 4.6 miles for treatment site, and 4.3 miles for control site;
- Temporal traffic control device: QWS and concrete barrier for treatment site, and concrete barrier only for control site;
- Major difference was found to be the difference in AADT before and during construction between treatment site ($AADT_{before}$ = 52,840; $AADT_{during}$ = 55,883) and control site ($AADT_{before}$ = 84,456; $AADT_{during}$ = 73,265) which will be discussed in detail in the following section.

3.5 TRAFFIC VOLUME DATA

The traffic volume data was collected from Alabama Traffic Data Manager (TDM) website maintained by ALDOT, as shown in Figure 3-3.

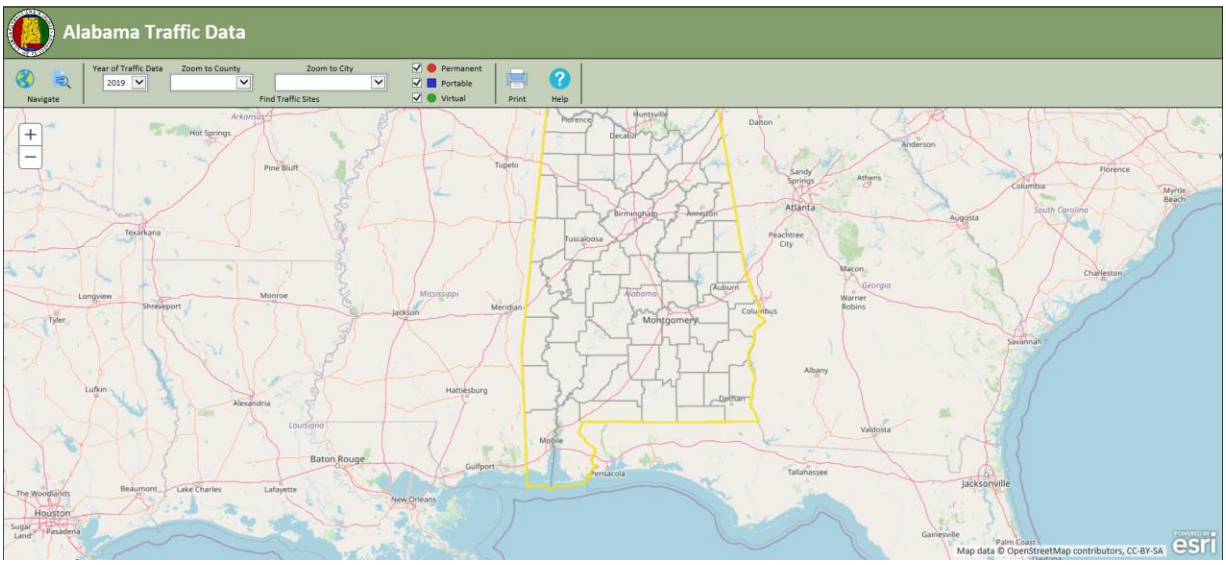

Figure 3-3: Traffic Data Manager (TDM) Map View
(Alabama Traffic Data Manager 2020)

Table 3-1 below summaries the annual average daily traffic (AADT) at the study sites from 2016 to 2019. Specifically, traffic volumes for the control site are from Continuous Count Station 91 (CCS# 91) located on I-65 near Exit 238 which can be found in Figure 3-2. As for the treatment site, since there is no permanent counter available within the work zone segment, the traffic volume for each study year was calculated by averaging the AADTs of two portable counters (Tuscaloosa 33 and Tuscaloosa 34) located within the work zone segment. An example of traffic volume information collection in 2019 is shown in Figure 3-4.

Table 3-1: Annual Average Daily Traffic (AADT) at Study Sites

	2016	2017	2018	2019
Control (I-65)	83,500	85,430	73,005	73,525
Treatment (I-59/I-20)	51,075	54,605	55,602	56,164

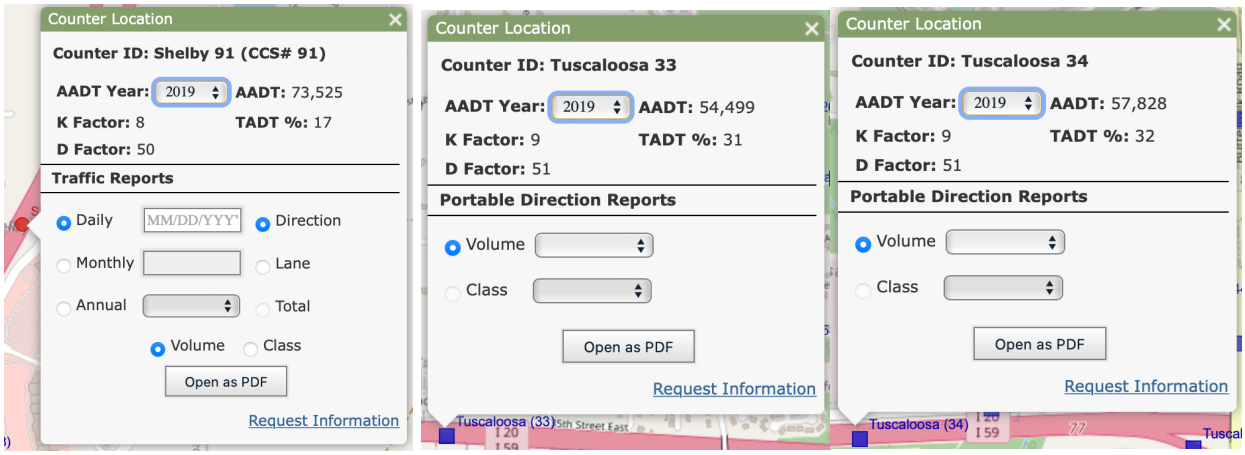

Figure 3-4: Traffic Volumes Information in 2019
(Alabama Traffic Data Manager 2020)

Since the methodology identified in this study to generate CMF was adjusted for an observational before-during study with comparison site, 2016 and 2017 AADT were combined as "before" construction period and data from 2018 to 2019 were combined as "during" construction period. The average traffic volumes after the combined years are summarized in Table 3-2.

Table 3-2: AADT in Before-During Period at Study Sites

	Before (2016-2017)	During (2018-2019)
Control (I-65)	84,465	73,265
Treatment (I-59/I-20)	52,840	55,883

3.6 CRASH DATA

As introduced before, the "during" construction period for both treatment and control site, I-59/I-20 project with QWS deployed and I-65 project without QWS deployed respectively, was from March 2018 to December 2019. Therefore, a same time span for both study sites was confirmed

from March 2016 to December 2017 as “before” construction period for the purpose of before-during CMF calculation.

Crash data for the before (March 2016 to December 2017) and during (March 2018 to December 2019) construction period mentioned above were collected from the Critical Analysis Reporting Environment (CARE) database maintained by the University of Alabama, which consists of traffic crash reports completed by corresponding law enforcement officers from Alabama. A statewide list of crash record of each year (2016 – 2019) were collected from CARE and then manually filtered to obtain the desired datasets. A series of filters such as County name, Month, Route name, crash type, and Milepost range etc. were created for the purpose of analysis. It should be noted that even though the lengths of work zone for both treatment and control site ranges are between milepost 72.61 – 77.15 and milepost 237.56 – 241.80, respectively, the exact number of 72.6 – 77.2 resulted in a 4.6 mi corridor for treatment site and 237.5 – 241.8 resulted in a 4.3 mi segment for control site were applied in the filter function for the purpose of covering entire project length.

In the literature review effort for the topic of QWS presented in Chapter 2, the most impacted crash types by QWS implementation were identified as rear-end crashes and sideswipe-same-direction crashes, therefore, only these two crash types were considered for filtering crash records. Meanwhile, only those crashes occurred on the freeway main segment within the identified milepost ranges were counted in the later process of CMF calculation, in other words, in CARE, the filter function of “Intersection Related” was selected as “No”. Table 3-3 below summarizes the crash number of study sites in the before and during construction period.

Table 3-3: Crash Number at Study Sites from CARE

	Before (2016-2017)	During (2018-2019)
Control (I-65)	76	113
Treatment (I-59/I-20)	49	143

3.7 DATA ANALYSIS AND RESULTS

Since the treatment site for this study (work zone with QWS deployed) on Interstate 59/Interstate 20 (I-59/I-20) was expanded from 4 to 6 lanes in both directions, there is one major difference that the control site (work zone without QWS deployed on I-65) resulted in an 8-lane highway from a 4-lane highway in both directions. After carefully examined and compared the relevant datasets including work zone data (e.g., work zone location, length of the work zone, and work zone duration), road geometric and traffic data (e.g., traffic volume, speed limit), as well as crash data involved (e.g., crash type, severity) (Edara et al. 2020), and identified that the main effect of this difference on crash frequency used for CMF calculation was the difference in traffic volume.

To address the impact of traffic volume difference on crash frequency, the number of crashes per year at the two study sites were adjusted using the crash rate formula expressed in Equation 3-5 to calculate crashes per 100 million vehicle-miles of travel (Golembiewski 2011). It is important to note that the length of each study site for analysis was 4.3 miles for I-65 and 4.6 miles for I-59, calculated from each milepost range mentioned before, to represent work zone length L in the following equation.

$$R = \frac{C \times 100{,}000{,}000}{V \times 365 \times N \times L} \quad \text{(Eq. 3-5)}$$

Where,

R: Crash rate for the road segment expressed as crashes per 100 million vehicle-miles of travel,

C: Total number of roadway departure crashes in the study period,

V: Traffic volumes using Average Annual Daily Traffic (AADT) volumes,

N: Number of years of data,

L: Length of the roadway segment in miles,

Table 3-4 summarizes the calculated crash rate of study sites in the before and during construction period, in which the raw crash numbers are from Table 3-3. Comparison ratio (r) for the control site was also calculated to be 1.71 using crash rate during construction divided by the crash rate in the before period as illustrated in Equation 3-1 of methodology section.

Table 3-4: Crash Rate at Study Sites

	Before (2016-2017)	**During (2018-2019)**	**Comparison Ratio**
Control (I-65)	31	54	1.71
Treatment (I-59/I-20)	30	83	

By applying Equation 3-2 to Equation 3-4 to the crash data in Table 3-4, the results as well as the calculated CMF can be found in Table 3-5.

Table 3-5: Crash Rate at Study Sites

$N_{exp, T, D}$	Var ($N_{exp, T, D}$)	CMF
52	224	1.49

To obtain a more precise estimate for conclusion, the variance of CMF, the standard error (SE) of the CMF, along with a 95% confidence interval can be calculated using the following equations (Gross et al. 2010).

$$\text{Variance (CMF)} = CMF^2[(1/N_{obs,\,T,\,D})+(Var(N_{exp,\,T,\,D})/N_{exp,\,T,\,D}^2)] / [1+(Var(N_{exp,\,T,\,D})/N_{exp,\,T,\,D}^2)]^2$$

$$= 1.49^2 * [(1 / 83) + (224 / 52^2)] / [1 + (224 / 52^2)]^2$$

$$= 0.18$$

$$\text{SE (CMF)} = \text{SQRT (0.18)} = 0.424$$

$$95\%\ CF = 1.49 \pm 1.96 * 0.424 = [0.654, 2.317]$$

Even though it can be concluded that the CMF estimate of 1.49 indicates that QWS deployment in freeway work zone results in a 49% increase in the number of rear-end and sideswipe-same-direction associated crashes, in this case, the 95% confidence interval is 0.654 to 2.317, which cannot be stated with 95% confidence that the true value of CMF is not 1.0. Specifically, it cannot be concluded with 95% confidence that this treatment has any effect, which seems to be reasonable because of differences exist under different work zone conditions. Most importantly, since the calculated CMF only used traffic data from 1 treatment site and 1 control site, the validity of this value is questionable.

In order to make the safety performance analysis more comprehensive, the impact of QWS deployment on crash reduction of study sites will be evaluated using crash numbers from the aforementioned same filtering process except for unselecting rear-end and sideswipe-same-direction to include all crash types. All types of crash number from CARE are summarized in Table 3-6.

Table 3-6: All Types of Crash Number at Study Sites from CARE

	Before (2016-2017)	During (2018-2019)
Control (I-65)	195	228
Treatment (I-59/I-20)	234	368

To address the difference in traffic volume, Equation 3-5 was applied again and the corresponding crash rate for each are calculated as shown in Table 3-7.

Table 3-7: All Types of Crash Rate at Study Sites

	Before (2016-2017)	During (2018-2019)
Control (I-65)	80	108
Treatment (I-59/I-20)	144	214

The crash increase percentage of control site when no QWS deployed was calculated to be 27% as shown in Table 3-8, in which 39% and 50% represent the proportion of rear-end (RE) and sideswipe-same-direction (SS) in all crash types in the before and during construction period, respectively.

Table 3-8: Control Site Crash Increase Percentage

Control	ALL Type	RE & SS	Percentage
Before	80	31	39%
During	108	54	50%
			27%

The crash increase percentage of treatment site when QWS in-place was calculated to be 86% as shown in Table 3-9, in which 21% and 39% represent the proportion of rear-end (RE) and

sideswipe-same-direction (SS) in all crash types in the before and during construction period, respectively.

Table 3-9: Treatment Site Crash Increase Percentage

Treatment	ALL Type	RE & SS	Percentage
Before	144	30	21%
During	214	83	39%
			86%

From the above two tables, it can be concluded that in this study, the percentage of increased rear-end and sideswipe crashes at the control site (without QWS) was less than that at the treatment site (with QWS). Even though this result can support the developed site-specific CMF indicating that QWS results in an increase in the rear-end and sideswipe-same-direction associated crashes, an important limitation is that the same site was not used for control and treatment, and this study only includes 1 control site and 1 treatment site and therefore the transferability of the developed CMF to other possible deployments is limited.

CHAPTER FOUR: TRAFFIC SIMULATION EVALUATION

4.1 INTRODUCTION

The purpose of this study was to present a comprehensive analysis of the safety and mobility impacts of queue warning system (QWS) deployed in Alabama work zones, in which the safety evaluation of the QWS on the basis of crash frequency analysis has been addressed in detail in Chapter 3, with a positive conclusion that the deployment of QWS under Alabama freeway work zone conditions has the ability to help reduce rear-end and sideswipe-in-same-direction crashes. To support the safety evaluation results from Chapter 3 and visually analyze the effectiveness of QWS on traffic flow, this chapter introduces the process of developing, calibrating, and validating a series of traffic microsimulation models in greater detail with a purpose of being able to replicate traffic operations observed in the field work zone area.

Based on the previous literature studies as presented in Chapter 2, traffic simulation tools such as QuickZone, FREVAL-WZ, CORSIM, and VISSIM have been developed and widely used by researchers and agencies for the purpose of analyzing relative traffic performance measures. While there are many traffic simulation software packages available, in this study, VISSIM was chosen to be utilized to develop a series of traffic simulation models with an aim of evaluating the mobility impacts of QWS deployment.

To start with the analysis, a brief overview of the study site along with the location of key sensors utilized for the data analysis is described (a detailed description of the study site can be found in Chapter 3). The methodology summarized from the literature review effort and relevant data analysis are discussed in significant detail and then applied to the VISSIM model development, calibration, and validation. Lastly, a series of sensitivity analyzes focusing on the

selected measures of effectiveness (MOEs), including travel time, vehicle delay, and queue length, are compared and evaluated between the simulated models of base condition and incident condition.

4.2 OVERVIEW OF STUDY SITE (I-59/I-20)

As introduced in Chapter 3, the I-59/I-20 widening project just south of Tuscaloosa, Alabama, resulting in a 6-lane highway from a 4-lane highway with a total construction period of approximately 22 months (March 2018 to December 2019), was ultimately selected as ALDOT's initial deployment of a queue warning system (QWS) in work zones and was used as the study site for the purpose of this research. Figure 4-1 shows the construction layout of the study site along with the location of key sensors utilized for relevant traffic data extraction and analysis, specifically the sensors used as part of the QWS are side-fire microwave radar sensors. A complete project location map from ALDOT construction plans for this project can be found in Appendix A.

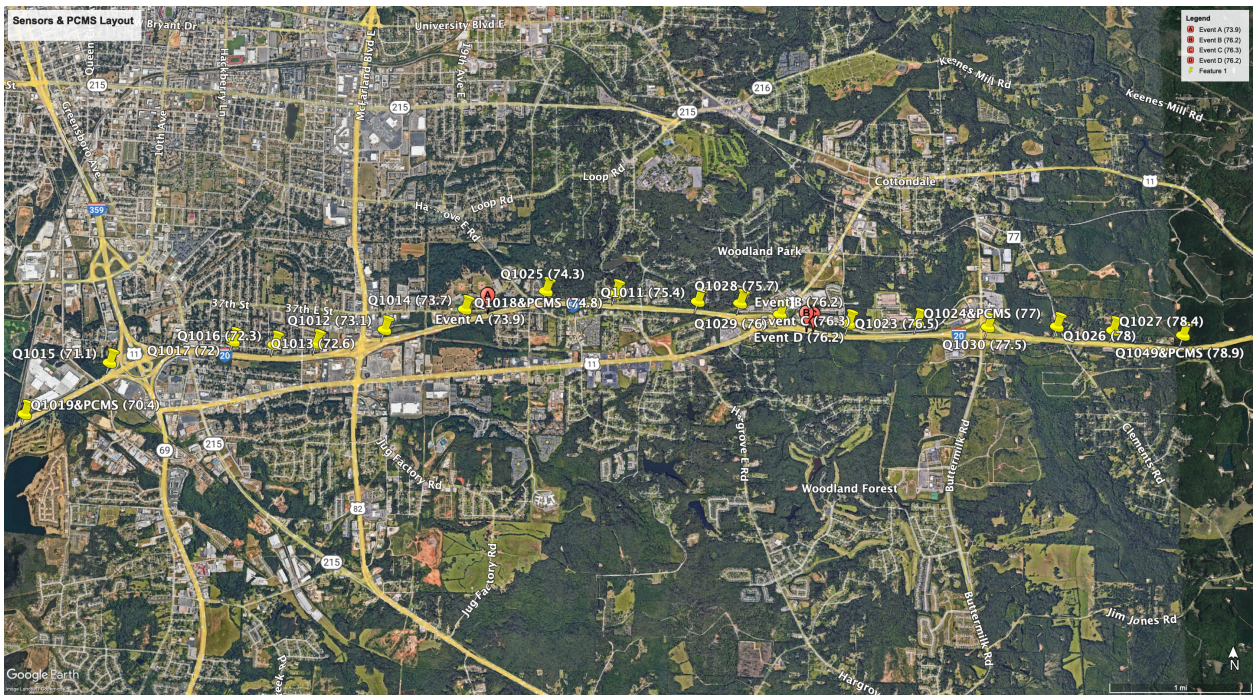

Figure 4-1: Study Site Overview (I-59/I-20)

4.3 METHODOLOGY

A major task of this research was to develop a series of traffic simulation models with the ability to replicate field-observed work zone traffic operation under specific situations to estimate the effect of QWS on traffic flow parameters within the freeway work zone. For this purpose, four incidents that occurred within the work zone during construction were identified and relevant traffic data for each incident were collected and processed to be utilized for the purpose of developing a traffic simulation model under incident condition. In order to intuitively evaluate the impacts of QWS on traffic flow after an incident, based on the evaluation of MOEs such as travel time, vehicle delay, and queue length, a base condition simulation model for each incident scenario was developed first and then calibrated to replicate traffic conditions observed in the field by comparing the simulated distribution of vehicle speed to the field observed speed distribution. Then, the incident condition simulation models were able to be developed associated with each

calibrated base condition scenario using the same network and calibrated parameters but different traffic inputs. Based on the literature studies, a logic flowchart developed by Tufuor et al. (2022) for the purpose of simulation model development and calibration is presented in Figure 4-2.

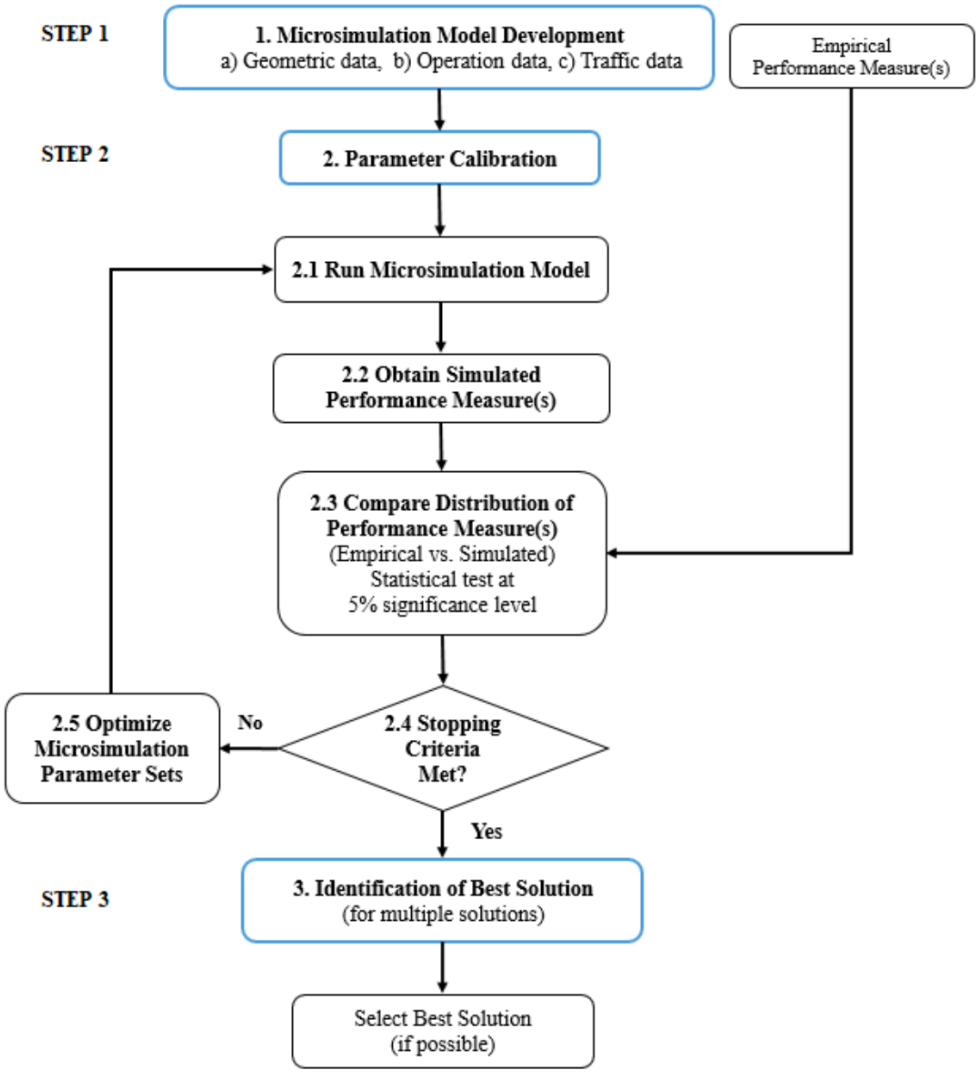

Figure 4-2: Logic Flowchart for VISSIM Model Development and Calibration (Tufuor et al. 2022)

As can be seen in Figure 4-2, three major steps were considered for the simulation model development, calibration, and validation. To start with the base condition model development,

work zone-related data such as study site geometry and traffic data (speed and volume), as well as relevant traffic operation data are needed to be collected and processed first for the purpose of preparing for the model development. Additionally, field-collected performance measures such as traffic flow and speed need to be conducted to evaluate the quality of the developed simulation models, and also to be utilized in the calibration process. Step 2 emphasizes the calibration of the model under base condition, which mainly focuses on the calibration of the driver-behavior parameters. Although different literatures suggested different parameters to be calibrated, it was determined in this study that the simulated models were able to acceptably replicate field-observed conditions by modifying three main parameters which are CC0 (desired standstill distance), CC1 (desired time headway) and the desired truck acceleration (Jehn and Turochy 2019). To achieve a well-calibrated simulation model, this process was in need to be iteratively performed until obtain an acceptable set of parameters to be utilized in step 3.

4.4 DATA COLLECTION, SCREENING, AND PROCESSING

Data collection effort was performed based on the associated information of identified incidents which will be introduced in detail below. From previous studies summarized in Chapter 2, rear-end crashes were considered to be the most frequent types of crashes due to the presence of a work zone. For the purpose of this study, a review of the crash database (named CARE, utilized in Chapter 3 as well) was conducted and ultimately identified four rear-end incidents that took place within the work zone during construction period (March 2018 to December 2019).

Specifically, incident A, at milepost (MP) 73.9, occurred on the southbound of I-59/I-20 at 22:30 on October 23,2018.

Incident B (MP 76.2) and C (MP 76.3) were recorded on November 26, 2019, at 14:10 and 17:45, respectively, on I-59/I-20 northbound.

Incident D (MP 76.2) was reported on March 19, 2019, at 13:33, northbound of I-59/I-20.

After identified the time and location of each incident, it was necessary to determine the time range and mileage affected by the corresponding incident according to the traffic data collected by the roadside sensors. In this project, side-fire microwave radar sensors were utilized to collect traffic volume and speed.

An extensive data review effort was performed and relevant affected sensors and time span were confirmed for the purpose of preparing for the simulation models development. Figure 4-3 shows an overview of each incident location along with the roadside sensor locations, as well as the entire length used for the simulation model development. Specifically, detailed field data analysis associated with each event, which represents a combination of base condition and incident condition, is described in the remaining portion of this section. It is noteworthy that data review also found that volumes on each side of interchange collected by sensor Q1028 and Q1029 were similar, therefore, the effect of ramps was not considered in the simulation model development.

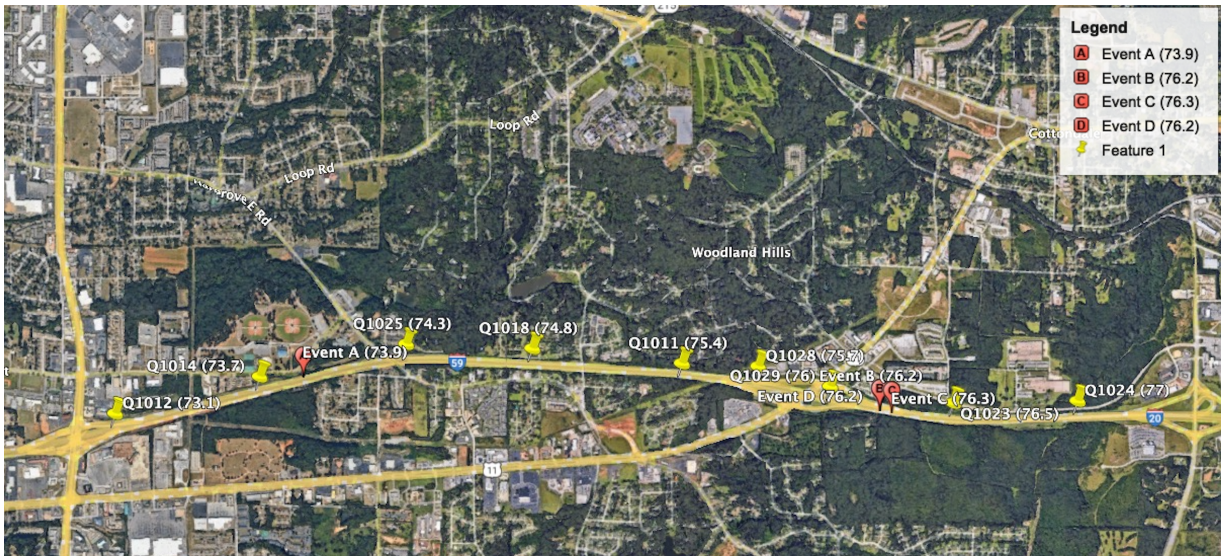

Figure 4-3: Overview Layout of Incidents and Roadside Sensor Locations

4.4.1 Field Data Analysis of Event A (Base vs. Incident Condition)

Specifically, Figure 4-4 presents a detailed layout related to event A, where the red triangle represents the approximate location of incident A. It is worth mentioning that each sensor was deployed outside of lane 1 (outside lane).

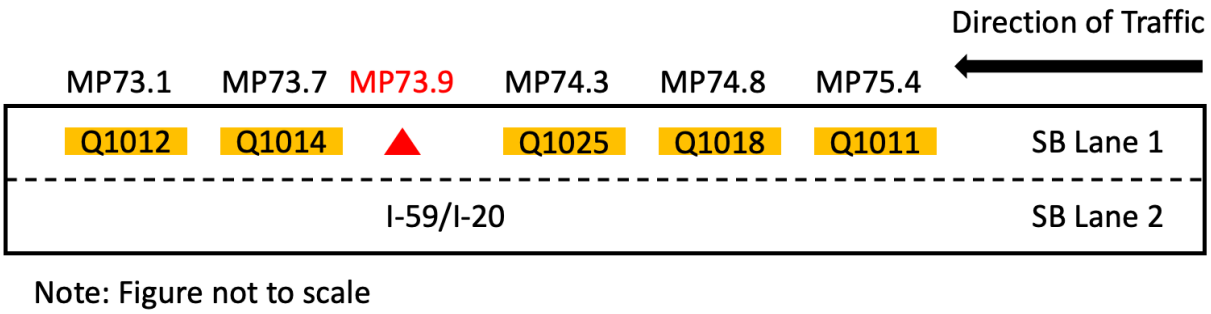

Figure 4-4: Layout of Event A

Under incident condition, data review of upstream and downstream sensors revealed that only the first upstream sensor Q1025 has a speed reduction recorded after the incident happened (22:30). As shown in Figure 4-5, the speed returned to normal around 23:15 for both lane 1 (southbound outside) and lane 2 (southbound inside). While passing the location of upstream second sensor Q1018 after incident occurred, upstream drivers can still operate at a normal speed as shown in Figure 4-6, which means the queue did not extend to this location.

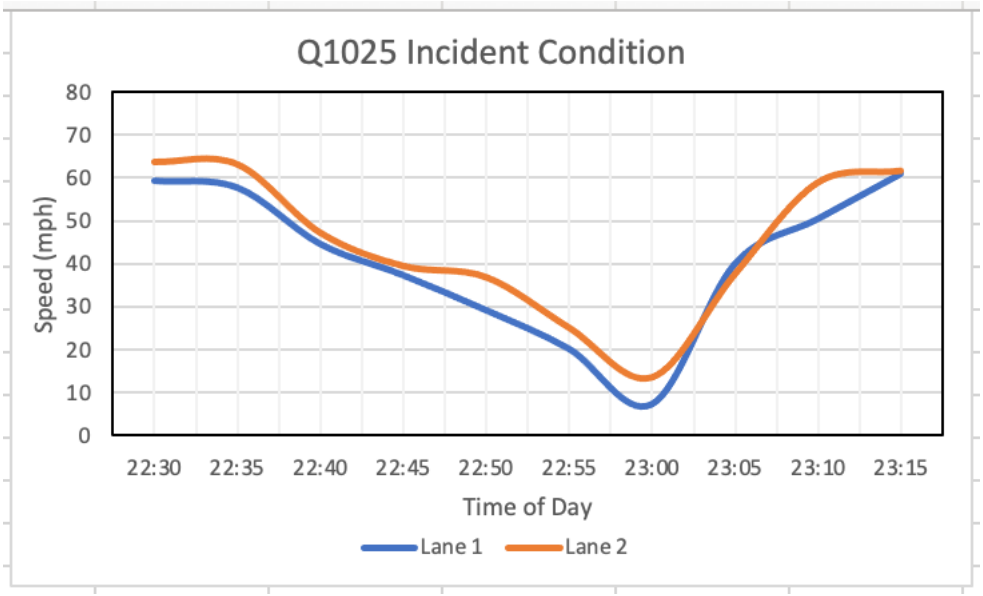

Figure 4-5: Affected Sensor Q1025 and Time Span of Incident A

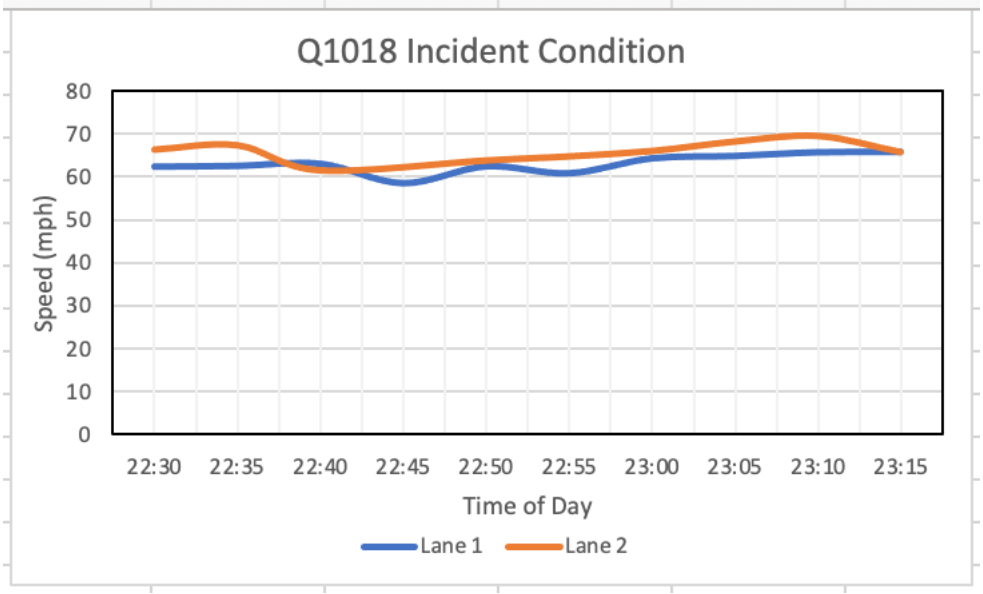

Figure 4-6: Non-Affected Sensor Q1018 and Time Span of Incident A

Even though there was only one sensor recorded a speed reduction, for the simulation purpose, three sensors upstream (Q1025, Q1018, Q1011) and two sensors downstream (Q1014

and Q1012) of the incident location were selected as shown in Figure 4-4 and the location of each sensor will be coded as a data collection point in the simulation models.

For the purpose of developing a base condition simulation model, based on the incident date (Tuesday on 10/23/2018), four Tuesdays (8/28/2018, 9/25/2018, 10/9/2018, and 10/16/2018) were randomly selected in the three months prior to the incident, and traffic data of each Tuesday were extracted from the five relevant sensors as mentioned beforehand. In order to create a robust dataset with minimal bias as input for simulation model development, these four Tuesdays of traffic data from each sensor were averaged to be representative of a base condition.

Based on a previous incident data review effort, the time window for both base and incident model simulations were determined to be from 21:00 to 24:00 for a total of 3-hour period as the incident occurred at 22:30. Figure 4-7 and Figure 4-8 show examples of field observed base condition speed trajectory from the first sensor Q1025 just upstream of the incident location and the second sensor Q1018 upstream of Q1025, respectively. It should be noted that the base condition speed trajectory for each sensor will be used for comparison with the simulated base condition distributions of selected traffic metrics for the purpose of model calibration.

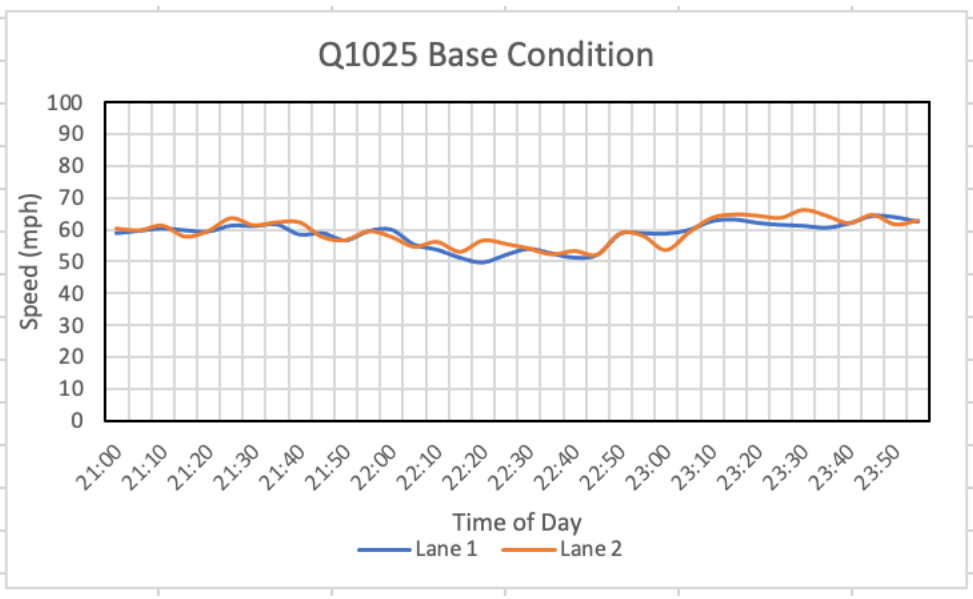

Figure 4-7: Sensor Q1025 Base Condition Speed Profile

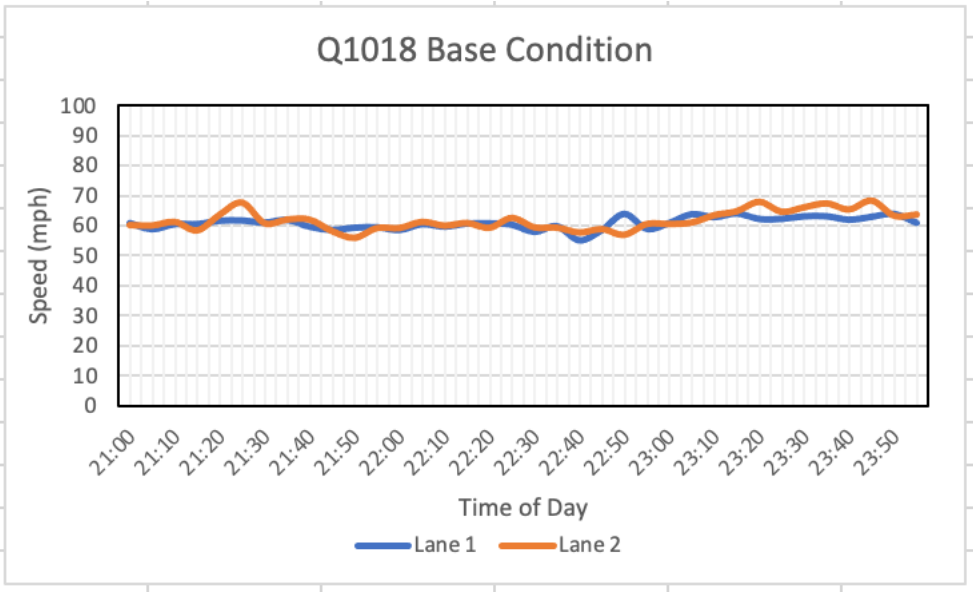

Figure 4-8: Sensor Q1018 Base Condition Speed Profile

4.4.2 Field Data Analysis of Event B&C (Base vs. Incident Condition)

Since incident B and C took place on the same day (11/26/2019) with 3 hours apart and close to each other, they were combined for analysis and simulation model development. Figure 4-9 shows the detailed layout associated with event B and event C, where the red triangle represents the approximate location of incident B&C.

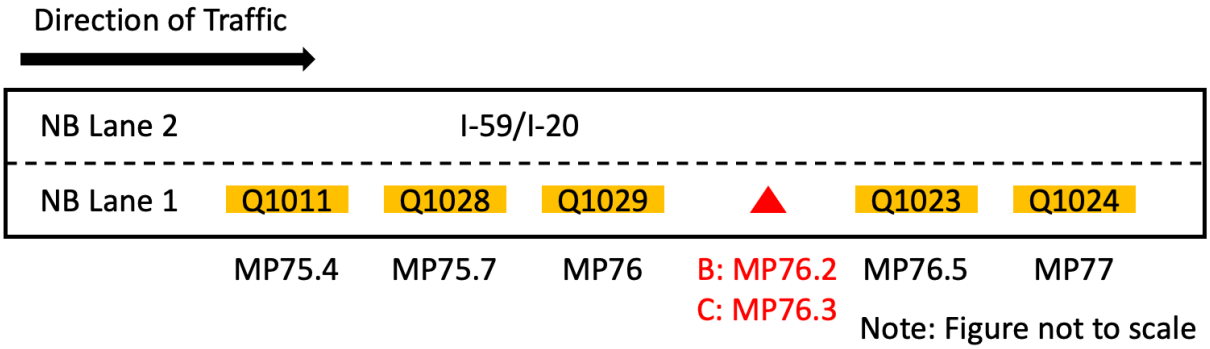

Figure 4-9: Layout of Event B&C

Following the same data review process as incident A, it was found that the recorded speed reductions extended to the second sensor Q1028 upstream of the incident location, but not to the third sensor Q1011 upstream.

As can be seen from Figure 4-10, the speed dropped below 10mph right after incident B (14:10) occurred and took about 90 minutes to returned to normal. The same phenomenal can be observed for incident C which occurred at 17:45. The speed recorded from sensor Q1028 reduced immediately after the incident and lasted for about an hour before returning to normal. In Figure 4-11, the speed trend from sensor Q1011 illustrates that traffic flow was not affected by the downstream incidents.

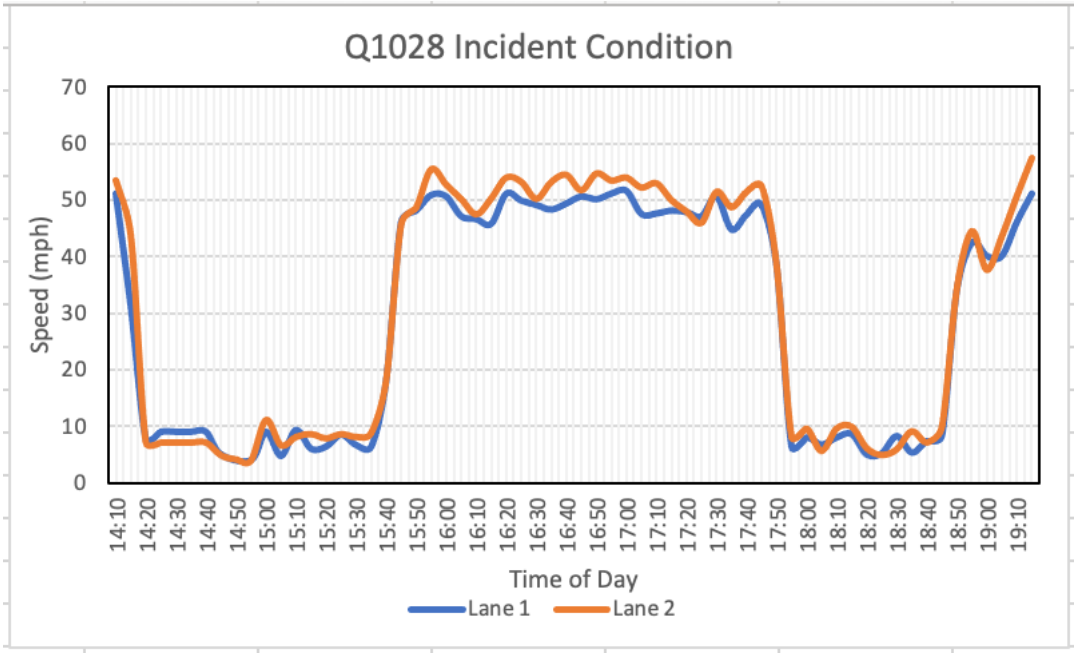

Figure 4-10: Affected Sensor Q1028 and Time Span of Incident B&C

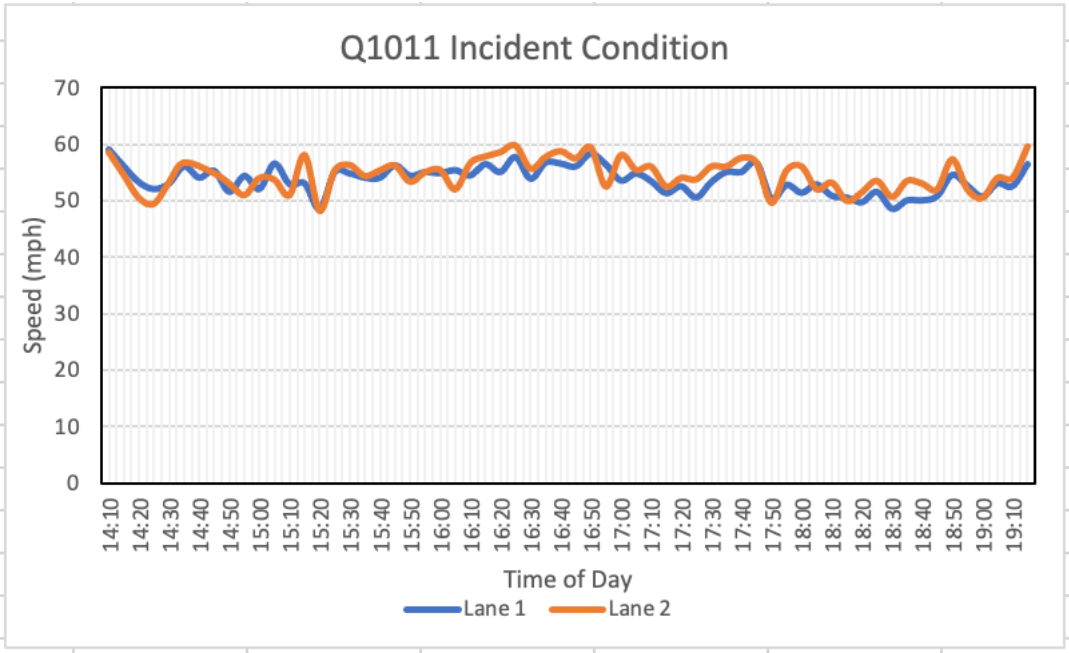

Figure 4-11: Non-Affected Sensor Q1011 and Time Span of Incident B&C

As with event A, for event B&C, three sensors upstream (Q1029, Q1028, Q1011) and two sensors downstream (Q1023 and Q1024) of the incident location were selected as noted in Figure 4-9 with the purpose of coding data collection points in VISSIM. The same process of date identification along with data collection were performed in preparation for the development of a base condition simulation model.

According to a previous review of incident-related data, a total of 6 hours analysis window from 13:45 to 19:45 capable of covering both incident B and incident C was confirmed for both base and incident simulation model development. Examples of field observed base condition speed trajectory for sensor Q1028 and sensor Q1011 are provided in Figure 4-12 and Figure 4-13, respectively. As mentioned beforehand, the field observed speed trend under base condition will be utilized for the simulated base condition model calibration by comparing to the simulated speed distributions.

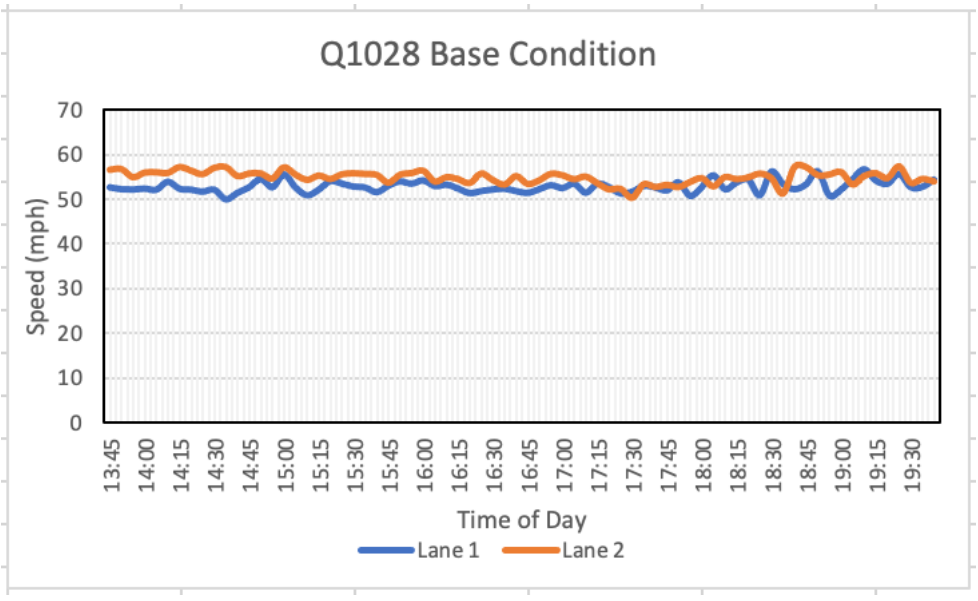

Figure 4-12: Sensor Q1028 Base Condition Speed Profile

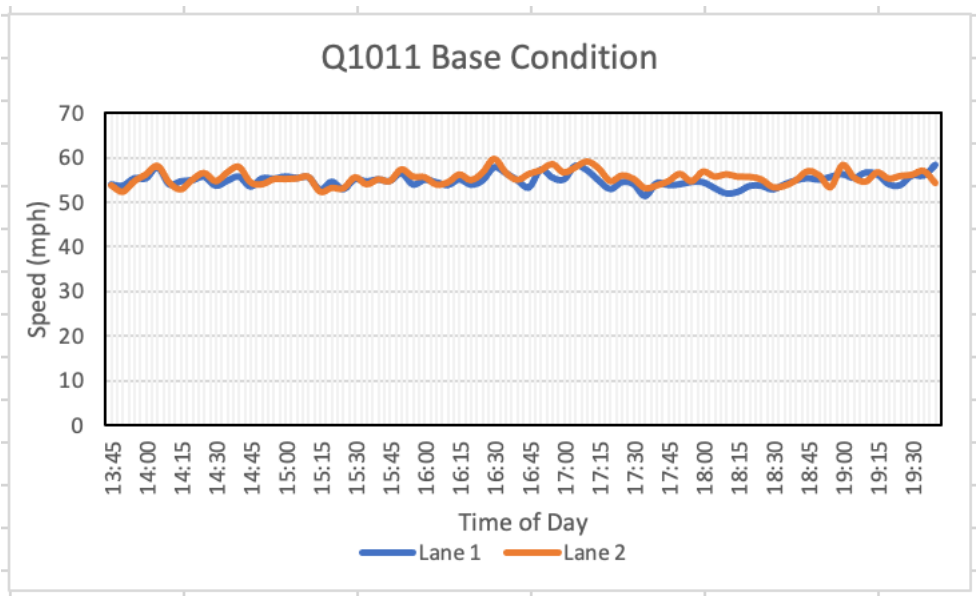

Figure 4-13: Sensor Q1011 Base Condition Speed Profile

4.4.3 Field Data Analysis of Event D (Base vs. Incident Condition)

Since incident D was reported from the same location as incident B (MP 76.2), same layout including both incident (marked as a red triangle) and associated sensor locations is given in Figure 4-14. The selected three sensors upstream and two sensors downstream of the incident location will be utilized for coding data collectors in VISSIM.

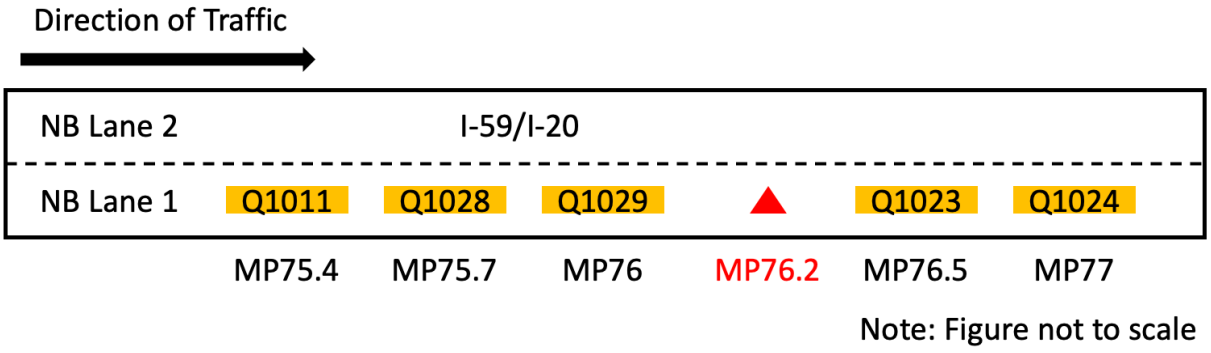

Figure 4-14: Layout of Event D

After reviewing field data related to the incident, it was found that the recorded speed reductions extended to the second sensor Q1028 upstream of the incident location as well but not to the location of upstream third sensor Q1011, as shown in Figure 4-15 and Figure 4-16.

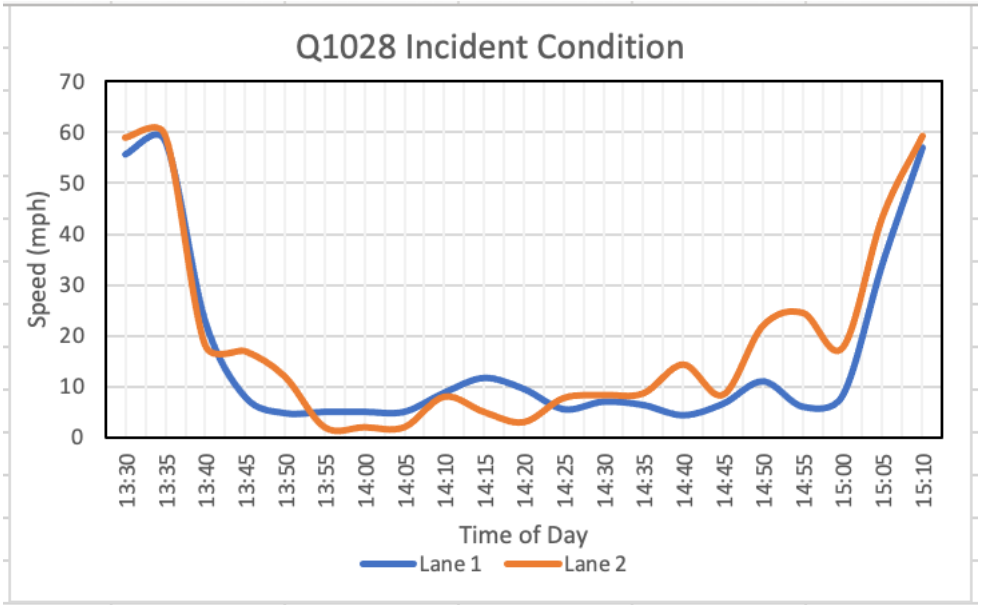

Figure 4-15: Affected Sensor Q1028 and Time Span of Incident D

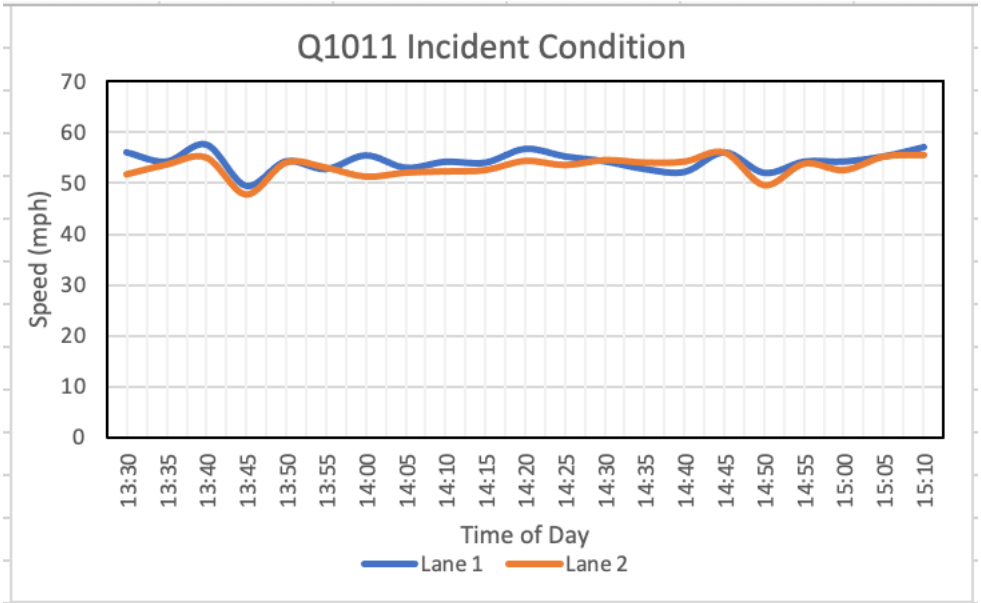

Figure 4-16: Non-Affected Sensor Q1011 and Time Span of Incident D

From Figure 4-15, it can be observed that the speed reduced to around 10mph after incident D (13:33) occurred and took about 80 minutes to back to normal for both lane 1 (northbound outside) and lane 2 (northbound inside). The speed trend from Figure 4-16 indicated that driver behaviors were not affected by the downstream incident.

To prepare for the development of a base condition simulation model, the same data processes as for the other incidents were conducted to obtain an averaged Tuesday traffic data for each sensor. Based on the incident data, a total of 3 hours analysis window from 13:00 to 16:00 was identified for both base and incident simulation models. Figure 4-17 and Figure 4-18 show examples of field collected speed trajectory under base condition from sensor Q1028 and Q1011, respectively. The field observed base condition speed trajectory will be used to calibrate the simulated base condition model as mentioned beforehand.

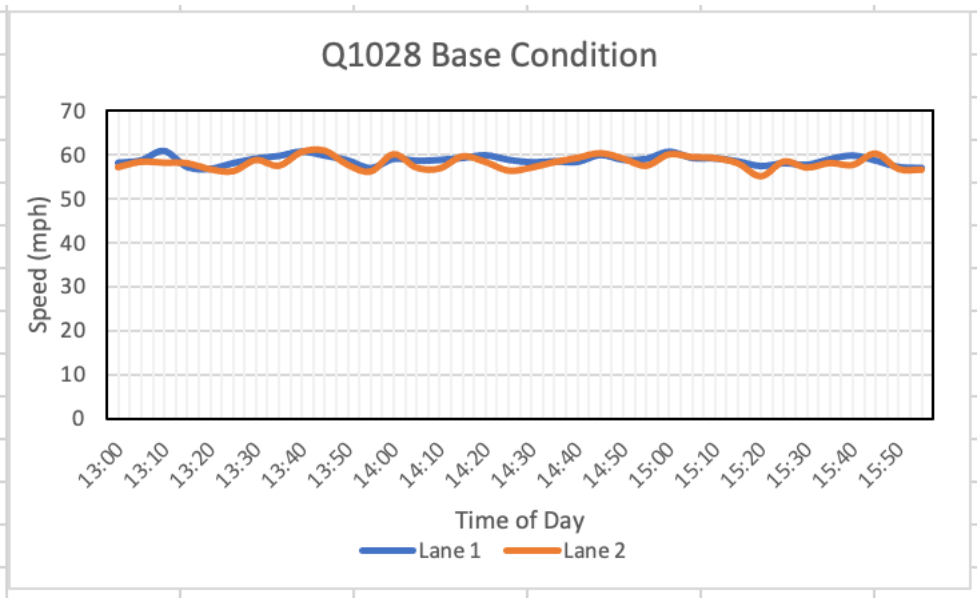

Figure 4-17: Sensor Q1028 Base Condition Speed Profile

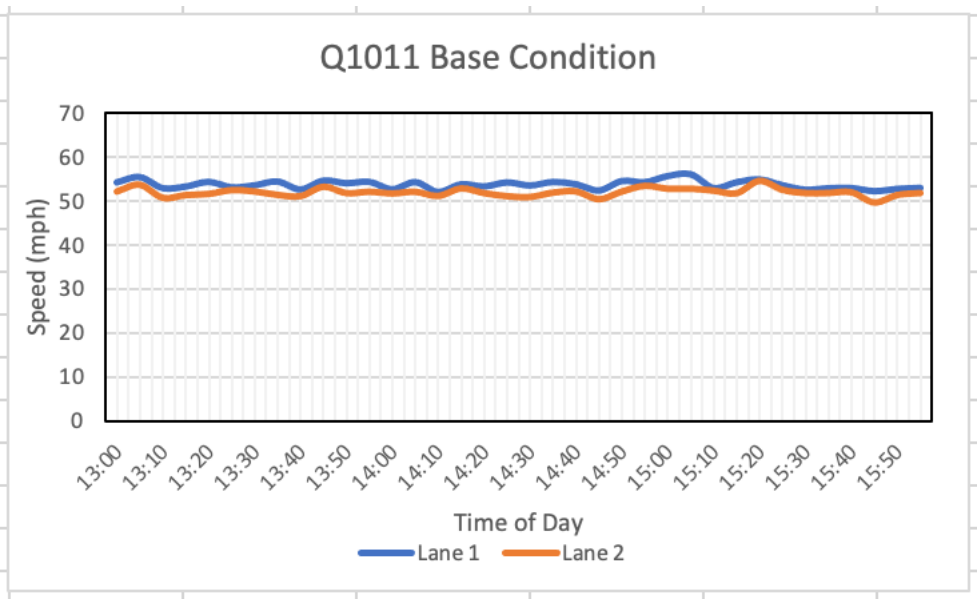

Figure 4-18: Sensor Q1011 Base Condition Speed Profile

4.5 VISSIM MODEL DEVELOPMENT, CALIBRATION, AND VALIDATION

The following subsections present procedures for the development of VISSIM simulation models in detail. Specifically, three sets of six different models were developed and analyzed separately based on the incident characteristics.

4.5.1 Event A: Base Condition vs. Incident Condition

a. Basic Network Creation

The first step in the VISSIM network development process was the creation of basic geometric elements specific to the event A condition since only incident A took place on the southbound direction of the study work zone (I-59/I-20). As mentioned beforehand, this widening project expanded from a 4-lane highway to a 6-lane highway and the only time that interstate was permitted to be reduced to one lane in either direction was at night or when necessary to move equipment or traffic control devices. Therefore, two lanes, with no lane closures, of the study site were generated in VISSIM with the use of embedded maps. It is noteworthy that both base condition and incident condition simulation models, herein collectively assigned to event A, share the same road network but different field-gathered inputs.

A sample drawing of the road network layout of event A is provided in Figure 4-19. It may be noticed that the drawing only represents a general layout related to event A and does not describe the horizontal curvature found at the site.

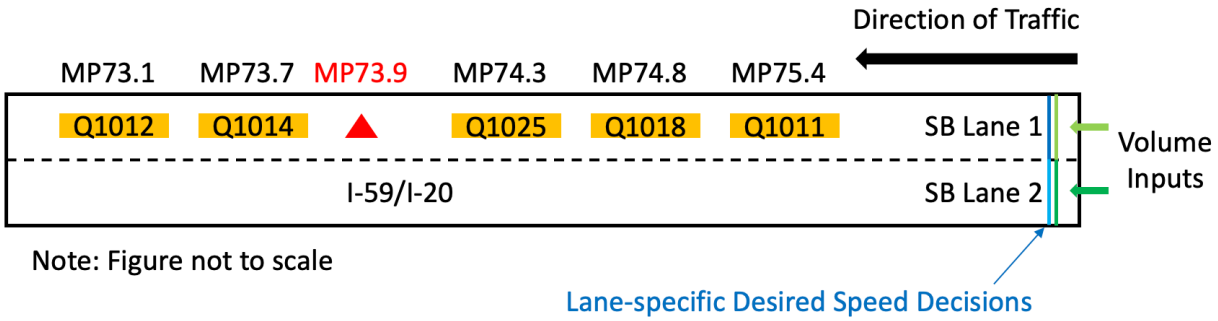

Figure 4-19: Road Network Layout of Event A

From Figure 4-19, it should be noted that the key components such as volume inputs, lane-specific desired speed decisions, and sensor locations were included in the drawing for the purpose of coding the basic network. Specifically, the location of each sensor set up in the field was coded as a data collection point in VISSIM, with the aim of calibrating the base condition simulation model by comparing the simulated traffic data such as vehicle flow and speed with the field-observed traffic data from each sensor. Each of the key components will be discussed in more detail in the following sections.

b. Volume Inputs and Vehicle Compositions

As discussed earlier, traffic data, including volume and speed, under base condition for each sensor was obtained from the averaged four Tuesdays. For the incident condition, traffic data was extracted from the day the incident occurred. Referring to Figure 4-19, traffic volume data from the farthest sensor Q1011 upstream of the incident location was utilized as inputs introduced at the beginning of the road network in VISSIM. For volume input purposes only, recorded traffic volumes from other sensors were not considered since it was assumed traffic volumes would not change while driving through the road network once the simulation was run.

Based on the time of the incident (22:30) and the review of incident-related data, a total of 3-hour time period from 21:00 to 24:00 was identified to be the analysis window for simulation as discussed beforehand. In addition, a 15-minute period from 20:45 to 21:00 was added to the analysis time window as a warm-up period for the simulation model to reach equilibrium. Examples of volume inputs at 5-minute intervals for the first hour of simulation under base condition and incident condition are provided in Table 4-1 and Table 4-2, respectively, and the full datasets can be found in Appendix B.

Table 4-1: Example of Base Condition Volume Inputs in VISSIM for Event A

Time	Raw Volumes (RL)	Flow Rates, vphpl (RL)	Raw Volumes (LL)	Flow Rates, vphpl (LL)
20:45	30	360	31	372
20:50	22	264	21	252
20:55	26	312	30	360
21:00	37	444	34	408
21:05	27	324	22	264
21:10	30	360	24	288
21:15	23	276	33	396
21:20	35	420	29	348
21:25	38	456	39	468
21:30	29	348	32	384
21:35	39	468	41	492
21:40	28	336	47	564

Table 4-2: Example of Incident Condition Volume Inputs in VISSIM for Event A

Time	Raw Volumes (RL)	Flow Rates, vphpl (RL)	Raw Volumes (LL)	Flow Rates, vphpl (LL)
20:45	48	576	39	468
20:50	23	276	15	180
20:55	31	372	25	300
21:00	43	516	27	324
21:05	37	444	33	396
21:10	21	252	13	156
21:15	21	252	37	444
21:20	22	264	23	276
21:25	30	360	47	564
21:30	55	660	38	456
21:35	31	372	27	324
21:40	35	420	22	264

From Tables 4-1 and 4-2, it should be noted that the way each sensor records data is lane-specific, therefore, the abbreviations for RL (right lane) and LL (left lane) in the table represent the recordings of the sensor Q1011 in the southbound outside lane and the southbound inside lane, respectively. In addition, to convert the raw volume of vehicles from sensor Q1011 recorded in 300 second intervals, a multiplication factor of 12 was applied to each raw volume to obtain a volume input in vehicles per hour to be encoded in VISSIM. The same volume translation process was applied to the rest of simulation hours for both base and incident conditions and can be found in Appendix B.

After the vehicle volumes was created in VISSIM, the next step was to assign relative vehicle compositions to the lane-specific volume inputs. It should be noted that the sensors utilized in this study only have the ability to record traffic data such as vehicle speed and volume, and are not applicable for the classification of vehicles such as passenger cars, single-unit trucks, and heavy trucks. Therefore, a surrogate method, with an assumption that the vehicle class distribution

should not have changed significantly on the same corridor, was performed to define vehicle compositions with relative vehicle class proportions as inputs in VISSIM.

The research team coordinated with ALDOT and was able to obtain length-based vehicle volume data from a continuous count station 51 within the study site at milepost 78.1 for the month of May 2022. Since incident A occurred on a Tuesday, length-based traffic data from 5 Tuesdays in May, which are May 3rd, May 10th, May 17th, May 24th, and May 31st, were extracted and processed with the goal of obtaining average traffic data for each vehicle composition in each lane and then calculating the relative flow associated with each vehicle type which enter the simulation. An example of before-processed daily class report by lane in 1-hour intervals from midnight to 2:00am on the day of May 3rd is provided in Figure 4-20.

Daily Class Report by Lane for CCS 51

Day of Tuesday-05/03/2022

Direction:**NB/SB** Lane:**1-3** County:**Tuscaloosa**

Hourly Class Report

Hour Begins	Lane & Dir	Classes CL1	CL2	CL3	Lane Total
0:00am	Lane 1-NB	40	3	98	141
	Lane 1-SB	72	6	89	167
	Lane 2-NB	61	5	52	118
	Lane 2-SB	91	9	66	166
	Total	264	23	305	592
1:00am	Lane 1-NB	21	2	92	115
	Lane 1-SB	41	13	84	138
	Lane 2-NB	48	2	38	88
	Lane 2-SB	57	6	44	107
	Total	167	23	258	448

Figure 4-20: Example of Before-Processed Vehicle Class Report by Lane

From Figure 4-20, it should be noted that the length-based breakdown for each vehicle class is 0 – 27’ as class 1 (CL1), 27’ – 40’ as class 2 (CL2), and greater than 40’ as class 3 (CL3);

this approximates Passenger Vehicles (FHWA 1 – 3), Single-Unit Trucks (FHWA 4 – 7), and Combination-Unit Trucks (FHWA 8 – 13). In addition, since incident A occurred southbound (SB) of the study site, therefore, only traffic data belonging to the SB direction was utilized for the relative vehicle class proportion calculations. Specifically, the lane designations assigned are as follows, with Lane 1 being the outside lane for that given direction, and Lane 2 being the inside lane for that given direction.

Same as the simulation analysis time period as discussed in section 4.4.1, a total of 3 hours analysis window from 21:00 to 24:00 was determined to calculate average traffic data from 5 Tuesdays for each vehicle type on each lane. The aggregated average volume data along with the lane-based proportions for each vehicle class in the traffic stream are provided in Table 4-3 as inputs to be introduced to the base and incident condition simulation models in VISSIM.

Table 4-3: Aggregated Average Volume Data with Relative Vehicle Flow for Event A

	SB1_RL	SB2_LL
PC	357	100
HGV	206	6
SUT	21	2
Total	584	108
RelFlo_PC	0.61	0.93
RelFlo_HGV	0.35	0.06
RelFlo_SUT	0.04	0.02

It can be seen from above Table 4-3, three sets of vehicle compositions, which are PC (Passenger Cars), HGV (Heavy Trucks), and SUT (Single-Unit Trucks), along with the lane-based relative flow proportional volumes during the 3 hours analysis period were developed and encoded in the simulation models. As mentioned previously, it was assumed that the distribution of vehicle classes along the same corridor should not have changed significantly, therefore, the above conducted relative flows were applied to both base and incident simulation models.

c. Desired Speed Distributions

Desired speed distributions along with the desired speed decisions were initially developed based on a combination of vehicle speed data collected from all five sensors during the 3-hour analysis window, where the desired speed decisions were placed at the same location as the volume input points (at the beginning of the road network). As mentioned beforehand, the way the sensors record is lane-specific and cannot be utilized for vehicle classification, therefore, a total of four lane-specific desired speed distributions (two for base condition model and two for incident condition model) were initially developed and coded in VISSIM.

To prepare for the development of the desired speed distributions, a statistical summary of all field-gathered speed data for each lane under base and incident conditions was conducted at first, as shown in Figure 4-21 and Figure 4-22.

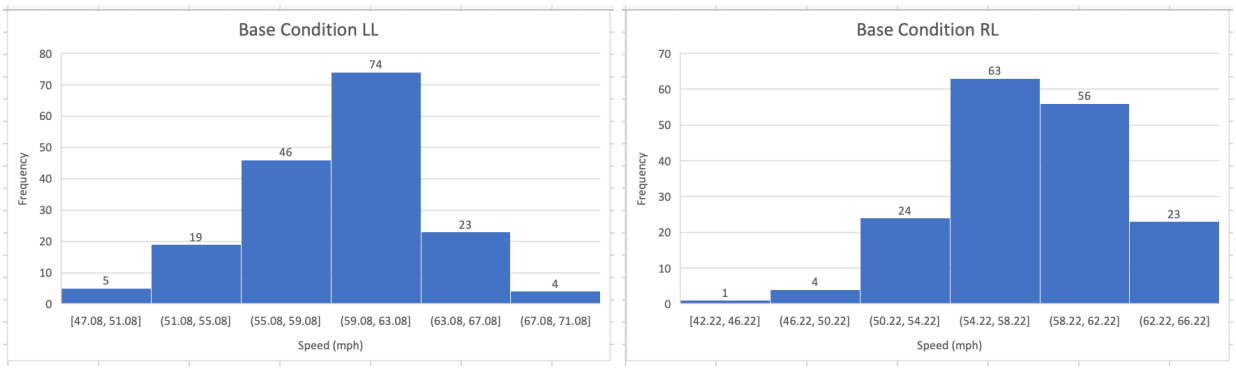

Figure 4-21: Lane-Specific Empirical Speed Frequency for Event A Base Condition

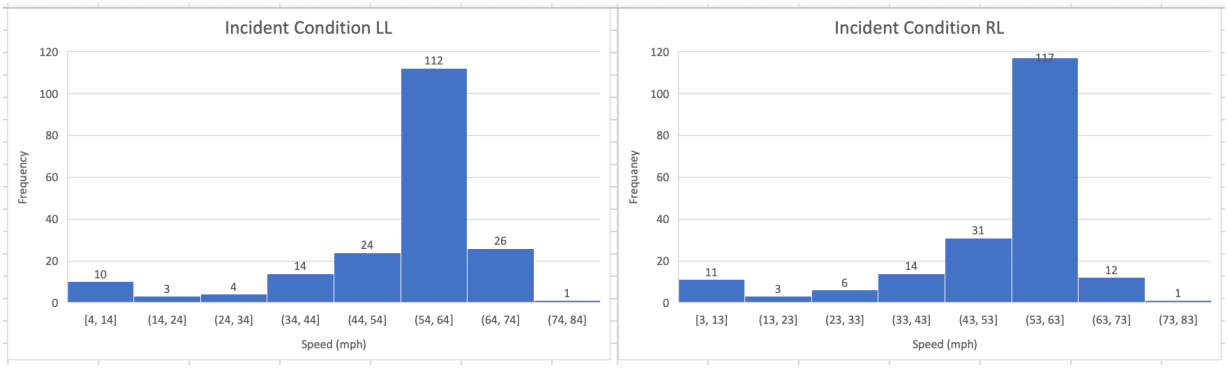

Figure 4-22: Lane-Specific Empirical Speed Frequency for Event A Incident Condition

Table 4-4 and Table 4-5 provide the calculated cumulative percentages related to speed, where the data were introduced in VISSIM for the purpose of creating a series of lane-specific desired speed distributions as shown in Figure 4-23 and Figure 4-24.

Table 4-4: Lane-Specific Speed Cumulative Percentage for Event A Base Condition

LL		RL	
Speed_avg	**Cumulative (%)**	**Speed_avg**	**Cumulative (%)**
49.08	2.9240	44.22	0
53.08	14.0351	48.22	2.9240
57.08	40.9357	52.22	16.9591
61.08	84.2105	56.22	53.8012
65.08	97.6608	60.22	86.5497
69.08	100	64.22	100

Table 4-5: Lane-Specific Speed Cumulative Percentage for Incident Condition

LL		RL	
Speed_avg	**Cumulative (%)**	**Speed_avg**	**Cumulative (%)**
9	5.1546	8	5.6410
19	6.7010	18	7.1795
29	8.7629	28	10.2564
39	15.9794	38	17.4359
49	28.3505	48	33.3333
59	86.0825	58	93.3333
69	99.4845	68	99.4872
79	100	78	100

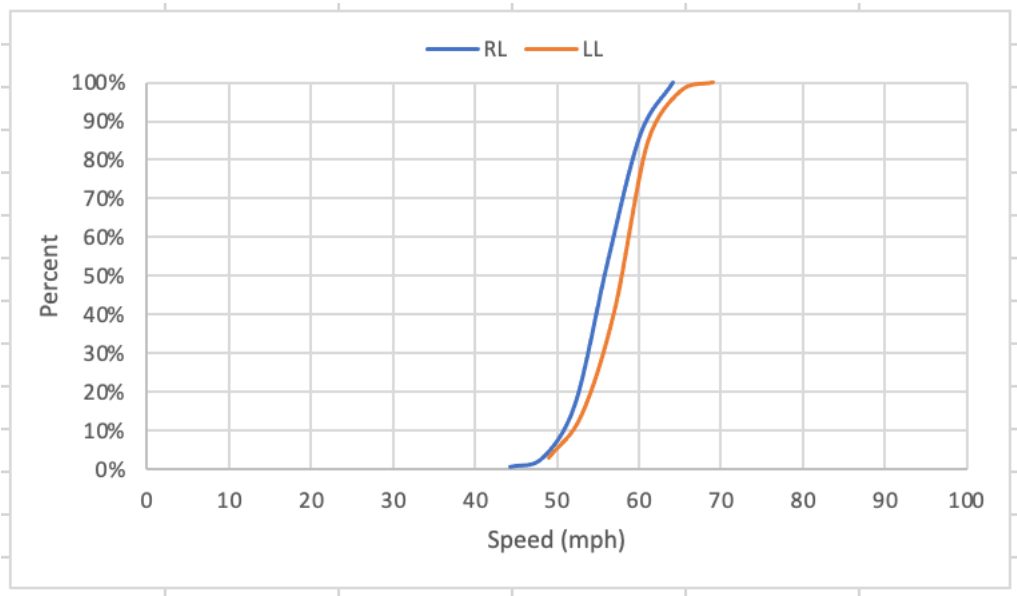

Figure 4-23: Base Condition Desired Speed Distribution of Event A

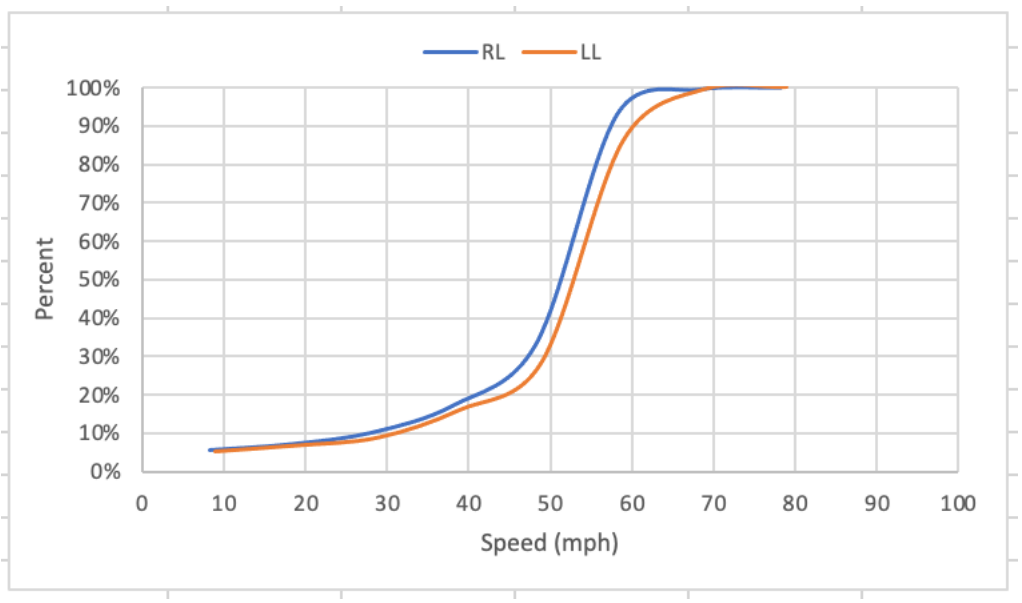

Figure 4-24: Incident Condition Desired Speed Distribution of Event A

As mentioned at the beginning of this section, the initially developed desired speed distributions were based on the combination of traffic speed data collected by all five sensors deployed throughout the work zone area. However, pilot simulation runs revealed that speed measured by the downstream data collectors was approximately 10-15mph lower than field-observed speed data under base condition. Speed trajectories conducted by the downstream data collectors under incident condition simulation model showed significant deviations from empirical speed distributions. Therefore, finer desired speed distributions were in need to be developed and calibrated to be able to best replicate field-observed distribution of key traffic parameters such as speed and volume. The following section presents this calibration procedures in great detail, and as well as the validation process of the incident condition simulation model using the well-calibrated base condition simulation model through the comparison of the simulated distribution of selected traffic metrics from incident condition to the field-gathered data.

d. Calibration and Validation

Pilot simulation runs under base condition have shown that simulation model was not able to competently replicate field-observed conditions if using VISSIM default vehicle characteristics and driving behavior parameters, even with careful input of processed field-gathered geometry, volume, and speed data. Therefore, iterative modification of VISSIM default parameters was in need to be conducted until the base simulation model yielded the same distribution of effectiveness measures collected in the field.

Based on the previous literature review effort, a study conducted by Jehn and Turochy presented a novel approach focused on the modification of key VISSIM input parameters such as heavy vehicle characteristics and driving behavior parameters for the purpose of calibrating generalizable microsimulation models for rural freeway work zones under Alabama condition (Jehn and Turochy 2019). The work zone area, started at a milepost of approximately 64, analyzed in that research located at the same interstate (I-59/I-20) and just a few miles downstream of the study site utilized in this research, specifically, the last sensor utilized for analysis within the work zone area was Q1012 with a milepost of 73.1 (refer to Figure 4-3).

The researchers were able to identify three parameters which are CC0 (desired standstill distance), CC1 (desired time headway) and the desired truck acceleration to be the most significant for replicating field conditions in the simulation model calibration process. Table 4-6 and Table 4-7 provide the calibrated results from their study regarding desired time headway (CC1) and related driving behavior parameters, respectively, as inputs to be introduced in VISSIM. Additionally, the default heavy truck parameters in VISSIM were found not to be representative of the U.S. truck fleet but of the lighter and faster trucks driven in Europe (Jehn & Turochy 2019; Edara & Chatterjee 2010; Harwood 2003; PTV Group 2017). The researchers calibrated the standstill

desired acceleration to be 2 ft/s^2 from the VISSIM default heavy truck acceleration of 8.2 ft/s^2. It should be noted that the detailed simulation model development and calibration processes for the purpose of obtaining these well-calibrated parameters could be found in their study.

Table 4-6: Calibrated Desired Headway Distributions (Jehn & Turochy 2019)

Headway (s) original	Headway (s) calibrated	Cumulative % below (passenger cars)	Cumulative % below (trucks)
1	0.65	1%	0%
2	1.65	43%	2%
3	2.65	76%	27%
4	3.65	89%	57%
5	4.65	96%	77%
6	5.65	100%	90%
7	6.65	100%	100%

Table 4-7: Calibrated Driving Behavior Parameters (Jehn & Turochy 2019)

Parameter	Description	Default Value	Calibrated Value
Car-Following Parameters			
CC0	desired standstill distance	4.92 ft	10 ft
CC1	desired time headway	0.9 s	Empirical Distribution with 0.35 s subtracted[a]
CC2	additional distance over desired safety distance	13.12 ft	Default
CC3 - CC9	--	--	Default
Lane-Changing Parameters			
Lane-Changing Distance	distance upstream of a required lane change that drivers will begin looking for gaps to merge	656.2 ft	3000 ft
SRF	safety distance reduction factor	0.6	Default
Cooperative Braking	check box (yes or no)	No	Yes
Maximum Deceleration for Cooperative Braking	maximum accepted deceleration when braking cooperatively	-9.84 ft/s^2	-20 ft/s^2
Waiting Time Before Diffusion	maximum waiting time before vehicle removed from network	60 s	200 s
All others	--	--	Default

[a]See Table 4-6 for original empirical distribution

Since the study work zone utilized to develop the calibration parameter sets such as driving behavior parameters and heavy truck characteristic in this literature was close to the study site of this research and with only one year apart of the construction period, it was assumed that the basic geometry and relevant traffic compositions utilized for the simulation model calibrations will not have changed significantly. Therefore, the calibrated parameter sets were applied to the simulation models developed for this study under both base and incident conditions.

After introduced all the above-mentioned calibrated parameters in VISSIM, the next calibration process performed focused on the development of appropriate desired speed distribution sets since the accuracy of the microsimulation results depends heavily on the quality of the developed desired speed distributions, therefore, if sufficient field-collected vehicle speed data are available, a finer set of desired speed distributions should be developed to best reflect the actual conditions in the work zone area (Zhao et al. 2022).

As described earlier in the subsection *c. Desired Speed Distributions*, the lane-specific desired speed distribution was initially developed based on a combination of traffic speed data collected by all five sensors deployed throughout the work zone area during the 3 hours analysis window. However, the speed trajectory results of the pilot simulation run presented consistent deviations from the speed distribution conducted under field conditions. Therefore, to be able to best replicate field observed conditions, a total of six desired speed distributions, along with six desired speed decisions as shown in Figure 4-25, were ultimately developed for the base condition simulation model based on the previous vehicle speed data review effort which revealed that speed reduction only occurred at the first upstream sensor Q1025 from the incident location.

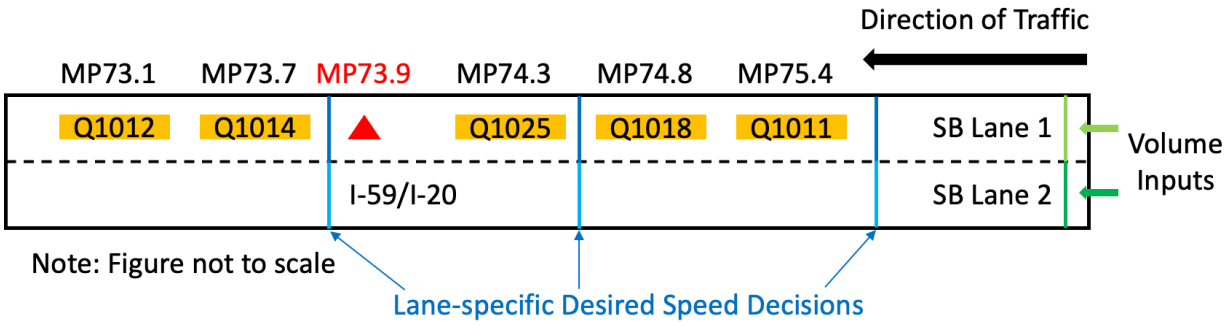

Figure 4-25: Road Network Layout with Key Components of Event A

Specifically, the first set of lane-specific desired speed decisions and associated desired speed distributions were placed at the beginning of the road network with speed data collected from the combination of sensor Q1011 and Q1018 under base condition. The second set of lane-specific desired speed decisions along with associated desired speed distributions were placed at the midpoint (approximately measured in VISSIM) between sensor Q1018 and Q1025; even though at base condition, the speed data utilized for the distribution development only from sensor Q1025 for consistency with incident condition. The last set of lane-specific desired speed decisions with related desired speed distributions under base condition were placed just downstream of the incident location; it should be noted that herein mentioned incident location was just an imaginary point and does not mean under the incident condition. The speed data utilized for the speed distribution development came from the combination of sensor Q1014 and Q1012.

After determined which sensor(s) would be utilized for the development of desired speed distributions, the same series of data processing procedures as described in the previous section *c* to obtain the cumulative percentages related speed collected from the desired sensors to be introduced into VISSIM were performed. Examples of this process performed on the first set of

desired speed distributions under base condition are provided in the following Figure 4-26, Table 4-8, and Figure 4-27.

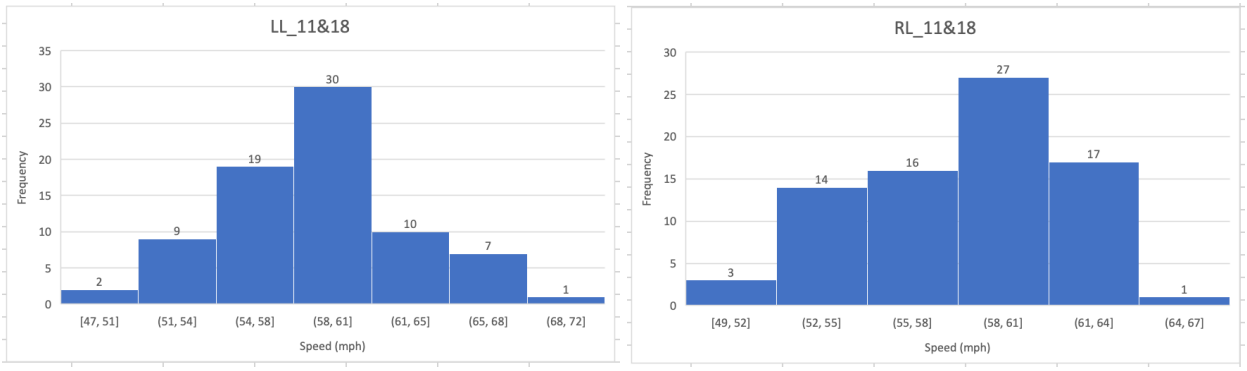

Figure 4-26: Lane-Specific Empirical Speed Frequency from Q1011 and Q1018

Table 4-8: Lane-Specific Speed Cumulative Percentage

LL		RL	
Speed_avg	**Cumulative (%)**	**Speed_avg**	**Cumulative (%)**
48.83	3%	50.11	4%
52.33	14%	53.21	22%
55.83	38%	56.31	42%
59.33	77%	59.41	77%
62.83	90%	62.51	99%
66.33	99%	65.61	100%
69.83	100%	-	-

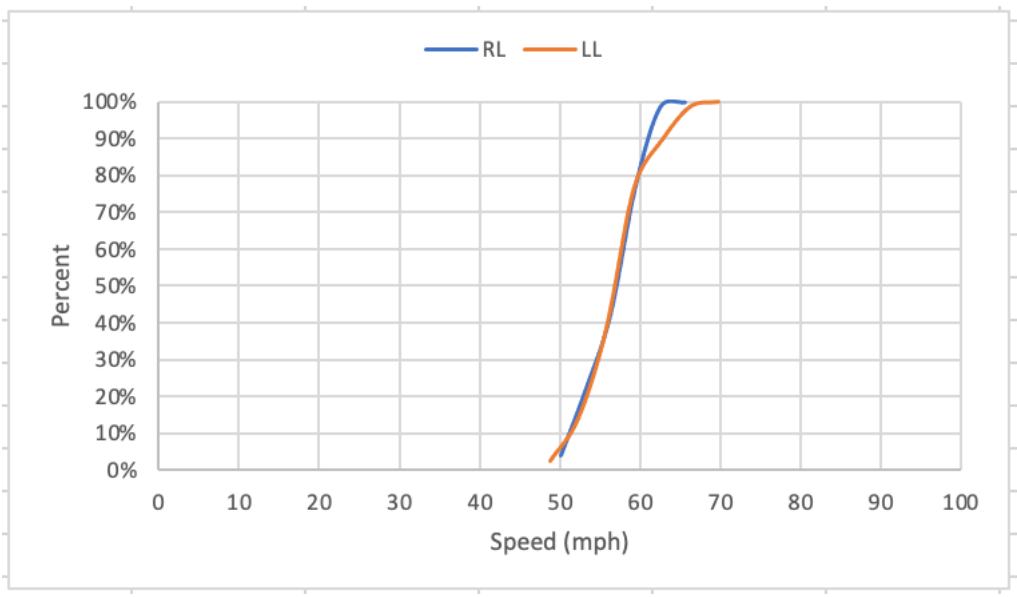

Figure 4-27: First Set of Desired Speed Distributions under Base Condition

The cumulative speed data from Table 4-8 then were introduced in VISSIM to be able to define the first set of desired speed decisions, as shown in Figure 4-28.

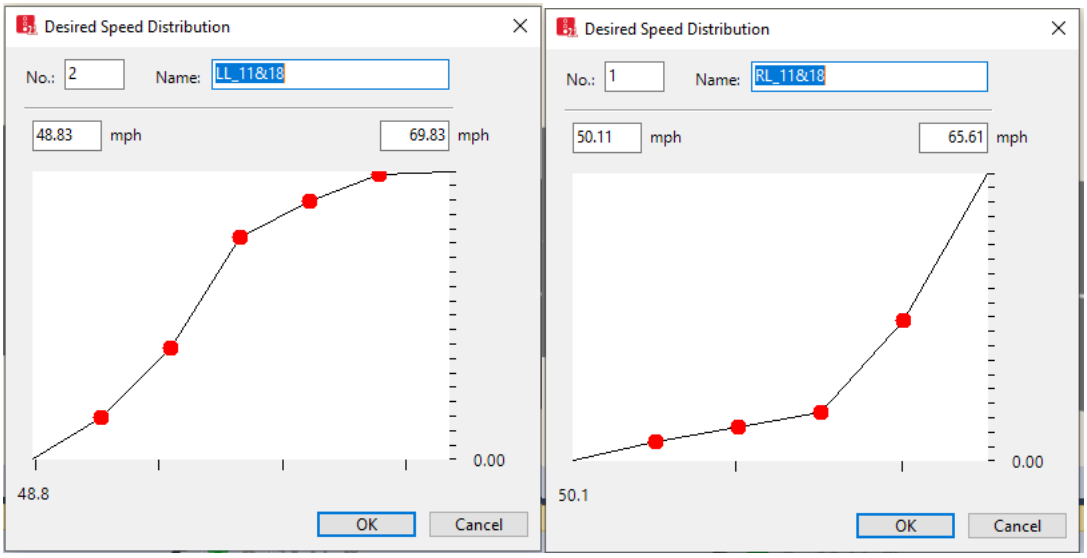

Figure 4-28: Cumulative Speed Distribution for Event A Base Condition

A total of six desired speed distributions with associated six desired speed decisions for a base condition simulation model were developed in VISSIM as shown in Figure 4-29.

Count: 6	No	Name	LowerBound	UpperBound
1	1	RL_11&18	50.11	65.61
2	2	LL_11&18	48.83	69.83
3	3	RL_25	47.12	66.72
4	4	LL_25	51.47	65.27
5	5	RL_14&12	52.82	64.82
6	6	LL_14&12	53.68	66.88

Figure 4-29: Base Condition Developed Desired Speed Distributions for Event A

After adjusted all the calibrated parameters obtained from literature and modified relevant desired speed distributions in VISSIM, the next step was to run the base condition simulation model to determine the calibration accuracy since the objective of model calibration is to obtain the best match between model performance estimates and field performance measurements (Dowling er al. 2004). For the purpose of this research, two performance measures, traffic flow and speed, with corresponding criteria were used to evaluate the accuracy of the calibration.

As such, 10 repeated runs of the base simulation model were performed using different random number seeds. The simulated flows and speeds of the ten replicate runs in a 5-minute time interval format during the 3 hours analysis window were then utilized to compare with the field-observed measurements to evaluate the base simulation model accuracy in representing field conditions.

For the purpose of measuring base simulation model accuracy, two criteria, GEH (Geoffrey E. Havers) statistic and Relative Root Mean Square Error (RRMSE), identified based on the previous literature review effort were utilized to quantitatively measure the closeness of the developed base condition simulation model to the actual traffic condition. Specifically, GEH statistic was found to be the most commonly used measure for flow calibration criteria, while

RRMSE was utilized for speed calibration criteria (Lu et al. 2014; Lu et al. 2017; Wisconsin DOT 2002; UK Highway Agency 1996; Dowling er al. 2004; Kan et al. 2019; Zhao et al. 2022; Jehn and Turochy 2019). The following addressed the use of each criterion performed on the simulation outputs under base condition in detail based on the findings of the literature studies mentioned above.

Criteria for Flow Calibration

The GEH statistic, developed by Wisconsin DOT for the purpose of assessing the developed simulation model of the Milwaukee highway system, was utilized for flow calibration criteria in this study.

The GEH statistic is computed as follow:

$$GEH\ (k) = \sqrt{\frac{2[S(k)-O(k)]^2}{[S(k)+O(k)]}} \quad \text{(Eq. 4-1)}$$

Where,

$S(k)$: Simulated flow during the k-th time interval (veh/hour)

$O(k)$: Observed flow measured in the field during the k-th time interval (veh/hour)

It should be noted that a satisfactory calibration requires that the flow should meet the condition of a GEH value less than 5 (GEH < 5) for at least 85% of all 5-minute time intervals, based on guidance from the FHWA *Traffic Analysis Toolbox Volume III: Guidelines for Applying Traffic Microsimulation Modeling Software* (Dowling er al. 2004).

Criteria for Speed Calibration

The Relative Root Mean Square Error (RRMSE) statistic was identified for speed calibration criteria in this study based on past best practices in literature. The RRMSE measures the closeness of speed by calculating the difference between the simulation output and the empirical data for every 5-minute time interval.

The RRMSE statistic is defined as follow:

$$RRMSE = \sqrt{\frac{1}{n}\sum_{k=1}^{n}\left(\frac{S(k)-O(k)}{O(k)}\right)^2} \quad \text{(Eq. 4-2)}$$

Where,

$S(k)$: Simulated speed during the k-th time interval (veh/hour)

$O(k)$: Observed speed measured in the field during the k-th time interval (veh/hour)

n: Total number of 5-minute time interval

It is worth noting that, based on past best practice from the aforementioned literature studies, the simulation model accuracy is deemed excellent when RRMSE is within 10%; if the RRMSE is between 10% and 25%, the model is considered acceptable.

The processes to obtain the desired value of GEH and RRMSE statistics for the purpose of evaluating calibration accuracy of base simulation model are presented in the following Tables.

Specifically, Table 4-9 shows an example of the processes to calculate the value of GEH and RRMSE for the first half-hour, based on the sensor Q1011 right-lane (RL) traffic data.

Same procedures were performed on the remaining nine datasets and the average GEH of each was summarized in Table 4-10 for the purpose of determining if the GEH of each case satisfy the target (GEH < 5). For better understanding, each "Location" in Table 4-10 under specific lane

(RL/LL) includes a total of 36 cases/GEH values which comes from 12 5-minute intervals per hour for a total of 3 hours; the case was deemed to meet the target if the associated GEH value was less than 5. In general, it can be seen that the simulated flows at all locations meet the calibration criteria.

Evaluation of RRMSE at each location only need to consider the average value of each lane during the 3 hours analysis window, as summarized in Table 4-11. As can be seen, the lane-specific RRMSE values for each location are below 10%, indicating that the simulated speeds meet the calibration criteria as well.

Table 4-9: Example of GEH and RRMSE Calculations for Event A Base Model

Q1011 RL	VISSIM_avg		Sensor		GEH	RRMSE
	Volume	Speed	Volume	Speed		
21:00	36	59.41	37	52.84	0.1	2%
21:05	30	59.04	27	52.15	0.5	2%
21:10	29	59.84	30	55.21	0.1	1%
21:15	30	59.72	23	54.15	1.4	1%
21:20	35	59.66	35	54.20	0.0	1%
21:25	39	58.87	38	54.25	0.2	1%

Table 4-10: GEH for Mean Flows at Each Location from Event A Base Model

Location	Target	Cases LL/RL	Cases Met		% Met		Target Met?	
			LL	RL	LL	RL	LL	RL
Q1011	GEH < 5 for > 85% of k (5-min interval)	36	36	36	100%	100%	Yes	Yes
Q1018		36	35	36	97%	100%	Yes	Yes
Q1025		36	36	34	100%	94%	Yes	Yes
Q1014		36	36	34	100%	94%	Yes	Yes
Q1012		36	36	36	100%	100%	Yes	Yes
Overall		**180**	**179**	**176**	**99%**	**98%**	**Yes**	**Yes**

Table 4-11: RRMSE for Mean Speeds at Each Location from Event A Base Model

Location	RRMSE	
	LL	RL
Q1011	4%	9%
Q1018	10%	7%
Q1025	6%	10%
Q1014	6%	7%
Q1012	4%	3%
Average	**6%**	**7%**

Considering the whole model comprehensively, the calibration results show that the selected two performance measures, traffic flow and speed, meet both calibration criteria (GEH and RRMSE statistic), meaning that the VISSIM calibration results of the base condition model match well with field observations and that all the calibration efforts indicating the base simulation model is ready to be used for the incident model simulation. The remainder of this section discusses the process for the development of the incident condition simulation model in greater detail.

As mentioned at the beginning of this section, both base and incident conditions share the same road network but have different field-gathered inputs, such as volumes and desired speed distributions. The volume inputs of the calibrated base condition model were changed to incident condition traffic data (see Table 4-2). Vehicle compositions with relative flows are consistent with those of the base simulation model as presented in Table 4-3.

The prior attempt of the desired speed distribution development for the base condition simulation model has shown that finer desired speed distributions need to be developed to better replicate field conditions. However, according to the previous field data analysis of Event A (subsection 4.4.1), there was a speed drop recorded by the first upstream sensor (Q1025) after the incident and lasted for approximately 40 minutes.

In order to allow VISSIM to replicate the speed reduction phenomenon after the incident, the reduced speed area was introduced in VISSIM along with two lane-specific desired speed distributions using speed data only from the abnormal time period (speed reduction period), as shown in Table 4-12. It is worth mentioning that although the recorded speed reduction period lasted about 40 minutes, only the period of the lowest speed (compared with other periods) was used when developing the reduced speed distribution.

Table 4-12: Speed Reduction Period of Incident A

LL		RL	
Time	**Speed**	**Time**	**Speed**
22:50	37	22:50	29.25
22:55	25.25	22:55	20.25
23:00	13.667	23:00	7.333

In general, a total of eight desired speed distributions, as shown in Figure 4-30, using data from incident condition were ultimately developed and the six lane-specific desired speed decisions were placed at the same location as the base simulation model (see Figure 4-25), plus two desired speed distributions specially developed for the reduced speed area.

Count: 8	No	Name	LowerBound	UpperBound
1	1	RL_11&18	7.40	75.40
2	2	LL_11&18	7.50	77.50
3	5	RL_25	34.75	64.75
4	6	LL_25	42.50	72.50
5	7	RL_14&12	9.83	61.83
6	8	LL_14&12	13.83	65.83
7	9	RL_Reduce_25	7.33	34.33
8	10	LL_Reduce_25	13.67	41.67

Figure 4-30: Incident Condition Developed Desired Speed Distributions for Event A

Examples of the first set of cumulative speed distribution under incident condition, as well as the two distributions specific for reduced speed area are presented in Figure 4-31 and Figure 4-32.

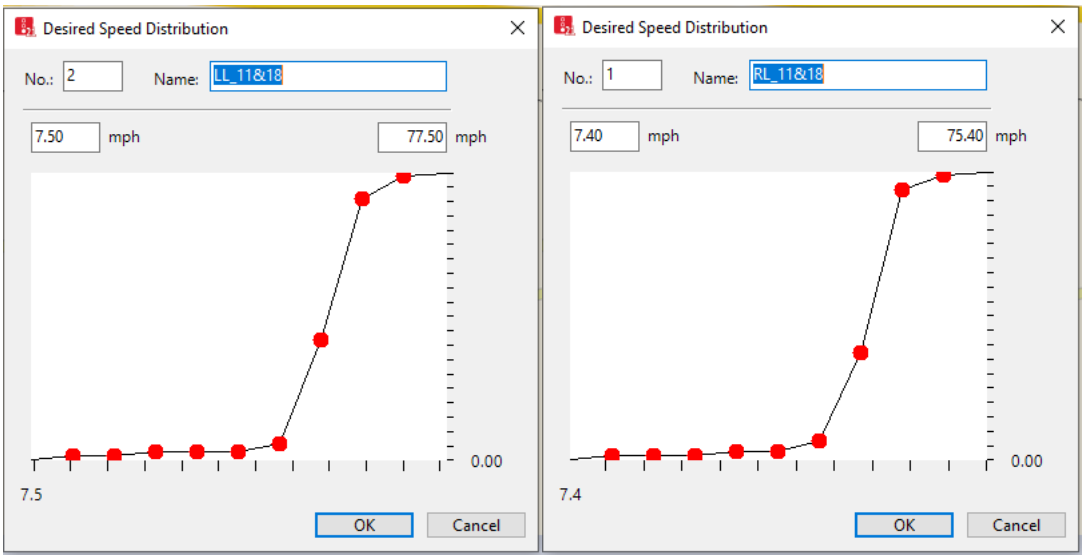

Figure 4-31: Cumulative Speed Distribution for Event A Incident Condition

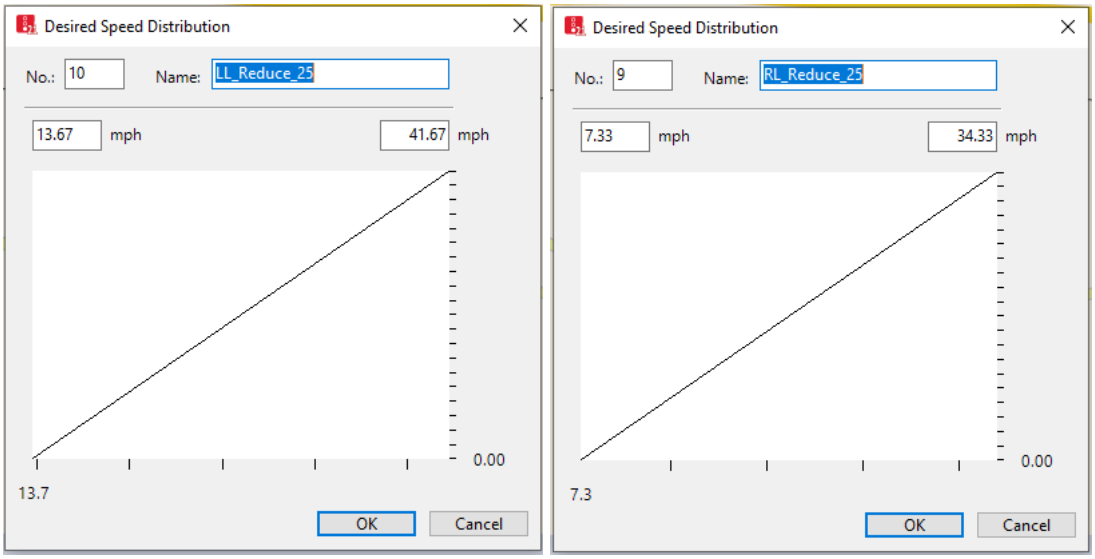

Figure 4-32: Cumulative Speed Distribution in Reduced Speed Area of Incident A

Although field collected data were able to be utilized to identify the affected time period with corresponding speed by incident, while coding the reduced speed area in VISSIM, the effective time period of the speed reduction area needs to be determined for the purpose of modifying desired speed of vehicles within the given time period. Example screenshot of the parameters, such as length, time from/to, identified to be coded for the reduced speed area, as shown in Figure 4-33.

No	Name	Lane	Pos	Length	TimeFrom	TimeTo
1	RL_Reduce_25	1 - 1	14000.000	1600.000	7500	8100
2	LL_Reduce_25	1 - 2	14000.000	1600.000	7500	8100

Figure 4-33: Reduced Speed Area Inputs for Incident A

It should be noted that the determination of the reduced speed area length is an iteration process. The best suitable length could be identified until the observed operations of traffic during the simulation and the simulated results match to the field condition. The effective time period of the reduced speed area was determined from 7500s to 8100s, which corresponding to the speed reduction period 22:50 to 23:05 as presented in Table 4-12.

Same process as used for the base model was performed to determine the quality of the incident condition simulation model. The evaluation results of GEH and RRMSE statistic are summarized and presented in Table 4-13.

Table 4-13: GEH and RRMSE at Each Location for Incident A

Location	GEH (% Match)		RRMSE	
	LL	RL	LL	RL
Q1011	100%	100%	12%	11%
Q1018	100%	100%	15%	13%
Q1025	92%	93%	23%	26%
Q1014	96%	98%	22%	21%
Q1012	99%	100%	18%	16%
Average	**97%**	**98%**	**18%**	**17%**

It can be seen from Table 4-13, the two performance measures, traffic flows and speed, meet both calibration criteria which corresponding to the GEH and RRMSE.

In conclusion, the results indicate that the developed simulation models (base and incident condition) with calibrated parameters reliably replicates the traffic operation at the study site with QWS deployed.

The impacts of the QWS will be discussed in the last part of this section by evaluating the selected measure of effectiveness (MOEs), travel time, queue length and delay, between the simulated base model and incident model.

4.5.2 Event B&C: Base Condition vs. Incident Condition

a. Basic Network Creation

As mentioned in previous field data analysis part (see subsection 4.4.2), since incident B and C occurred on the same day (11/26/2019) with 3 hours apart and close to each other, they were combined for analysis and simulation model development. It is worth mentioning that the term of "Event" includes both base condition and incident condition as stated beforehand.

Following the same procedure as Event A, the first step of the simulation model development was the creation of basic geometric elements. Since both incidents took place on the

northbound of the study work zone (I-59/I-20), the same roadway network from Event A developed, but in opposite direction and with different location of key components such as volume inputs, lane-specific desired speed decisions and sensor locations, was created in VISSIM. Figure 4-34 provides a sample drawing of the road network layout.

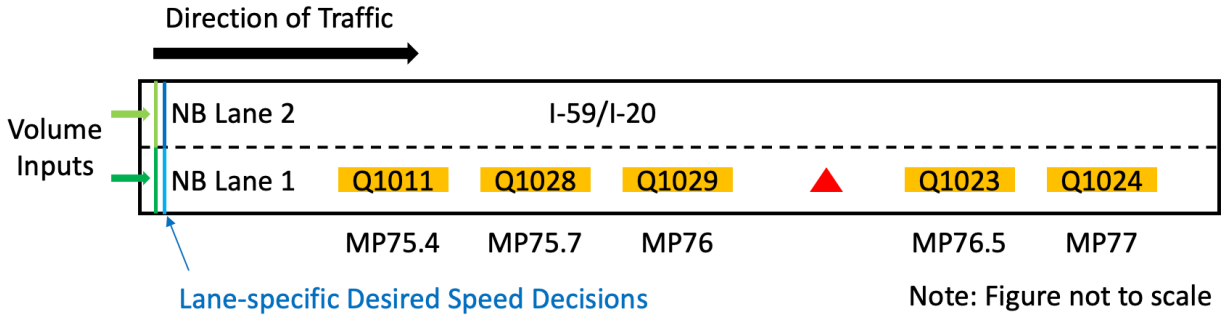

Figure 4-34: Road Network Layout of Event B&C

Each sensor location included in the drawing was introduced as a data collection point in VISSIM for the purpose of calibrating the base condition simulation model. The key components mentioned above will be discussed in detail in the following sections.

b. Volume Inputs and Vehicle Compositions

Traffic volumes for both base and incident conditions were obtained from the farthest sensor Q1011 upstream of the incident location and introduced at the beginning of the road network in VISSIM. Follow the same incident-related data review process as event A, a total of 6 hours analysis window from 13:45 to 19:45 capable of covering both incident B and incident C was confirmed for simulation as discussed beforehand. Additionally, a 15-minute warm-up period from 13:30 to 13:45 was added to the simulation analysis window. Table 4-14 and Table 4-15 provide examples of volume inputs at 5-minute intervals for the first hour of simulation under base and

incident conditions, respectively. It is worth mentioning that as with event A, the same volume translation process was applied in this step.

Table 4-14: Example of Base Condition Volume Inputs in VISSIM for Event B&C

Time	Raw Volumes (RL)	Flow Rates, vphpl (RL)	Raw Volumes (LL)	Flow Rates, vphpl (LL)
13:30	64	768	55	660
13:35	60	720	43	516
13:40	50	600	37	444
13:45	65	780	60	720
13:50	55	660	52	624
13:55	74	888	54	648
14:00	73	876	59	708
14:05	69	828	53	636
14:10	73	876	64	768
14:15	85	1020	77	924
14:20	63	756	57	684
14:25	59	708	30	360

Table 4-15: Example of Incident Condition Volume Inputs in VISSIM for Event B&C

Time	Raw Volumes (RL)	Flow Rates, vphpl (RL)	Raw Volumes (LL)	Flow Rates, vphpl (LL)
13:30	30	360	32	384
13:35	71	852	43	516
13:40	64	768	72	864
13:45	75	900	43	516
13:50	35	420	21	252
13:55	59	708	67	804
14:00	48	576	16	192
14:05	67	804	47	564
14:10	86	1032	61	732
14:15	70	840	74	888
14:20	77	924	68	816
14:25	71	852	36	432

The same determination process of vehicle compositions with relative flows as discussed in event A was applied to event B&C. Based on the previous determined analysis time period, a total of 7 hours analysis window from 13:00 to 20:00 was identified to calculate average traffic data from 5 Tuesdays in May for each vehicle type on each lane. It should be noted that even though the simulation time period was identified from 13:30 to 19:45 for a total of 6-hour, the traffic volume data used for vehicle composition with relative flow calculations were provided in 1-hour interval format. Therefore, 7 hours were ultimately determined to be able to cover the entire time period. The aggregated average volume data along with the lane-based proportions for each vehicle class in the traffic stream are provided in Table 4-16 as inputs to be introduced to the base and incident condition simulation models in VISSIM.

Table 4-16: Aggregated Average Volume Data with Relative Vehicle Flow for Event B&C

	NB1_RL	NB2_LL
PC	842	575
HGV	350	19
SUT	76	18
Total	1268	612
RelFlo_PC	0.66	0.94
RelFlo_HGV	0.28	0.03
RelFlo_SUT	0.06	0.03

c. Desired Speed Distributions

The prior attempt (from event A) of the desired speed distribution development for the base condition simulation model has shown that finer desired speed distributions need to be developed to better replicate field conditions, if sufficient field-collected speed data are available. Therefore, same procedures as discussed in the subsection *d. Calibration and Validation* of event A for the purpose of identifying which sensor(s) would be utilized for the development of a finer set of

desired speed distributions as well as the location of the desired speed decisions were performed, and the results can be found in Figure 4-35, Table 4-17.

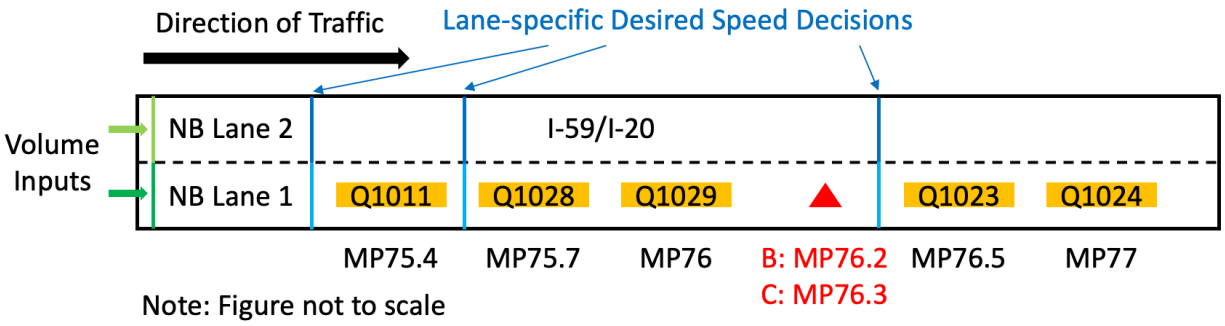

Figure 4-35: Road Network Layout with Key Components of Event B&C

Table 4-17: First Set of Speed Cumulative Percentage for Event B&C Base Condition

LL		RL	
Speed_avg	**Cumulative (%)**	**Speed_avg**	**Cumulative (%)**
52.9	12%	52.07	4%
54.2	35%	53.17	15%
55.5	68%	54.27	49%
56.8	89%	55.37	83%
58.1	97%	56.47	92%
59.4	100%	57.57	99%
-	-	58.67	100%

The cumulative speed data from Table 4-17 were then introduced into VISSIM to define the first set of desired speed decisions, as shown in Figure 4-36.

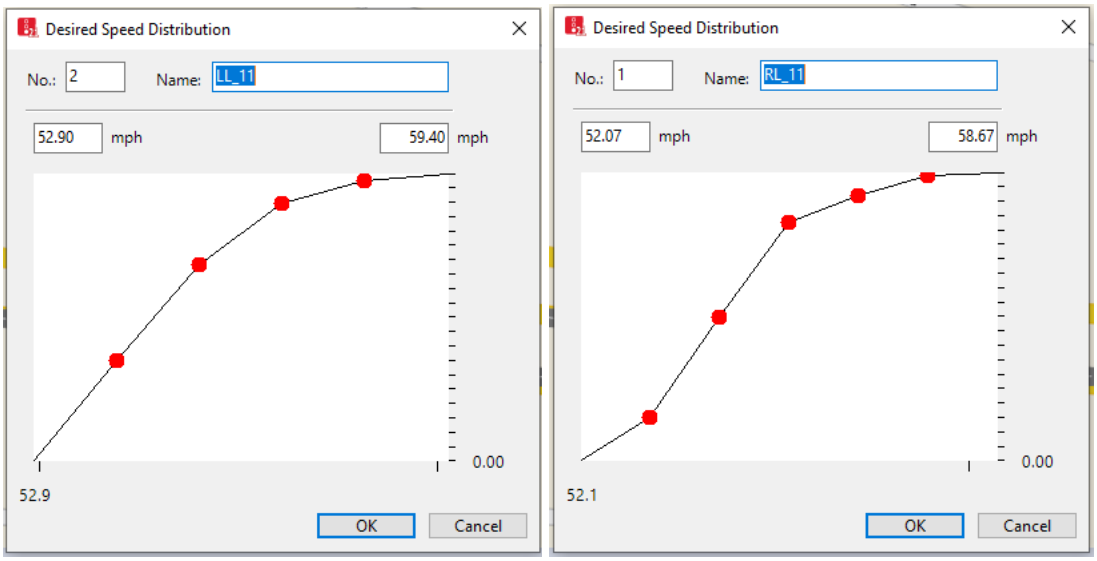

Figure 4-36: Cumulative Speed Distribution for Event B&C Base Condition

A total of six desired speed distributions along with associated six desired speed decisions for a base condition simulation model were developed in VISSIM as shown in Figure 4-37.

Count: 6	No	Name	LowerBound	UpperBound
1	1	RL_11	52.07	58.67
2	2	LL_11	52.90	59.40
3	3	RL_28&29	50.30	56.77
4	4	LL_28&29	47.70	64.50
5	5	RL_23&24	36.41	63.21
6	6	LL_23&24	40.71	72.51

Figure 4-37: Desired Speed Distributions for Event B&C Base Condition

d. Calibration and Validation

The same calibration parameter sets utilized in event A were applied for the base condition simulation model development. With the developed finer set of desired speed distributions, the same process as previously analyzed for event A was performed to determine the calibration accuracy using the selected two performance measures (traffic flow and speed). The evaluation results of GEH and RRMSE statistic are summarized in Table 4-18.

Table 4-18: GEH and RRMSE at Each Location for Event A Base Condition

Location	GEH (% Match)		RRMSE	
	LL	RL	LL	RL
Q1011	99%	99%	4%	3%
Q1028	99%	99%	5%	3%
Q1029	90%	94%	6%	3%
Q1023	89%	88%	12%	20%
Q1024	98%	99%	26%	25%
Average	**95%**	**96%**	**11%**	**11%**

The calibration results from above table 4-18 show that the selected two performance measures, traffic flow and speed, meet both calibration criteria (GEH and RRMSE statistic), meaning that the VISSIM calibration results of the base condition model agree well with field observations and that all the calibration efforts indicating the base simulation model is ready to be used for the incident model simulation.

Following the same procedure as discussed in event A – incident simulation model development, after modified the desired volume inputs and speed distributions with the use of traffic data from incident day, the reduced speed area was then created in to be able to replicate the speed reduction phenomenon after the incident.

According to the previous field data analysis of Event B&C (subsection 4.4.2), the speed reduction was extended to the upstream second sensor (Q1028) for both incident B and C, therefore, a combination of the speed data only from the speed reduction period recorded from the upstream two sensors (Q1028 and Q1029) was used to develop desired speed distributions specific to the reduced speed area.

Since incidents B (14:10) and C (17:45) occurred at different times of the day, two separate speed reduction periods were identified to be 14:15 – 15:45 and 17:50 – 19:00, respectively, based on the combination of speed data from two sensors. The cumulative percentages of speed for each

reduction period are summarized in Table 4-19 and Table 4-20 for incident B and incident C, respectively.

Table 4-19: Cumulative Speed Reduction Distribution of Incident B

LL		RL	
Speed_avg	**Cumulative (%)**	**Speed_avg**	**Cumulative (%)**
6.3	77%	4.7	48%
11.3	86%	8.1	97%
16.3	100%	11.5	97%
-	-	14.9	97%
-	-	18.3	100%

Table 4-20: Cumulative Speed Reduction Distribution of Incident C

LL		RL	
Speed_avg	**Cumulative (%)**	**Speed_avg**	**Cumulative (%)**
6.1	43%	6.717	88%
8.7	100%	12.817	92%
-	-	18.917	96%
-	-	25.017	100%

The cumulative speed data from Table 4-19 and Table 4-20 then were introduced in VISSIM to be able to define the reduced speed area, as shown in Figure 4-38 and Figure 4-39.

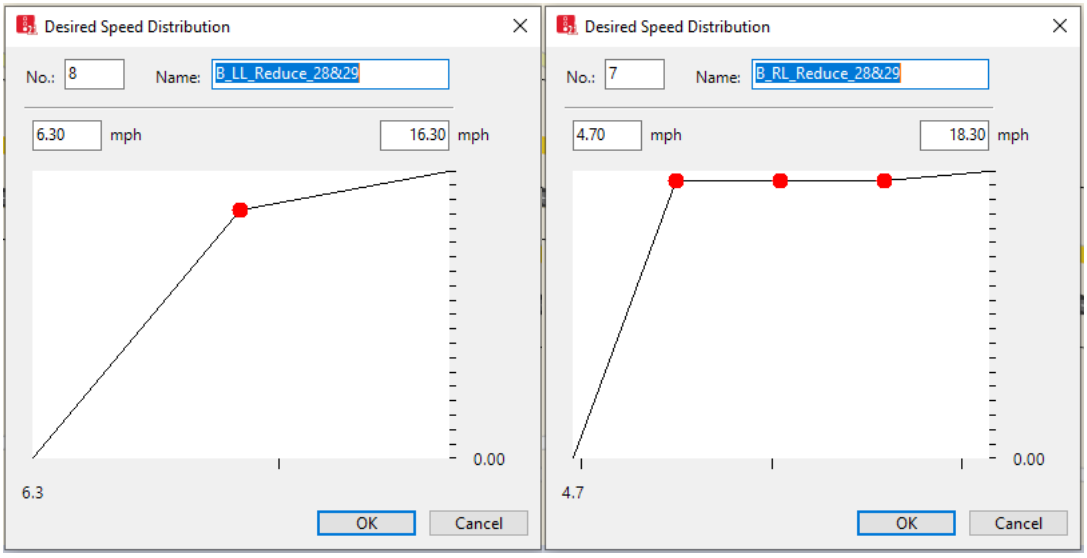

Figure 4-38: Cumulative Speed Distribution in Reduced Speed Area of Incident B

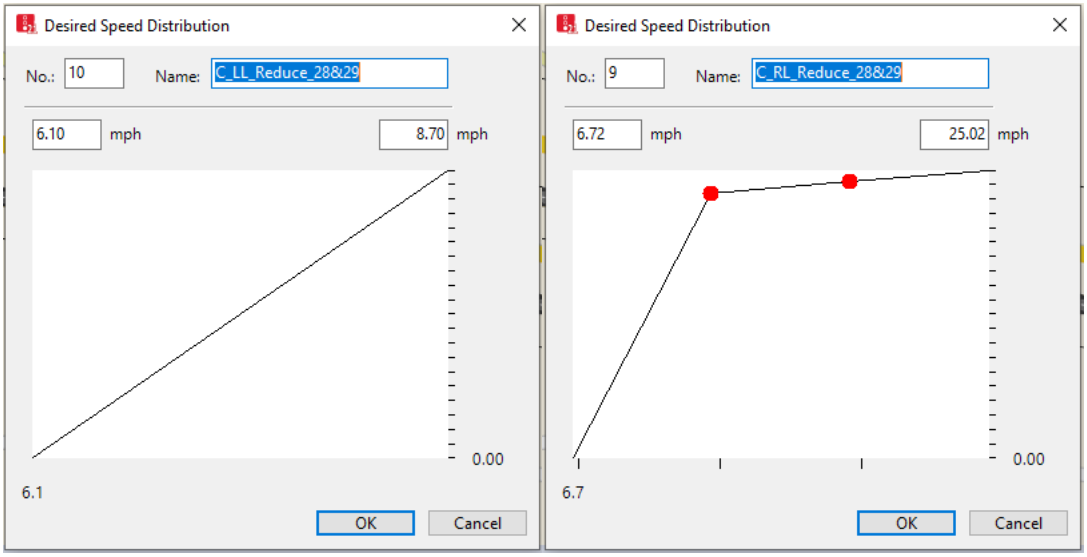

Figure 4-39: Cumulative Speed Distribution in Reduced Speed Area of Incident C

The determination of the effective time period and length of the reduced speed area is an iteration process as previously discussed in event A. The identified parameters, such as length and time from/to, as inputs for the reduced speed area in VISSIM are shown in Figure 4-40.

No	Name	Lane	Pos	Length	TimeFrom	TimeTo
1	B_RL_Reduce_1028-1029	1 - 1	21700.000	700.000	2400	6900
2	B_LL_Reduce_1028-1029	1 - 2	21700.000	700.000	2700	6900
3	C_RL_Reduce_1028-1029	1 - 1	21700.000	700.000	15300	18600
4	C_LL_Reduce_1028-1029	1 - 2	21700.000	700.000	15600	18000

Figure 4-40: Reduced Speed Area Inputs for Incident B&C

In general, a total of ten desired speed distributions using data from incident condition were ultimately developed, as shown in Figure 4-41.

Count: 10	No	Name	LowerBound	UpperBound
1	1	RL_11	49.50	59.50
2	2	LL_11	49.55	62.55
3	3	RL_28&29	32.80	54.40
4	4	LL_28&29	36.85	59.65
5	5	RL_23&24	19.57	69.57
6	6	LL_23&24	25.55	125.65
7	7	B_RL_Reduce_28&29	4.70	18.30
8	8	B_LL_Reduce_28&29	6.30	16.30
9	9	C_RL_Reduce_28&29	6.72	25.02
10	10	C_LL_Reduce_28&29	6.10	8.70

Figure 4-41: Desired Speed Distributions for Event B&C Incident Condition

Same process as used in previous corresponding step was performed to determine the quality of the incident condition simulation model. The evaluation results of GEH and RRMSE statistic are summarized and presented in Table 4-21.

Table 4-21: GEH and RRMSE at Each Location for Incident B&C

Location	GEH (% Match)		RRMSE	
	LL	RL	LL	RL
Q1011	98%	99%	18%	18%
Q1028	96%	98%	30%	25%
Q1029	88%	90%	36%	37%
Q1023	95%	94%	24%	25%
Q1024	92%	93%	15%	13%
Average	**94%**	**95%**	**25%**	**24%**

It can be seen from Table 4-21, on average, the two performance measures, traffic flows and speed, meet both calibration criteria which corresponding to the GEH (< 5 for at least 85% of the records) and RRMSE (< 25%). At the location of sensor Q1028 and Q1029, even though the evaluation results of RRMSE which used for speed calibration criteria are greater than the threshold, it was assumed that this deviation might be caused by the beginning and the end of the simulation period. Example of this phenomenon from the location of Q1028 left lane (LL) can be found in Figure 4-42, which provides a comparison of speed profiles generated in VISSIM with that observed in the field. This graph demonstrates that simulation models cannot fully simulate real-world traffic variability especially when there is an incident traffic flows tend to be more stochastic. Nevertheless, the general speed profiles between VISSIM generated and field observed math well and the incident simulation model was considered successfully validated.

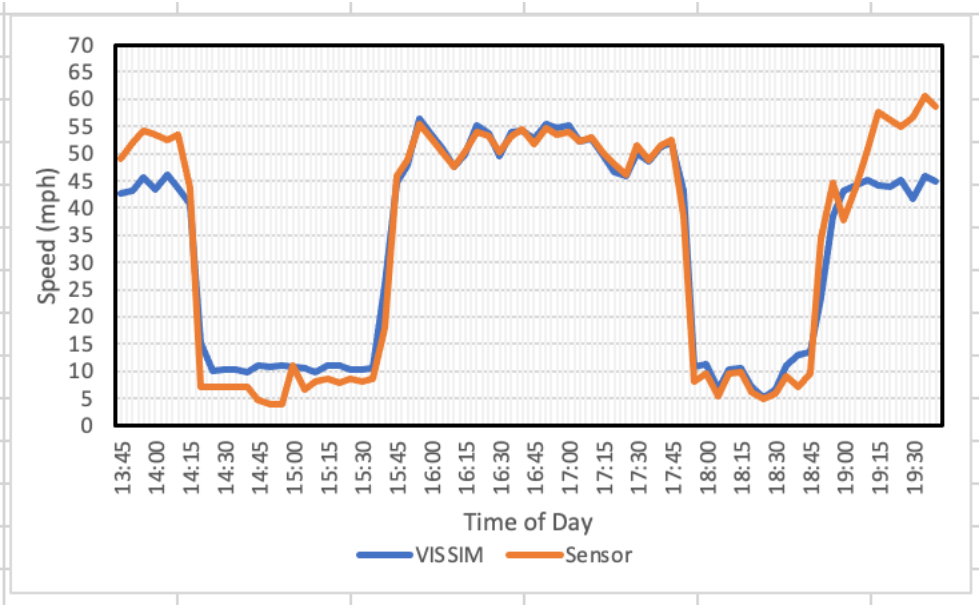

Figure 4-42: Q1028 Left-Lane Speed Profile Comparison Under Incident Condition

In generally, the results from both base and incident conditions indicate that the developed simulation models with calibrated parameters reliably replicates the traffic operations at the study

site with QWS deployed. The evaluation of the selected measures of effectiveness (MOEs), such as travel time, delay, and queue length, between the simulation base model and incident model will be discussed in detail at the end of this chapter.

4.5.3 Event D: Base Condition vs. Incident Condition

a. Basic Network Creation

The basic roadway network of event D shares the same road network and the key component locations as event B&C since incident D occurred at the same location as incident B (MP 76.2, NB) as described in the previous section. Figure 4-43 provides a sample drawing of the road network layout utilized for the development of the event D base and incident condition simulation models.

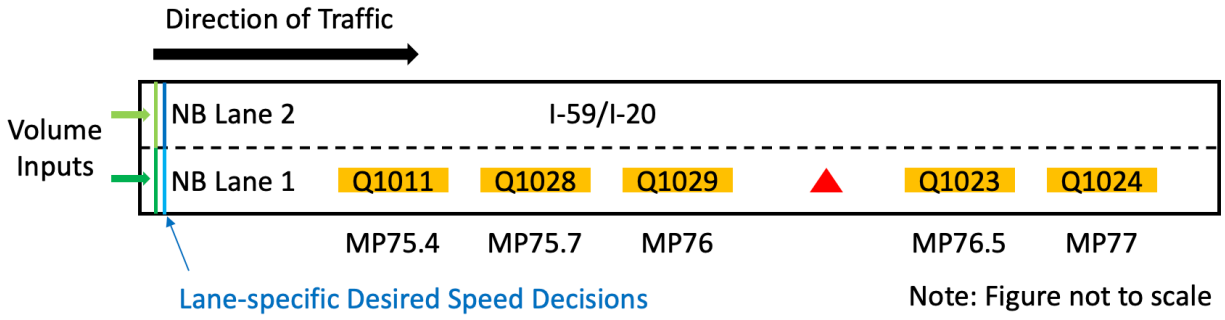

Figure 4-43: Road Network Layout of Event D

b. Volume Inputs and Vehicle Compositions

Same as event B&C, the farthest sensor Q1011 upstream of the incident location was utilized to extract traffic data specific to base and incident conditions, and the desired traffic data was introduced at the beginning of the road network in VISSIM. The same incident-related data review

process as event A was performed and a total of 3-hour period from 13:00 to 16:00 plus a 15-minute warm-up period from 12:45 to 13:00 was identified for simulation.

Table 4-22 and Table 4-23 provide examples of volume inputs at 5-minute intervals for the first hour of simulation under base and incident conditions, respectively, following the same volume translation process as used before.

Table 4-22: Example of Base Condition Volume Inputs in VISSIM for Event D

Time	Raw Volumes (RL)	Flow Rates, vphpl (RL)	Raw Volumes (LL)	Flow Rates, vphpl (LL)
12:45	57	684	48	576
12:50	59	708	52	624
12:55	57	684	37	444
13:00	43	516	44	528
13:05	42	504	37	444
13:10	48	576	37	444
13:15	55	660	59	708
13:20	57	684	44	528
13:25	46	552	41	492
13:30	52	624	39	468
13:35	50	600	48	576
13:40	60	720	49	588

Table 4-23: Example of Incident Condition Volume Inputs in VISSIM for Event D

Time	Raw Volumes (RL)	Flow Rates, vphpl (RL)	Raw Volumes (LL)	Flow Rates, vphpl (LL)
12:45	44	528	24	288
12:50	83	996	38	456
12:55	58	696	67	804
13:00	61	732	50	600
13:05	50	600	33	396
13:10	61	732	55	660
13:15	29	348	51	612
13:20	62	744	62	744
13:25	50	600	35	420
13:30	45	540	35	420
13:35	83	996	63	756
13:40	56	672	37	444

The vehicle type composition with relative flows were calculated and shown in Table 4-24 following the same analysis process as applied before.

Table 4-24: Aggregated Average Volume Data with Relative Vehicle Flow for Event D

	NB1_RL	NB2_LL
PC	797	523
HGV	385	23
SUT	86	17
Total	1268	563
RelFlo_PC	0.63	0.93
RelFlo_HGV	0.30	0.04
RelFlo_SUT	0.07	0.03

c. Desired Speed Distributions

A finer set of desired speed distributions was developed based on previous simulation model validation experience. As can be seen in Figure 4-44 and Figure 4-45, a total of six desired speed decisions along with six speed distributions were introduced in VISSIM.

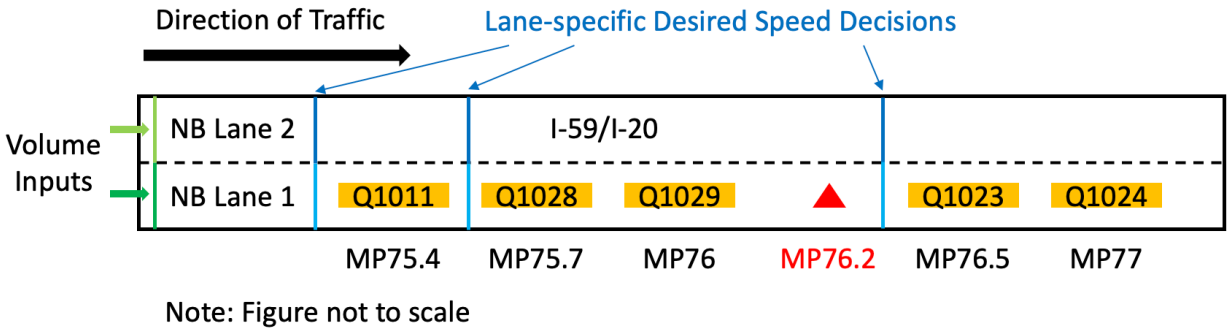

Figure 4-44: Road Network Layout with Key Components of Event D

Count: 6	No	Name	LowerBound	UpperBound
1	1	RL_11	52.50	56.50
2	2	LL_11	50.04	54.79
3	3	RL_28&29	57.46	62.66
4	4	LL_28&29	55.88	62.38
5	5	RL_23&24	54.56	65.56
6	6	LL_23&24	54.32	65.15

Figure 4-45: Desired Speed Distributions for Event D Base Condition

The cumulative speed percentages for the first set of the lane-specific desired speed distributions are provided in Table 4-25 and introduced in VISSIM to define the first set of desired speed decisions as shown in Figure 4-46.

Table 4-25: First Set of Speed Cumulative Percentage for Event D Base Condition

LL		RL	
Speed_avg	**Cumulative (%)**	**Speed_avg**	**Cumulative (%)**
50.0	5%	52.5	33%
51.0	28%	53.5	56%
51.9	79%	54.5	92%
52.9	95%	55.5	97%
53.8	97%	56.5	100%
54.8	100%	-	-

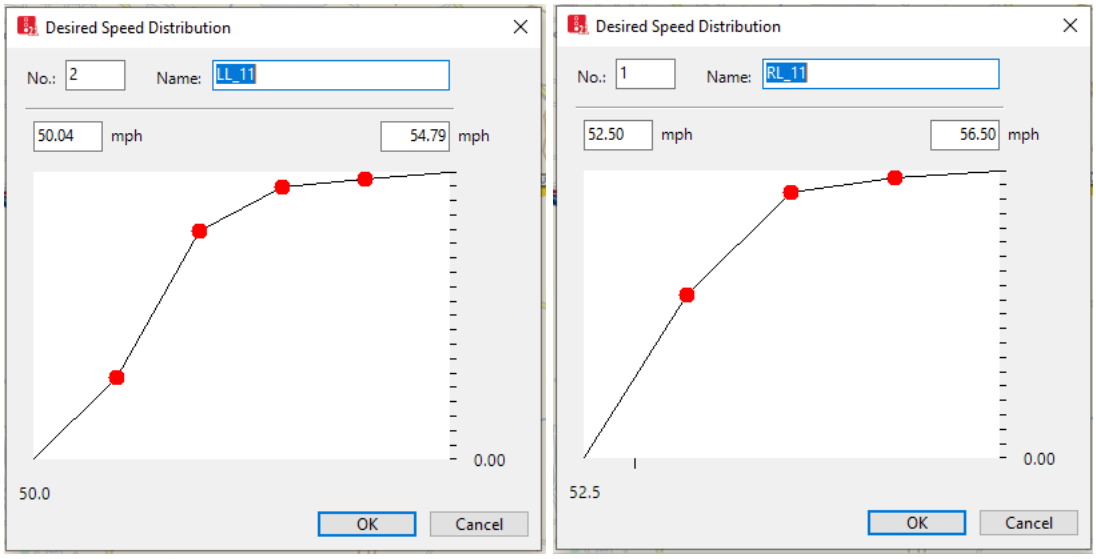

Figure 4-46: Cumulative Speed Distribution for Event D Base Condition

d. Calibration and Validation

The same calibration analysis procedure as described in the previous corresponding steps was performed to evaluate the accuracy of the base simulation model. Table 4-26 summarizes the evaluation results of GEH and RRMSE statistic.

Table 4-26: GEH and RRMSE at Each Location for Event D Base Condition

Location	GEH (% Match)		RRMSE	
	LL	RL	LL	RL
Q1011	100%	100%	2%	2%
Q1028	100%	100%	3%	3%
Q1029	100%	100%	4%	5%
Q1023	100%	100%	4%	2%
Q1024	85%	89%	11%	7%
Average	**97%**	**98%**	**5%**	**4%**

The calibration results from Table 4-26 show that the selected two performance measures, traffic flow and speed, meet both calibration criteria (GEH < 5 for at least 85% of all records and RRMSE < 25%), meaning that the VISSIM calibration results of the base condition model match

well with field observations and that all the calibration efforts indicating the base simulation model is ready to be used for the incident model simulation.

The same procedure as discussed in the previous incident simulation model development was performed and identified that the incident D simulation model shares the same reduced speed area as the incident B&C simulation model, but with different desired speed distribution inputs, since the location of incident B and D and the scope of impact (both speed reduction extended to the upstream second sensor Q1028 as discussed previously in the field data analysis section) are the same.

A combination of the speed data only from the speed reduction period recorded from the upstream two sensors (Q1028 and Q1029) was used to develop desired speed distributions specific to the reduced speed area. The speed reduction period was identified to be 13:40 – 15:05. The cumulative speed percentages for the reduction period are summarized in Table 4-27 and introduced in VISSIM to define the reduced speed area as shown in Figure 4-47.

Table 4-27: Cumulative Speed Reduction Distribution of Incident D

LL		RL	
Speed_avg	**Cumulative (%)**	**Speed_avg**	**Cumulative (%)**
4.3	47%	3.3	58%
10.8	79%	7.9	87%
17.3	94%	12.5	94%
23.8	100%	17.1	97%
-	-	21.7	100%

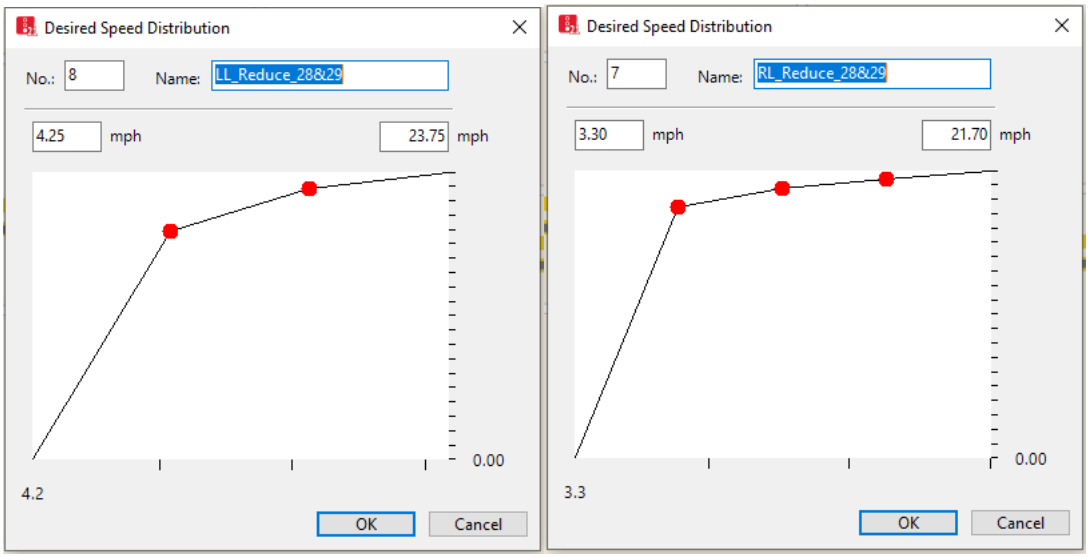

Figure 4-47: Cumulative Speed Distribution in Reduced Speed Area of Incident D

The determination of the effective time period of the reduced speed area is an iteration process as previously discussed. The identified parameters, such as length and time from/to, as inputs for the reduced speed area in VISSIM are shown in Figure 4-48. It should be noted that the identification of the length of the reduced speed area has been discussed at the beginning of the development of the incident D simulation model.

No	Name	Lane	Pos	Length	TimeFrom	TimeTo
1	RL_Reduce_28&29	1 - 1	21700.000	700.000	3300	7200
2	LL_Reduce_28&29	1 - 2	21700.000	700.000	3300	7200

Figure 4-48: Reduced Speed Area Inputs for Incident D

In general, a total of eight desired speed distributions using data from incident condition were ultimately developed, as shown in Figure 4-49.

Count: 8	No	Name	LowerBound	UpperBound
1	1	RL_11	50.40	57.60
2	2	LL_11	48.57	55.77
3	3	RL_28&29	29.00	62.00
4	4	LL_28&29	27.75	63.75
5	5	RL_23&24	38.20	75.20
6	6	LL_23&24	36.85	75.35
7	7	RL_Reduce_28&29	3.30	21.70
8	8	LL_Reduce_28&29	4.25	23.75

Figure 4-49: Desired Speed Distributions Under Incident D Condition

The same process as was used in the models of the other events was performed to determine the quality of the incident condition simulation model. The evaluation results of GEH and RRMSE statistic are summarized and presented in Table 4-28.

Table 4-28: GEH and RRMSE at Each Location under Incident D Condition

Location	GEH (% Match)		RRMSE	
	LL	RL	LL	RL
Q1011	92%	97%	20%	21%
Q1028	87%	88%	23%	20%
Q1029	86%	86%	30%	28%
Q1023	91%	90%	18%	15%
Q1024	92%	93%	23%	21%
Average	**90%**	**91%**	**23%**	**21%**

It may be noticed that at the location of sensor Q1029, even though the RRMSE values are greater than the threshold, on average, the two performance measures, traffic flows and speed, meet both calibration criteria which corresponding to the GEH (< 5 for at least 85% of the records) and RRMSE (< 25%), meaning that the developed incident simulation model was considered successfully validated.

Overall, the results from both base and incident conditions indicate that the developed simulation models with calibrated parameters reliably replicates the traffic operations at the study work zone with QWS deployed. The evaluation of the selected measures of effectiveness (MOEs),

such as travel time, delay, and queue length, between the simulation base model and incident model will be discussed in detail in the following section.

4.6 SENSITIVITY ANALYSIS OF TRAFFIC PERFORMANCE MEASURES

Three measures of effectiveness (MOEs), which are travel time, vehicle delay, and queue length from the simulation outputs, were utilized for the sensitivity analysis between the validated simulation models (base and incident conditions) for each event.

Specifically, travel time: measures the average travel time of the individual vehicle through the work zone; vehicle delay: refers to the average delay of all vehicles; queue length: the current queue length is measured upstream by the queue counter at each time step and the arithmetic mean is calculated per time interval (PTV Group 2021).

Due to the limited number of work zones with queue warning system deployment currently available for analysis in Alabama, each of the effectiveness measure analysis will only focus on the comparison from the incident simulation model to the base simulation model, since the traffic data utilized for the simulation model developments were collected under the use of QWS. In other words, a true control condition in which QWS was not deployed did not occur.

4.6.1 Travel Time and Vehicle Delay

Since travel time and delay measurements correspond to each other, they are combined for effectiveness analysis.

The comparison of travel time and vehicle delay between the incident model and the base model are provided in Figure 4-50, Figure 4-51, and Figure 4-52. It can be seen from the following Figures that after each incident occurred, the time period of increased travel time agrees with that

of the field-observed speed reduction period as discussed in the previous incident model development. With the increases of travel time, the corresponding vehicle delays increase over the same period.

Compared with the incident model, the travel times generated by each base model are consistent and stable across the work zone segment, and generally there is no vehicle delay under base conditions.

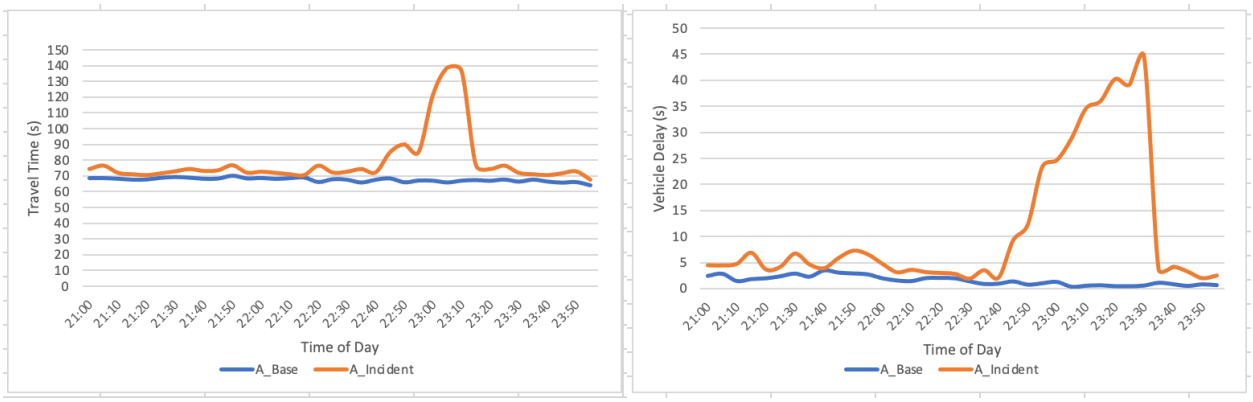

Figure 4-50: Travel Time and Vehicle Delay of Event A

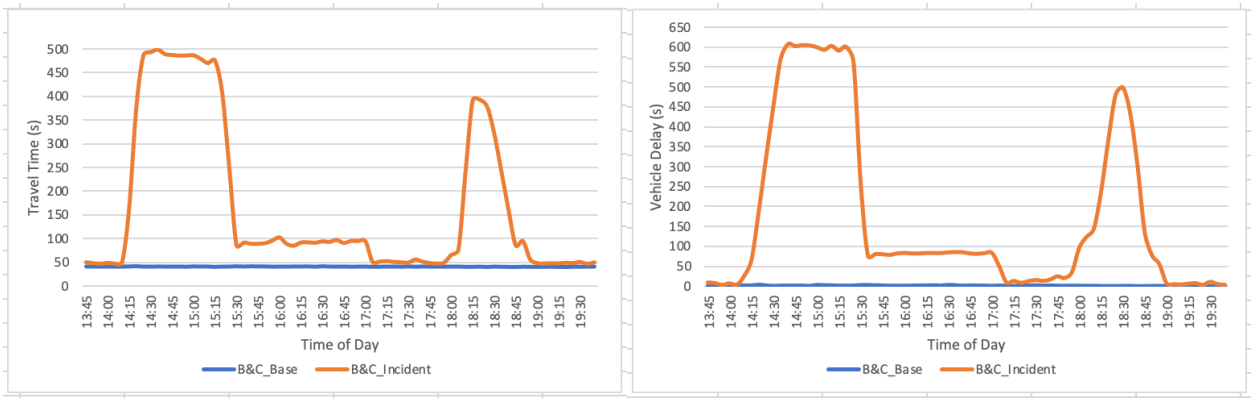

Figure 4-51: Travel Time and Vehicle Delay of Event B&C

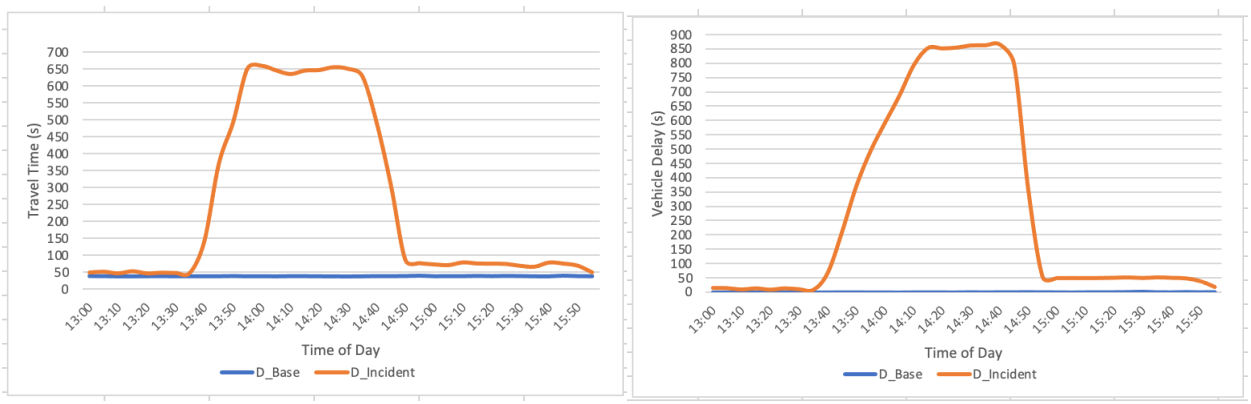

Figure 4-52: Travel Time and Vehicle Delay of Event D

4.6.2 Queue Length

The method used to evaluate the effectiveness of queue length is to compare the degree of agreement between the queue length data generated by the incident condition simulation model and the field-observed queue data (an estimation). Based on the previous literature review work, 35 mph was identified as the queue detection threshold which corresponds a "Stop" traffic condition (Pesti et al. 2013).

Table 4-29 provides an example of the queue length evaluation process specific to incident A. Time period from 22:50 to 23:05 is the identified speed reduction period as discussed beforehand where the recorded speeds from the upstream first sensor Q1025 are all below 35 mph. The second column represents the generated queue length from incident model. The third column represents the field-measured length between the upstream first sensor Q1025 to the upstream second sensor Q1018 based on the incident A location. Since the speed reduction was only recorded by the first sensor Q1025, it can be estimated that the approximate queue length will be between these two sensors, corresponding to a length range of 2112 to 4752 ft. The length calculation refers to Figure 4-3 which includes milepost for each location, and it is worth mentioning that due to the spacing of the sensors, the field-estimated queue lengths are only in

very broad ranges. The last column represents whether the queue length generated from the incident simulation model is within the desired range.

Table 4-29: Queue Length Evaluation for Incident A

Time	QLen, ft (Model)	Q1025 - Q1018, ft	Match?
22:50	2123	2112 - 4752	Y
22:55	2190	2112 - 4752	Y
23:00	2176	2112 - 4752	Y
% Match	**-**	**-**	**100%**

Queue length evaluation for incident B and C are provided in Table 4-30 and Table 4-31, respectively. It is worth mentioning that since both sensor Q1029 and Q1028 recorded a speed reduction, the expected queue length observed in the field will be between the first sensor Q1029 to the third sensor Q1011, corresponding to a length range of 1056 to 4224 ft.

Table 4-30: Queue Length Evaluation for Incident B

Time	QLen, ft (Model)	Q1029 - Q1011, ft	Match?
14:15	0	1056 - 4224	N
14:20	2442	1056 - 4224	Y
14:25	2540	1056 - 4224	Y
14:30	2840	1056 - 4224	Y
14:35	3540	1056 - 4224	Y
14:40	3535	1056 - 4224	Y
14:45	3538	1056 - 4224	Y
14:50	3529	1056 - 4224	Y
14:55	3555	1056 - 4224	Y
15:00	3523	1056 - 4224	Y
15:05	3526	1056 - 4224	Y
15:10	3523	1056 - 4224	Y
15:15	3548	1056 - 4224	Y
15:20	3563	1056 - 4224	Y
15:25	2544	1056 - 4224	Y
15:30	2037	1056 - 4224	Y
15:35	1978	1056 - 4224	Y
15:40	1863	1056 - 4224	Y
15:45	0	1056 - 4224	N
% Match	**-**	**-**	**89%**

Table 4-31: Queue Length Evaluation for Incident C

Time	QLen, ft (Model)	Q1029 - Q1011, ft	Match?
17:50	1697	1056 - 4224	Y
17:55	1909	1056 - 4224	Y
18:00	2970	1056 - 4224	Y
18:05	3890	1056 - 4224	Y
18:10	4099	1056 - 4224	Y
18:15	4465	1056 - 4224	N
18:20	4216	1056 - 4224	Y
18:25	4153	1056 - 4224	Y
18:30	4150	1056 - 4224	Y
18:35	3927	1056 - 4224	Y
18:40	3190	1056 - 4224	Y
18:45	2603	1056 - 4224	Y
18:50	2375	1056 - 4224	Y
18:55	1523	1056 - 4224	Y
% Match	**-**	**-**	**93%**

Queue length evaluation for incident D is provided in Table 4-32. Same as event B&C, speed reduction extended to the upstream second sensor Q1028, therefore, the expected queue length observed in the field will be the same.

Table 4-32: Queue Length Evaluation for Incident D

Time	QLen, ft (Model)	Q1029 - Q1011, ft	Match?
13:40	0	1056 - 4224	N
13:45	1059	1056 - 4224	Y
13:50	1099	1056 - 4224	Y
13:55	1222	1056 - 4224	Y
14:00	1986	1056 - 4224	Y
14:05	2585	1056 - 4224	Y
14:10	2610	1056 - 4224	Y
14:15	2618	1056 - 4224	Y
14:20	3009	1056 - 4224	Y
14:25	3106	1056 - 4224	Y
14:30	2912	1056 - 4224	Y
14:35	2626	1056 - 4224	Y
14:40	2617	1056 - 4224	Y
14:45	2309	1056 - 4224	Y
14:50	1214	1056 - 4224	Y
14:55	1029	1056 - 4224	Y
15:00	0	1056 - 4224	N
% Match	**-**	**-**	**88%**

The effectiveness evaluation of queue length indicates the simulation model outputs match well with the field data.

In general, the analysis of the three MOEs indicate that 1) the developed simulation models (base and incident condition) reliably replicates the field traffic operations; 2) if the incident occurred near midnight (low-volume conditions) such as incident A, there would be less impact on travel time and vehicle delay as well as the queue length; and 3) if the incident occurred around noon (higher-volume conditions), such as incident B, there will be an increase in travel time and the queue length compared to other time periods.

In addition, it may be noticed that although incident C (17:45pm) occurred at PM peak period, the impacts on travel time, vehicle delay and queue length are not significant, which possible due to the presence of QWS.

CHAPTER FIVE: CONCLUSIONS AND RECOMMENDATIONS

5.1 INTRODUCTION

The purpose of this study was to present a comprehensive analysis of the safety and mobility impacts of a queue warning system deployed in a freeway work zone environment. To achieve this purpose, two major tasks were conducted to evaluate the impact of QWS on traffic safety and mobility. Specifically, the safety performance evaluation of QWS focuses on the development of an approach to estimate expected crashes that would potentially be mitigated by QWS. In order to visually analyze the effectiveness of QWS on traffic flow, a series of traffic simulation models were developed and validated with the aim of being able to replicate field-observed traffic operations within the work zone area.

5.2 CONCLUSION

A site-specific crash modification factor (CMF) for QWS deployment was developed to be 1.49, indicating that a 49% increase in the rear-end and sideswipe associated crashes may be expected at the treatment site (with QWS) during construction. The crash reduction analysis of the study sites also concluded that the percentage of crash increased at the control site is lower than that at the treatment site, and as noted earlier this may be due to some differences in conditions between the two sites such as AADT and TTC deployment. It is important to note that these findings were conducted from a very limited study that only included 1 control and 1 treatment site, and the option of having control and treatment conditions at the same site was not available as mentioned before, therefore, the transferability to other locations is limited until further study with more study sites can be performed.

In addition, three sets of six different microsimulation models were developed in VISSIM for the purpose of intuitively analyzing the effectiveness of QWS on traffic flow under base and incident conditions within the freeway work zone. Based on the selected incident characteristics, this study presented a detailed analysis of VISSIM model development, calibration, and validation for each condition. Each of the developed simulation model with calibrated parameters reliably replicates the traffic operations at the study work zone with QWS deployed.

Based on the evaluation of effectiveness measures (i.e., travel time, vehicle delay, and queue length), this study concluded that 1) with the deployment of a QWS, midnight (low-volume conditions) incident tends to have less impact on the selected three MOEs and 2) incident occurred around noon (higher-volume conditions) will result in increased travel times and queue lengths through the work zone segment. An interesting finding driven from this process was that the PM peak period incident does not significantly affect travel times, vehicle delays, and queue lengths.

5.3 RECOMMENDATIONS FOR FUTURE RESEARCH

This thesis is a component of ongoing research aimed to evaluate the safety impact and performance of an initial deployment of QWS and provide guidelines for ALDOT on future applications. While the results of this research suggest that QWS deployed in freeway work zone has positive safety and mobility effects, the limited number of work zones with QWS deployment utilized for analysis is a concern. In continuation of this study, future recommendations on the analysis of the effectiveness of QWS deployment in freeway work zones can be found below:

- Increase the sample size of the study site with QWS for safety and mobility analysis.
- An Empirical Bayes before-after analysis can be used for the development of the site-specific CMF for QWS deployment in freeway work zone if field data is sufficient.

- Increase the number of the desired speed distributions along with the desired speed decisions in VISSIM to be able to best replicate the field conditions.
- For the development of an incident condition simulation model, the speed reduction length, position, and the effective time of the reduced speed area could be tested to obtain the most suitable parameter set.
- Transportation agencies should consider deploying QWS in freeway work zones in which flow rates are high enough that queuing may be expected to occur. This study faced limitations in experiment design due to how the QWS was deployed; therefore, the estimated safety benefits were relatively small. However, these results, combined with results of other studies, support consideration of QWS deployment in similar situations.

The methodology utilized in this study for the development of the site-specific crash modification factor related to the QWS deployment in freeway work zones when true control conditions could not be evaluated, and for the VISSIM model development, calibration and validation can be applicable to other state highway agencies and practitioners.

REFERENCES

1. Al-Kaisy, A., & Hall, F. (2003). Guidelines for estimating capacity at freeway reconstruction zones. *Journal of Transportation Engineering*, *129*(5), 572-577.
2. Alabama Department of Transportation (ALDOT) (2011). "2011 Crash Facts".
3. Alabama Department of Transportation (ALDOT) (2012). "2012 Crash Facts".
4. Alabama Department of Transportation (ALDOT) (2013). "2013 Crash Facts".
5. Alabama Department of Transportation (ALDOT) (2014). "2014 Crash Facts".
6. Alabama Department of Transportation (ALDOT) (2015). "2015 Crash Facts".
7. Alabama Department of Transportation (ALDOT) (2016). "2016 Crash Facts".
8. Alabama Department of Transportation (ALDOT) (2017). "2017 Crash Facts".
9. Alabama Department of Transportation (ALDOT) (2018). "2018 Crash Facts".
10. Alabama Department of Transportation (ALDOT) (2019). "2019 Crash Facts".
11. Alexiadis, V., Jeannotte, K., Chandra, A., Skabardonis, A., & Dowling, R. (2004). *Traffic analysis toolbox volume I, traffic analysis tools primer* (No. FHWA-HRT-04-038). United States. Federal Highway Administration. Office of Research, Development, and Technology.
12. American Association of State Highway and Transportation Officials (AASHTO). (2014). *Highway Safety Manual.* Washington, D.C.
13. American Road & Transportation Builders Association (ARTBA) (2022). Smart Work Zones.
14. Federal Highway Administration (2022). Crash Modification Factors (CMF) Clearinghouse.
15. Dimitrakopoulos, G., & Demestichas, P. (2010). Intelligent transportation systems. *IEEE Vehicular Technology Magazine*, *5*(1), 77-84.
16. Domenichini, L., La Torre, F., Branzi, V., & Nocentini, A. (2017). Speed behaviour in work zone crossovers. A driving simulator study. *Accident Analysis & Prevention*, *98*, 10-24.

17. Dowling, R., Skabardonis, A., & Alexiadis, V. (2004). *Traffic analysis toolbox, volume III: Guidelines for applying traffic microsimulation modeling software* (No. FHWA-HRT-04-040). United States. Federal Highway Administration. Office of Operations.
18. Edara, P., & Chatterjee, I. (2010). Multivariate regression for estimating driving behavior parameters in work zone simulation to replicate field capacities. *Transportation Letters*, *2*(3), 175-186.
19. Edara, P., Brown, H., Sun, C., & Savolainen, P. (2020). *Development and Application of Work Zone Crash Modification Factors (2nd Ed.)*. United States. Federal Highway Administration.
20. Federal Highway Administration (2011). ITS Research Fact Sheets - Benefits of Intelligent Transportation Systems.
21. Federal Highway Administration (2014). Local and Rural Road Safety Briefing Sheets – Crash Modification Factors (CMFs).
22. Federal Highway Administration (2017). Smart Work Zone Systems.
23. Federal Highway Administration (2020). Highway Statistics 2020.
24. Federal Highway Administration (2020). Status of the Nation's Highways, Bridges, and Transit Conditions & Performance 23rd Edition.
25. Federal Highway Administration (2022). Intelligent Transportation Systems (ITS) & Technology.
26. Federal Highway Administration (2022). Smarter Work Zones.
27. Federal Highway Administration (2022). Work Zone Facts and Statistics.
28. Federal Highway Administration (2022). Work Zone safety.
29. Garber, N. J., & Zhao, M. (2002). Distribution and characteristics of crashes at different work zone locations in Virginia. *Transportation Research Record*, *1794*(1), 19-25.

30. Golembiewski, G. A., Chandler, B., & Anderson, R. (2011). *Roadway departure safety: a manual for local rural road owners* (No. FHWA-SA-11-009). United States. Federal Highway Administration.
31. Gross, F., Persaud, B. N., & Lyon, C. (2010). *A guide to developing quality crash modification factors* (No. FHWA-SA-10-032). United States. Federal Highway Administration. Office of Safety.
32. Harb, R., Radwan, E., Yan, X., Pande, A., & Abdel-Aty, M. (2008). Freeway work-zone crash analysis and risk identification using multiple and conditional logistic regression. *Journal of Transportation Engineering*, *134*(5), 203.
33. Hardy, M., & Wunderlich, K. (2008). *Traffic Analysis Toolbox Volume VIII, Work Zone Modeling and Simulation: A Guide for Decision-Makers* (No. FHWA-HOP-08-029). United States. Federal Highway Administration. Office of Operations.
34. Harwood, D. W. (2003). *Review of truck characteristics as factors in roadway design* (Vol. 505). Transportation Research Board.
35. Hourdos, J., Liu, Z., Dirks, P., Liu, H. X., Huang, S., Sun, W., & Xiao, L. (2017). *Development of a queue warning system utilizing ATM infrastructure system development and field-testing* (No. MN/RC 2017-20). Minnesota. Dept. of Transportation. Research Services & Library.
36. Ishak, S., Qi, Y., & Rayaprolu, P. (2012). Safety evaluation of joint and conventional lane merge configurations for freeway work zones. *Traffic injury prevention*, *13*(2), 199-208.
37. Jehn, N. (2018). Development of Breakdown Probability Models for Rural Freeway Work Zones Using Field Data and Simulation. Master's Thesis, Auburn University.

38. Jehn, N. L., & Turochy, R. E. (2019). Calibration of vissim models for rural freeway lane closures: Novel approach to the modification of key parameters. *Transportation Research Record*, *2673*(5), 574-583.
39. Kan, X. D., Xiao, L., Liu, H., Wang, M., Schakel, W. J., Lu, X. Y., ... & Ferlis, R. A. (2019). Cross-comparison and calibration of two microscopic traffic simulation models for complex freeway corridors with dedicated lanes. *Journal of Advanced Transportation*, *2019*.
40. Khazraeian, S., Hadi, M., & Xiao, Y. (2017). Safety impacts of queue warning in a connected vehicle environment. *Transportation Research Record*, *2621*(1), 31-37.
41. Lu, X. Y., Kan, X., Shladover, S. E., Wei, D., & Ferlis, R. A. (2017). An enhanced microscopic traffic simulation model for application to connected automated vehicles. In *Proceedings of the Transportation Research Board 96th Annual Meeting*.
42. Lu, X. Y., Lee, J., Chen, D., Bared, J., Dailey, D., & Shladover, S. E. (2014). Freeway micro-simulation calibration: Case study using aimsun and VISSIM with detailed field data. In *93rd Annual Meeting of the Transportation Research Board, Washington, DC*.
43. Luttrell, T., Robinson, M., Rephlo, J. A., Haas, R., Srour, J., Benekohal, R. F., ... & Scriba, T. (2008). *Comparative analysis report: The benefits of using intelligent transportation systems in work zones* (No. FHWA-HOP-09-002).
44. Manual on Uniform Traffic Control Devices (MUTCD). Federal Highway Administration, 2009 edition.
45. Pesti, G., Chu, C. L., Charara, H., Ullman, G. L., & Balke, K. (2013). *Simulation based evaluation of dynamic queue warning system performance* (No. 13-5086).
46. Prichard, B. (2015). Exploration of Crash Severity and Location in Work Zone-Related Crashes in Alabama. Master's Thesis, Auburn University.

47. PTV Group. (2017). *PTV VISSIM 10 User Manual*.

48. PTV Group. (2021). *PTV VISSIM 2021 User Manual*.

49. Ramirez, V. (2017). Evaluating the effects of queue warning systems on freeway work zones using traffic simulation software. Master's Thesis, Auburn University.

50. Srinivasan, R., Ullman, G., Finley, M., & Council, F. (2011). Use of empirical bayesian methods to estimate crash modification factors for daytime versus nighttime work zones. *Transportation research record*, *2241*(1), 29-38.

51. Steger-Vonmetz, D. C. (2005). Improving modal choice and transport efficiency with the virtual ridesharing agency. In *Proceedings. 2005 IEEE Intelligent Transportation Systems, 2005.* (pp. 994-999). IEEE.

52. Texas Department of Transportation (TxDOT). (2018). Design Guidelines for Deployment of Work Zone Intelligent Transportation Systems.

53. Tufuor, E., Zhao, L., Haque, M., Rilett, L. R., Anderson, J. E., & Thompson, E. C. (2022). *Estimating System and Traveler Costs Due to Lane Closures During Construction and Maintenance Operations* (No. FY21-008).

54. UK Highways Agency, *Design Manual for Roads and Bridges:* Volume 12, Section 2, Department for Transport, London, England, May 1996.

55. Ullman, G. L., Iragavarapu, V., & Brydia, R. E. (2016). Safety effects of portable end-of-queue warning system deployments at Texas work zones. *Transportation Research Record*, *2555*(1), 46-52.

56. Ullman, G. L., Pratt, M., Geedipally, S., Dadashova, B., Porter, R. J., Medina, J., & Fontaine, M. D. (2018). *Analysis of work zone crash characteristics and countermeasures* (No. NCHRP Project 17-61).

57. Ullman, G., Schroeder, J., & Gopalakrishna, D. (2014). *Work zone intelligent transportation systems implementation guide: Use of technology and data for effective work zone management* (No. FHWA-HOP-14-008).

58. Venugopal, S., & Tarko, A. (2000). Safety models for rural freeway work zones. *Transportation Research Record*, *1715*(1), 1-9.

59. Wisconsin DOT. (2002). Freeway System Operational Assessment-PARAMICS Calibration and Validation Guidelines (Draft), Technical Report I-33. *Wisconsin DOT, District*, *2*.

60. Yang, H., Ozbay, K., Ozturk, O., & Xie, K. (2015). Work zone safety analysis and modeling: a state-of-the-art review. *Traffic injury prevention*, *16*(4), 387-396.

61. Zhao, L., Rilett, L. R., & Shakiul Haque, M. (2022). Calibration and Validation Methodology for Simulation Models of Intelligent Work Zones. *Transportation Research Record*, 03611981221082591.

APPENDIX A: SMART WORK ZONE PROJECT LOCATION MAP

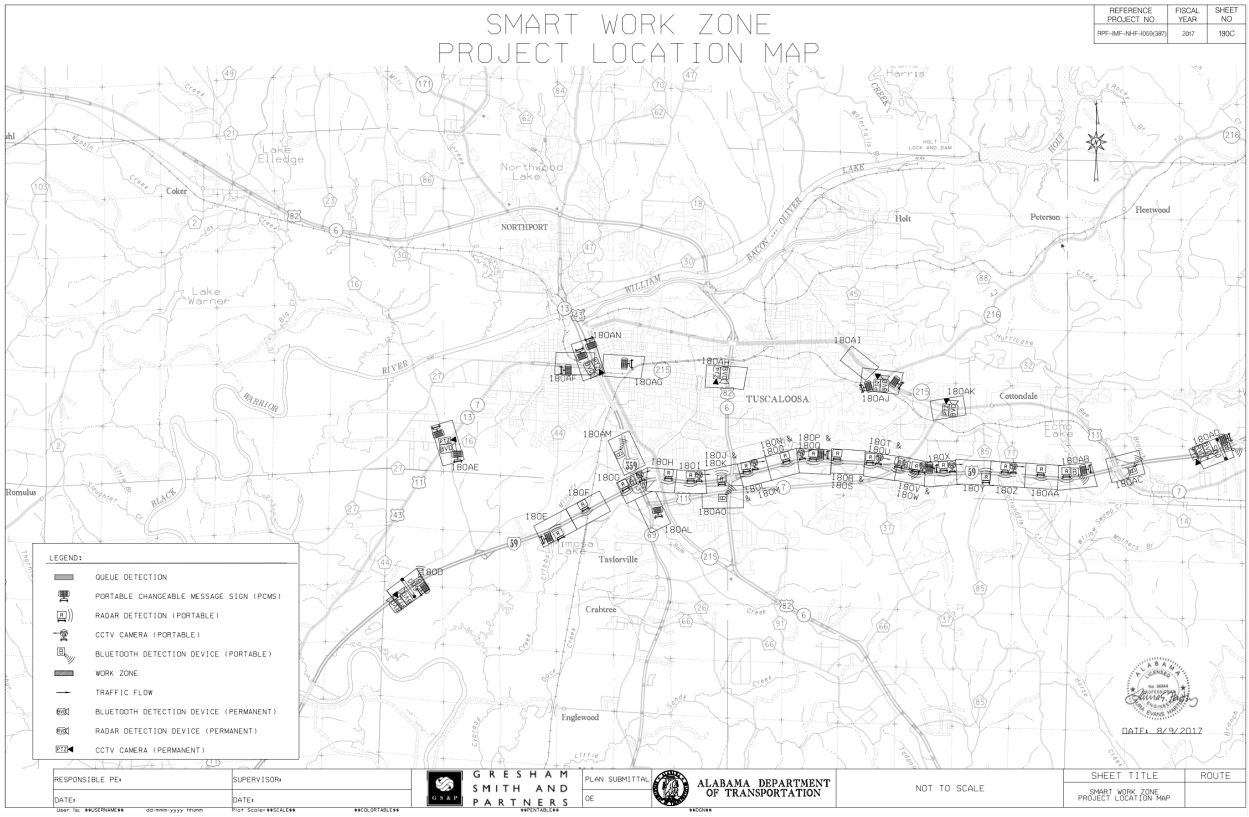

Figure A-1: Project Location Map

APPENDIX B: FIELD-COLLECTED VEHICLE VOLUMES

Table B-1: Base Condition Volume Inputs for Event A

Time	Raw Volumes (RL)	Flow Rates, vphpl (RL)	Raw Volumes (LL)	Flow Rates, vphpl (LL)
20:45	30	360	31	372
20:50	22	264	21	252
20:55	26	312	30	360
21:00	37	444	34	408
21:05	27	324	22	264
21:10	30	360	24	288
21:15	23	276	33	396
21:20	35	420	29	348
21:25	38	456	39	468
21:30	29	348	32	384
21:35	39	468	41	492
21:40	28	336	47	564
21:45	33	396	33	396
21:50	31	372	34	408
21:55	32	384	28	336
22:00	19	228	32	384
22:05	20	240	23	276
22:10	26	312	32	384
22:15	29	348	27	324
22:20	26	312	24	288
22:25	25	300	17	204
22:30	15	180	14	168
22:35	9	108	17	204
22:40	21	252	20	240
22:45	18	216	9	108
22:50	21	252	17	204
22:55	20	240	20	240
23:00	18	216	12	144
23:05	13	156	10	120
23:10	17	204	16	192
23:15	19	228	13	156
23:20	20	240	10	120
23:25	13	156	15	180
23:30	28	336	15	180
23:35	16	192	19	228
23:40	16	192	12	144
23:45	16	192	14	168
23:50	11	132	11	132
23:55	12	144	13	156

Table B-2: Incident Condition Volume Inputs for Event A

Time	Raw Volumes (RL)	Flow Rates, vphpl (RL)	Raw Volumes (LL)	Flow Rates, vphpl (LL)
20:45	48	576	39	468
20:50	23	276	15	180
20:55	31	372	25	300
21:00	43	516	27	324
21:05	37	444	33	396
21:10	21	252	13	156
21:15	21	252	37	444
21:20	22	264	23	276
21:25	30	360	47	564
21:30	55	660	38	456
21:35	31	372	27	324
21:40	35	420	22	264
21:45	13	156	14	168
21:50	16	192	40	480
21:55	23	276	31	372
22:00	28	336	33	396
22:05	48	576	43	516
22:10	18	216	23	276
22:15	33	396	40	480
22:20	22	264	2	24
22:25	18	216	14	168
22:30	23	276	18	216
22:35	16	192	15	180
22:40	16	192	10	120
22:45	22	264	13	156
22:50	20	240	25	300
22:55	18	216	12	144
23:00	8	96	9	108
23:05	18	216	17	204
23:10	13	156	9	108
23:15	40	480	17	204
23:20	34	408	17	204
23:25	29	348	18	216
23:30	20	240	13	156
23:35	30	360	16	192
23:40	20	240	13	156
23:45	18	216	8	96
23:50	22	264	11	132
23:55	13	156	10	120

Table B-3: Base Condition Volume Inputs for Event B&C

Time	Raw Volumes (RL)	Flow Rates, vphpl (RL)	Raw Volumes (LL)	Flow Rates, vphpl (LL)
13:30	64	768	55	660
13:35	60	720	43	516
13:40	50	600	37	444
13:45	65	780	60	720
13:50	55	660	52	624
13:55	74	888	54	648
14:00	73	876	59	708
14:05	69	828	53	636
14:10	73	876	64	768
14:15	85	1020	77	924
14:20	63	756	57	684
14:25	59	708	30	360
14:30	69	828	49	588
14:35	63	756	57	684
14:40	68	816	43	516
14:45	67	804	54	648
14:50	51	612	30	360
14:55	96	1152	75	900
15:00	76	912	57	684
15:05	78	936	59	708
15:10	59	708	56	672
15:15	63	756	49	588
15:20	67	804	46	552
15:25	93	1116	77	924
15:30	68	816	66	792
15:35	83	996	61	732
15:40	78	936	57	684
15:45	58	696	55	660
15:50	64	768	49	588
15:55	68	816	52	624
16:00	72	864	53	636
16:05	76	912	56	672
16:10	78	936	59	708
16:15	87	1044	66	792
16:20	70	840	52	624
16:25	87	1044	78	936
16:30	70	840	54	648
16:35	60	720	47	564
16:40	72	864	54	648
16:45	68	816	52	624

16:50	61	732	49	588
16:55	51	612	43	516
17:00	62	744	55	660
17:05	56	672	43	516
17:10	42	504	37	444
17:15	65	780	39	468
17:20	67	804	47	564
17:25	75	900	68	816
17:30	52	624	42	504
17:35	80	960	62	744
17:40	58	696	44	528
17:45	60	720	46	552
17:50	58	696	43	516
17:55	62	744	39	468
18:00	53	636	40	480
18:05	56	672	38	456
18:10	42	504	35	420
18:15	44	528	33	396
18:20	42	504	29	348
18:25	52	624	37	444
18:30	53	636	33	396
18:35	43	516	24	288
18:40	32	384	34	408
18:45	43	516	33	396
18:50	49	588	42	504
18:55	36	432	22	264
19:00	33	396	21	252
19:05	35	420	30	360
19:10	33	396	22	264
19:15	30	360	21	252
19:20	41	492	32	384
19:25	36	432	18	216
19:30	41	492	32	384
19:35	33	396	19	228
19:40	19	228	12	144

Table B-4: Incident Condition Volume Inputs for Event B&C

Time	Raw Volumes (RL)	Flow Rates, vphpl (RL)	Raw Volumes (LL)	Flow Rates, vphpl (LL)
13:30	30	360	32	384
13:35	71	852	43	516
13:40	64	768	72	864
13:45	75	900	43	516
13:50	35	420	21	252
13:55	59	708	67	804
14:00	48	576	16	192
14:05	67	804	47	564
14:10	86	1032	61	732
14:15	70	840	74	888
14:20	77	924	68	816
14:25	71	852	36	432
14:30	57	684	76	912
14:35	54	648	57	684
14:40	40	480	0	0
14:45	70	840	81	972
14:50	99	1188	96	1152
14:55	58	696	29	348
15:00	46	552	17	204
15:05	41	492	50	600
15:10	120	1440	68	816
15:15	56	672	18	216
15:20	72	864	71	852
15:25	73	876	54	648
15:30	68	816	80	960
15:35	73	876	65	780
15:40	48	576	52	624
15:45	115	1380	119	1428
15:50	68	816	69	828
15:55	85	1020	52	624
16:00	92	1104	89	1068
16:05	44	528	20	240
16:10	98	1176	129	1548
16:15	82	984	80	960
16:20	77	924	63	756
16:25	53	636	54	648
16:30	85	1020	92	1104
16:35	39	468	35	420
16:40	107	1284	95	1140
16:45	87	1044	93	1116

16:50	82	984	49	588
16:55	49	588	44	528
17:00	33	396	18	216
17:05	66	792	89	1068
17:10	94	1128	67	804
17:15	71	852	32	384
17:20	97	1164	82	984
17:25	79	948	70	840
17:30	90	1080	77	924
17:35	93	1116	72	864
17:40	54	648	42	504
17:45	42	504	41	492
17:50	74	888	40	480
17:55	58	696	35	420
18:00	51	612	45	540
18:05	81	972	80	960
18:10	92	1104	68	816
18:15	67	804	59	708
18:20	49	588	37	444
18:25	88	1056	47	564
18:30	24	288	46	552
18:35	63	756	67	804
18:40	75	900	68	816
18:45	44	528	32	384
18:50	44	528	38	456
18:55	74	888	50	600
19:00	43	516	40	480
19:05	62	744	23	276
19:10	54	648	53	636
19:15	63	756	58	696
19:20	41	492	8	96
19:25	86	1032	72	864
19:30	40	480	24	288
19:35	34	408	37	444
19:40	51	612	41	492

Table B-5: Base Condition Volume Inputs for Event D

Time	Raw Volumes (RL)	Flow Rates, vphpl (RL)	Raw Volumes (LL)	Flow Rates, vphpl (LL)
12:45	57	684	48	576
12:50	59	708	52	624
12:55	57	684	37	444
13:00	43	516	44	528
13:05	42	504	37	444
13:10	48	576	37	444
13:15	55	660	59	708
13:20	57	684	44	528
13:25	46	552	41	492
13:30	52	624	39	468
13:35	50	600	48	576
13:40	60	720	49	588
13:45	64	768	41	492
13:50	49	588	46	552
13:55	48	576	42	504
14:00	48	576	33	396
14:05	57	684	42	504
14:10	52	624	41	492
14:15	54	648	49	588
14:20	47	564	45	540
14:25	64	768	48	576
14:30	54	648	46	552
14:35	57	684	55	660
14:40	61	732	49	588
14:45	58	696	44	528
14:50	62	744	44	528
14:55	59	708	51	612
15:00	48	576	50	600
15:05	57	684	57	684
15:10	67	804	53	636
15:15	64	768	58	696
15:20	77	924	51	612
15:25	74	888	76	912
15:30	62	744	42	504
15:35	61	732	56	672
15:40	71	852	52	624
15:45	60	720	56	672
15:50	72	864	58	696
15:55	73	876	62	744

Table B-6: Incident Condition Volume Inputs for Event D

Time	Raw Volumes (RL)	Flow Rates, vphpl (RL)	Raw Volumes (LL)	Flow Rates, vphpl (LL)
12:45	44	528	24	288
12:50	83	996	38	456
12:55	58	696	67	804
13:00	61	732	50	600
13:05	50	600	33	396
13:10	61	732	55	660
13:15	29	348	51	612
13:20	62	744	62	744
13:25	50	600	35	420
13:30	45	540	35	420
13:35	83	996	63	756
13:40	56	672	37	444
13:45	53	636	41	492
13:50	54	648	47	564
13:55	53	636	58	696
14:00	59	708	74	888
14:05	59	708	51	612
14:10	86	1032	48	576
14:15	43	516	43	516
14:20	38	456	33	396
14:25	69	828	56	672
14:30	61	732	49	588
14:35	55	660	56	672
14:40	59	708	62	744
14:45	59	708	11	132
14:50	43	516	30	360
14:55	86	1032	81	972
15:00	103	1236	69	828
15:05	86	1032	91	1092
15:10	82	984	74	888
15:15	53	636	50	600
15:20	70	840	38	456
15:25	70	840	67	804
15:30	85	1020	69	828
15:35	53	636	61	732
15:40	77	924	68	816
15:45	74	888	52	624
15:50	84	1008	60	720
15:55	39	468	29	348